DESIGN OF HIGH PERFORMANCE RC-ACTIVE FILTERS

Wasfy Boushra Mikhael

A THESIS

in

The Faculty

of

Engineering

Presented in Partial Fulfillment of the Requirements
for the Degree of Doctor of Engineering at
Sir George Williams University
Montreal, Canada

May, 1973

This thesis is dedicated to the memory of my father, my idol,

DR. BOUSHRA MIKHAEL

who served humanity as a physician for more than fourty years. His life was a candle burning to make life brighter for others.

TABLE OF CONTENTS

LIST OF TABLES ix

LIST OF FIGURES x

LIST OF IMPORTANT ABBREVIATIONS AND SYMBOLS xvi

ACKNOWLEDGEMENTS xix

ABSTRACT xx

1. INTRODUCTION 1

1.1 GENERAL 1

1.2 RC-ACTIVE SYNTHESIS METHODS 5

1.3 ACTIVE DEVICES 7

1.3.1 THE OPERATIONAL AMPLIFIER 7

1.3.2 THE CURRENT CONVERSION TYPE GENERALIZED IMMITANCE CONVERTER 9

1.4 RECENT DESIGN CONSIDERATIONS IN ACTIVE FILTERS 12

1.5 SCOPE OF THE THESIS 14

2. DIRECT SYNTHESIS OF RC-ACTIVE FILTERS USING CURRENT CONVERSION TYPE GENERALIZED IMMITTANCE CONVERTERS 18

2.1 INTRODUCTION 18

2.2 STRUCTURE A - THE RC-ACTIVE NETWORK CONFIGURATION USING CGICA 18

2.3 NEW MINIMAL CAPACITOR LOW SENSITIVITY REALIZATION 21

2.3.1 SENSITIVITY ANALYSIS 24
2.3.2 AN INTERESTING FEATURE OF THE REALIZATION 26
2.4 STRUCTURE B - THE RC-ACTIVE NETWORK CONFIGURATION USING CGICB 31
2.4.1 ANTONIOU'S REALIZATION 33
2.4.2 COBB AND SU'S REALIZATIONS 35
2.5 CONCLUSIONS 36
3. FIRST CASCADE REALIZATION 39
3.1 INTRODUCTION 39
3.2 STABILITY PROPERTIES OF THE MINIMAL CAPACITOR REALIZATION 40
3.3 NEW STRUCTURES 46
3.4 SYNTHESIS USING BIQUAD A 53
3.4.1 SENSITIVITY ANALYSIS 57
3.4.2 DESIGN I - ZERO $S_{A_o}^{Q_{pa}}$ AND $S_{A_o}^{\omega_{pa}}$ DESIGN 61
3.4.3 DESIGN II - LOW SPREAD, LOW $S_{A_o}^{Q_{pa}}$ AND ZERO $S_{A_o}^{\omega_{pa}}$ DESIGN 63
3.4.4 THE INFLUENCE OF THE AMPLIFIER POLE ON BIQUAD A RESPONSE 64
3.5 DESIGN PROCEDURE 72
3.6 COMPARISON WITH KERWIN, HUELSMAN AND NEWCOMB, TARMI AND GHAUSI, AND THOMAS REALIZATIONS ... 72

3.7 EXPERIMENTAL RESULTS 76
3.7.1 LOW-PASS FILTER 77
3.7.2 BAND-PASS FILTER 77
3.8 CONCLUSIONS 82

4. SECOND CASCADE REALIZATION 84

4.1 INTRODUCTION 84
4.2 BIQUAD B - A NEW RC-ACTIVE NETWORK CONFIGURATION 84
4.3 STABILITY PROPERTIES 91
4.4 SENSITIVITY ANALYSIS 92
4.5 THE INFLUENCE OF THE AMPLIFIER POLE 97
4.6 DESIGN PROCEDURE 104
4.7 COMPARISON WITH KHN, TG AND TH REALIZATIONS 107
4.8 EXPERIMENTAL RESULTS 109
4.8.1 LOW-PASS FILTER 110
4 8.2 BAND-PASS FILTER 110
4.9 CONCLUSIONS 115

5. COMPARISON OF THE PERFORMANCES OF BIQUAD A AND BIQUAD B 117

5.1 INTRODUCTION 117
5.2 COMPARISON PART I 117
5.3 COMPARISON PART II 121
5.4 COMPARISON PART III 145

6. CONCLUSIONS 151

REFERENCES 157

APPENDIX A 161

A.1 THE INFLUENCE OF THE AMPLIFIER POLE ON Q_p AND ω_p OF BIQUAD A - DESIGN I 161

A.2 THE COMPUTER PROGRAM FOR CALCULATING THE EXACT VALUES OF $\hat{Q}_{pa}$ and $\hat{\omega}_{pa}$, OF BIQUAD A - DESIGN I IMPLEMENTED USING μA7410A, FOR DIFFERENT VALUES OF Q_p AND ω_p 169

APPENDIX B 171

B.1 THE INFLUENCE OF THE AMPLIFIER POLE ON Q_p AND ω_p OF BIQUAD A - DESIGN II 171

B.2 THE COMPUTER PROGRAM FOR CALCULATING THE EXACT VALUES OF $\hat{Q}_{pa}$ AND $\hat{\omega}_{pa}$, OF BIQUAD A - DESIGN II IMPLEMENTED USING μA7410A, FOR DIFFERENT VALUES OF Q_p and ω_p 175

APPENDIX C 177

C.1 THE INFLUENCE OF THE AMPLIFIER POLE ON Q_p AND ω_p OF BIQUAD B 177

C.2 THE COMPUTER PROGRAM FOR CALCULATING THE EXACT VALUES OF $\hat{Q}_{pa}$ and $\hat{\omega}_{pa}$, OF BIQUAD B IMPLEMENTED USING μA741 FOR DIFFERENT VALUES OF Q_p AND ω_p 180

LIST OF TABLES

Table 2.1 SENSITIVITY TO ELEMENT VARIATIONS 27

Table 3.1 Z_1 TO Z_6 OF CIRCUITS III, IV AND VI 51

Table 3.2 ELEMENT IDENTIFICATION FOR REALIZING THE MOST COMMONLY USED TRANSFER FUNCTIONS 56

Table 3.3 DESIGN VALUES AND TUNING PROCEDURE 73

Table 3.4 COMPARISON WITH KHN, TG AND TH REALIZATIONS 75

Table 4.1 ELEMENT IDENTIFICATION FOR REALIZING THE MOST COMMONLY USED TRANSFER FUNCTIONS 89

Table 4.2 DESIGN VALUES AND TUNING PROCEDURE 105

Table 4.3 COMPARISON WITH KHN, TG AND TH REALIZATIONS 108

Table 5.1 COMPARISON OF THE PERFORMANCES OF BIQUAD A AND BIQUAD B 118

Table 5.2 COMPARISON OF THE PERFORMANCES OF BIQUAD A AND BIQUAD B 120

Table 5.3 COMPARISON OF A-II AND B DESIGNS OF THE SIXTH ORDER LOW-PASS FILTER 146

Table 5.4 COMPARISON OF A-II AND B DESIGNS OF THE SIXTH ORDER BAND-PASS FILTER 147

LIST OF FIGURES

Fig. 1.1	THE OPERATIONAL AMPLIFIER	8
Fig. 1.2	THE CGICA	10
Fig. 1.3	THE CGICB	11
Fig. 1.4	THE SYMBOLIC REPRESENTATION OF THE CGIC	12
Fig. 2.1	STRUCTURE A - ACTIVE RC CONFIGURATION USING CGICA	19
Fig. 2.2	NEW MINIMAL CAPACITOR REALIZATION ..	23
Fig. 2.3	REALIZATION OF A SECOND ORDER BUTTERWORTH FILTER	29
Fig. 2.3a	LOW-PASS FILTER	29
Fig 2.3b	THE CORRESPONDING HIGH-PASS FILTER .	29
Fig. 2.3c	THE CORRESPONDING BAND-PASS FILTER .	30
Fig. 2.4	STRUCTURE B - THE RC-ACTIVE CONFIGURATION USING CGICB	32
Fig. 3.1	CIRCUIT I - SECOND ORDER REALIZATION OBTAINED FROM SECTION 2.3	41
Fig. 3.2	NATURAL FREQUENCY LOCUS OF CIRCUIT I	45
Fig. 3.3	SINGULAR ELEMENTS	46
Fig. 3.4	CIRCUIT II OBTAINED BY NULLATOR - NORATOR PAIRING	48
Fig. 3.5	CIRCUIT V OBTAINED BY NULLATOR - NORATOR PAIRING	49

Fig. 3.6	BIQUAD A	53
Fig. 3.7a	ΔQ_n% VERSUS f_p FOR BIQUAD A - DESIGN I USING μA7410A	67
Fig. 3.7b	$\Delta \omega_n$% VERSUS f_p FOR BIQUAD A - DESIGN I USING μA7410A	68
Fig. 3.8a	ΔQ_n% VERSUS f_p FOR BIQUAD A - DESIGN II USING μA7410A	70
Fig. 3.8b	$\Delta \omega_n$% VERSUS f_p FOR BIQUAD A - DESIGN II USING μA7410A	71
Fig. 3.9a	REALIZATION OF THE SIXTH ORDER CHEBYCHEV LOW-PASS FILTER (ELEMENT VALUES)	78
Fig. 3.9b-3.9e	FREQUENCY RESPONSE	79
Fig. 3.9b	LOGARITHMIC GAIN AND LINEAR FREQUENCY SCALES	79
Fig. 3.9c	LINEAR GAIN AND FREQUENCY SCALES	79
Fig. 3.9d	FREQUENCY RESPONSE FOR SUPPLY VOLTAGES ± 5 (LOWER CURVE) AND ± 15V, INPUT LEVEL = 0.05V	79
Fig. 3.9e	FREQUENCY RESPONSE AT TEMPERATURES -10°C (RIGHT-HAND CURVE), 20°C AND 70°C (LEFT-HAND CURVE)	79
Fig. 3.10a	REALIZATION OF THE SIXTH ORDER ELLIPTIC BAND-PASS FILTER (ELEMENT VALUES)	80

Fig. 3.10b-3.10f	FREQUENCY RESPONSE (REFERENCE LEVEL = 6 dB)	81
Fig. 3.10b	LOGARITHMIC GAIN AND LINEAR FREQUENCY SCALES	81
Fig. 3.10c	LINEAR GAIN AND FREQUENCY SCALES ...	81
Fig. 3.10d	FREQUENCY RESPONSE FOR SUPPLY VOLTAGES OF ± 7.5V (LOWER CURVE) AND ± 15V, INPUT LEVEL OF 0.3V	81
Fig. 3.10e-3.10f	FREQUENCY RESPONSE AT TEMPERATURES OF $-10^{\circ}C$ (RIGHT-HAND CURVE), $20^{\circ}C$ AND $70^{\circ}C$ (LEFT-HAND CURVE)	81
Fig. 4.1	SPECIAL CASE OF STRUCTURE B	85
Fig. 4.2	THE CGICB WITH ADDITIONAL PORTS 3G AND 4G	85
Fig. 4.3	SYMBOLIC REPRESENTATION OF THE CGICB IN FIG. 4.2	87
Fig. 4.4	THE BASIC CONFIGURATION	87
Fig. 4.5a	ΔQ_n% VERSUS f_p FOR BIQUAD B USING μA7410A	102
Fig. 4.5b	$\Delta\omega_n$% VERSUS f_p FOR BIQUAD B USING μA7410A	103
Fig. 4.6a	REALIZATION OF THE SIXTH ORDER CHEBYCHEV LOW-PASS FILTER	111
Fig. 4.6b-4.6e	FREQUENCY RESPONSE	112
Fig. 4.6b	LOGARITHMIC GAIN SCALE AND LINEAR FREQUENCY SCALE	112

Fig. 4.6c	LINEAR GAIN AND FREQUENCY SCALES	112
Fig. 4.6d	FREQUENCY RESPONSE FOR SUPPLY VOLTAGES ± 5V (LOWER CURVE) AND ± 15V, INPUT LEVEL = 0.05V	112
Fig. 4.6e	FREQUENCY RESPONSE AT TEMPERATURES -10°C (RIGHT-HAND CURVE), 20°C AND 70°C (LEFT-HAND CURVE)	112
Fig. 4.7a	REALIZATION OF THE SIXTH ORDER ELLIPTIC BAND-PASS FILTER	113
Fig. 4.7b-4.7f	FREQUENCY RESPONSE	114
Fig. 4.7b	LOGARITHMIC GAIN AND LINEAR FREQUENCY SCALES	114
Fig. 4.7c	LINEAR GAIN AND FREQUENCY SCALES	114
Fig. 4.7d	FREQUENCY RESPONSE FOR SUPPLY VOLTAGES OF ± 7.5V (LOWER CURVE) AND ± 15V, INPUT LEVEL OF 0.3V	114
Fig. 4.7e-4.7f	FREQUENCY RESPONSE AT TEMPERATURES OF -10°C (RIGHT-HAND CURVE), 20°C AND 70°C (LEFT-HAND CURVE)	114
Fig. 5.1a	ΔQ_n% VERSUS f_p FOR BIQUAD A - DESIGN I	123
Fig. 5.1b	ΔQ_n% VERSUS f_p FOR BIQUAD A - DESIGN II	124
Fig. 5.1c	ΔQ_n% VERSUS f_p FOR BIQUAD B	125
Fig. 5.2a	$\Delta\omega_n$% VERSUS f_p FOR BIQUAD A-DESIGN I	128

Fig. 5.2b — $\Delta\omega_n$% VERSUS f_p FOR BIQUAD A - DESIGN II 129

Fig. 5.2c — $\Delta\omega_n$% VERSUS f_p FOR BIQUAD B 130

Fig. 5.3a — ΔQ_n% VERSUS ΔA_{on}% FOR BIQUAD A - DESIGN I 132

Fig. 5.3b — ΔQ_n% VERSUS ΔA_{on}% FOR BIQUAD A - DESIGN II 133

Fig. 5.3c — ΔQ_n% VERSUS ΔA_{on}% FOR BIQUAD B 134

Fig. 5.4a — $\Delta\omega_n$% VERSUS ΔA_{on}% FOR BIQUAD A - DESIGN I 135

Fig. 5.4b — $\Delta\omega_n$% VERSUS ΔA_{on}% FOR BIQUAD A - DESIGN II 136

Fig. 5.4c — $\Delta\omega_n$% VERSUS ΔA_{on}% FOR BIQUAD B 137

Fig. 5.5a — ΔQ_n% VERSUS $\Delta\omega_{cn}$% FOR BIQUAD A - DESIGN I 139

Fig. 5.5b — ΔQ_n% VERSUS $\Delta\omega_{cn}$% FOR BIQUAD A - DESIGN II 140

Fig. 5.5c — ΔQ_n% VERSUS $\Delta\omega_{cn}$% FOR BIQUAD B 141

Fig. 5.6a — $\Delta\omega_n$% VERSUS $\Delta\omega_{cn}$% FOR BIQUAD A - DESIGN I 142

Fig. 5.6b — $\Delta\omega_n$% VERSUS $\Delta\omega_{cn}$% FOR BIQUAD A - DESIGN I 143

Fig. 5.6c — $\Delta\omega_n$% VERSUS $\Delta\omega_{cn}$% FOR BIQUAD B 144

Fig. 5.7 — THE EFFECT OF VARIATION OF ACTIVE PARAMETERS (DUE TO POWER SUPPLY CHANGES FROM ± 5V TO ± 15V) ON THE

Fig. 5.7 FREQUENCY RESPONSE OF THE SIXTH ORDER CHEBYCHEV LOW-PASS FILTER, (a) USING A-II AND (b) USING B 149

Fig. 5.8 THE EFFECT OF VARIATION OF ACTIVE PARAMETERS (DUE TO POWER SUPPLY) CHANGES FROM ± 7.5V TO ± 15V) ON THE FREQUENCY RESPONSE OF THE SIXTH ORDER ELLIPTIC BAND-PASS FILTER, (a) USING A-II AND (b) USING B 150

LIST OF IMPORTANT ABBREVIATIONS AND SYMBOLS

A	Operational amplifier gain
A_o	Operational amplifier d.c. gain
AP	All-pass
a_i	Coefficient of s^i in N(s)
B	Gain-bandwidth product
b_i	Coefficient of s^i in D(s)
BW	Bandwidth
BP	Band-pass
C_T	Total capacitance per section
C_{max}	Maximum capacitor value
C_{min}	Minimum capacitor value
C_{spread}	Capacitor spread = C_{max}/C_{min}
C_N	Number of capacitors per section
CGIC	Current conversion type generalized immitance converter
CGICA	CGIC type A
CGICB	CGIC type B
D(s)	Denominator of T(s)
f_p	Pole resonant frequency in cycles/sec.
GIC	Generalized immitance converter
H	Multiplier constant of the transfer function
HP	High-pass
h(s)	Conversion function of the CGIC
LP	Low-pass

N	Notch
N(s)	Numerator of T(s)
OA	Differential input single output operational amplifier
Q_p	Pole Q-factor
Q_{pa}	Pole Q-factor actually realized when the finite d.c. gain of the amplifier is taken into consideration
$\hat{Q}_{pa}$	Pole Q-factor actually realized when both the finite d.c. gain and the corner frequency of the amplifier are taken into consideration
Q_z	Zero Q-factor
R_T	Total resistance per section
R_{max}	Maximum resistor value
R_{min}	Minimum resistor value
R_{spread}	Resistor spread = R_{max}/R_{min}
R_N	Number of resistors per section
s	Complex frequency variable
S_e^x	Sensitivity of x due to small changes in e
T(s)	Open circuit voltage transfer function
$\Delta A_{on}\%$	Normalized percentage deviation of A_o $= [\{A_o - A_{o(typical)}\}/A_{o(typical)}] \times 100$
$\Delta Q_n\%$	Normalized percentage deviation of Q_p $= [(\hat{Q}_{pa} - Q_p)/Q_p] \times 100$
$\Delta \omega_{cn}\%$	Normalized percentage deviation of ω_c $= [\{\omega_c - \omega_{c(typical)}\}/\omega_{c(typical)}] \times 100$

$\Delta\omega_n$%	Normalized percentage deviation of ω_p $= [(\hat{\omega}_{pa}-\omega_p)/\omega_p] \times 100$
ω_c	Operational amplifier corner frequency
ω_n	Notch frequency
ω_p	Pole resonant frequency in rad/sec
ω_{pa}	Pole resonant frequency actually realized when the finite d.c. gain of the amplifier is taken into consideration
$\hat{\omega}_{pa}$	Pole resonant frequency actually realized when both the finite d.c. gain and corner frequency of the amplifier are taken into consideration
ω_z	Zero resonant frequency

ACKNOWLEDGEMENTS

The author wishes to record his appreciation and deep sense of gratitude to Dr. B. B. Bhattacharyya for his guidance and assistance during the entire preparation of this thesis.

Appreciation is also extended to Dr. M. N. S. Swamy for going through the manuscript and providing constant encouragement during the course of the work. Thanks are also due to Dr. A. Antoniou for many useful discussions. The author also gratefully acknowledges the various sacrifices made, inspiration, understanding and patience accorded to him by his wife, Mrs. Rifka Mikhael and his son, Victor Mikhael, throughout the period of the study.

The author also wishes to acknowledge Miss Geri Phillips for her efficiency in typing the manuscript.

This work was supported under the National Research Council of Canada, Grant No. A-7740 awarded to Dr. B. B. Bhattacharyya.

ABSTRACT

Designs of RC-active filters, using generalized impedance converters have been developed and studied in detail. These designs are found to be attractive from the point of view of implementation by currently available hybrid integrated technologies.

Two general configurations (termed Structure A and Structure B in the thesis), suitable for direct synthesis procedures, have been proposed. Structure B contains, as special cases, Antoniou's structure as well as that of Cobb and Su, while Structure A leads to a new minimal capacitor low sensitivity realization of RC-active filters. This one, in addition, is found to retain all the other attractive features of Antoniou's realization.

Two new configurations are then derived from structures A and B. These configurations are found to be convenient for cascade synthesis procedures. Several second order transfer functions, frequently encountered in practice, such as low-pass, high-pass, band-pass, notch and all-pass functions have been designed using these two configurations. All these sections are found to possess several attractive features such as (i) freedom from low frequency unstable modes of operation; (ii) low sensitivity to passive and active parameters; (iii) ability to be tuned in a simple manner by trimming only resistors.

The configuration resulting from Structure B (termed Biquad B in the thesis), leads to second order realizations using only two operational amplifiers. The properties of Biquad B have been compared with those due to Kerwin, Huelsman and Newcomb, Tarmi and Ghausi, and that due to Thomas, and have been found to be similar. The above mentioned realizations use three or more operational amplifiers.

The configuration resulting from Structure A (termed Biquad A in the thesis), yields second order realizations that use three operational amplifiers. The properties of Biquad A offer attractive advantages over those due to Kerwin, Huelsman and Newcomb, Tarmi and Ghausi, and Thomas such as reduced dependence on the operational amplifier parameters, lower element spreads, lower total resistance for the same total capacitance and vice-versa, etc.

With the exception of one section obtained from Biquad B, all the second order sections obtained from the Biquads can be directly cascaded without additional isolating amplifiers.

Theoretical predictions about the design techniques presented in this thesis have been verified by detailed computer simulations as well as experimental results. Further, these results show that the resulting filters are insensitive to power supply and temperature variations.

CHAPTER I

INTRODUCTION

CHAPTER I

INTRODUCTION

1.1 GENERAL

The origin of inductorless or active RC filters can be traced as far back as the thirties when these filters were designed using vacuum tubes, resistors and capacitors. Unfortunately, these techniques did not receive much attention in view of the bulky size and high prices of the vacuum tubes. Discovery of transistors led to a renewed interest in the area of active RC - filters and continued through the fifties before losing ground again to the LC filter design techniques, mainly because of the latter's superior sensitivity and stability properties. The recent surge of activity in this area can be attributed to a number of factors. Probably the strongest incentive has come from the rapidly developing technology of integrated circuits where a complex network, with all its elements and interconnections, is fabricated on a single chip. The main attractions of integrated circuit fabrication are the following [1,2] :

1) Increased system reliability

2) Reduction of size and weight, and an increased equipment density obtained by reducing the packaging levels and electronically inactive structural materials.

3) Increased functional performances obtained by regular and compact distribution of circuit elements.

4) Increased operating speeds due to the absence of parasitics and decreased propagation delay.

5) Reduction in power consumption.

Unfortunately, it has not yet been possible to fabricate inductors with reasonable values of inductances and quality factors by integrated circuit techniques. On the other hand, conventional inductors when miniturized to be consistent in size with other integrated circuit components, are extremely poor in quality to be of any use for many applications. [3]

The magnetic coupling between inductive elements may also create an additional problem, for example, in satellites carrying instruments for measuring very weak signals. Further, the nonlinear frequency dependence of the quality factor Q of the inductors, coupled with the variation of Q from one inductor to another inductor makes an accurate design of passive LC filters fairly complicated. Probably, the major difficulty in the use of inductors arises in the case of low frequency applications, like control systems and analog computers. At these frequencies (less than 1 KHZ), practical inductors of

reasonable Q tend to become unrealistically bulky and expensive.

A promising way of overcoming these difficulties is to disign filter networks without inductors, using active elements, resistors and capacitors which are easily integrable.

RC-active filters can be designed to have several other desirable features over the LC filters. Some of them are [4] :

1) The filter output impedance can be made very low, thereby making the filter response independent of the load impedance. Consequently, the filters can be cascaded without additional buffers.
2) Frequently, the input impedance of the filter is high compared with the source of impedance. Hence, very little signal power may be required.
3) The filters often provide insertion gain, thereby eliminating the need for additional amplifiers.

4) The use of active elements removes the two fundamental restrictions from RLC networks, passivity and reciprocity. Thus, active networks can not only realize network functions which are realizable by passive RLC networks, but also can be used to realize characteristics not achievable with passive networks.

However, while a passive filter can never become unstable, an improperly designed active filter can start oscillating with a slight variation of passive or active element parameters. Thus, special care should be exercised in designing active filters to avoid instability problems. Anothr problem that requires more attention in active filters than in passive filters is that of the sensitivity of the network function due to variation of network parameters. The sensitivity problem is not serious for most standard resistively terminated LC Ladder filters. However, active RC filters which are extremely frequency selective are, in general, more sensitive to parameter variations than the passive filters. Thus, particular attention should be given to the minimization of sensitivity to variation of one or more components in the design of active filters.

1.2 RC-ACTIVE SYNTHESIS METHODS

A large number of RC-active network synthesis procedures, using a variety of active elements, have been suggested in the literature [5]. These methods can be classified in several ways [6,7]. For example, they can be grouped according to the way in which the passive and active parameters in the realization are identified. The identification may be achieved by using one of the following:

1) The polynomial decomposition approach.[9,10,11]

2) The coefficient-matching approach. [10-28]

3) The simulated-inductor approach. [29-31]

In the first two methods of realization, a network configuration, which contains one or more ideal active elements and a passive RC subnetwork, is chosen. The parameters characterizing the passive subnetwork are then obtained in the first approach by properly decomposing and partitioning the specified network function and then comparing it with the appropriate network function of the selected configuration.

In the second approach, the design procedure starts from the analysis of the selected network. The element values of the passive RC subnetwork are then related to the parameters of the network function by

equating like coefficients of the complex frequency variable s. Usually, the number of equations is less than the number of unknowns. This offers the designer degrees of freedom that can be used to obtain a realization with a number of other desirable properties.

In the third approach, the design is accomplished in two steps. First, an LC filter is designed. Then the inductors are replaced by capacitively terminated gyrators. This approach is attractive due to the low-sensitivity features of resistively terminated LC filters.

Synthesis procedures can also be classified as direct [24,26,31] or cascade. [14-23,27,32] In direct synthesis procedures, the transfer function is realized as a single section. In cascade synthesis procedures, the transfer function is expressed as a product of first and second-order transfer functions and each of these is realized independently. The overall network is then obtained by cascading the individual sections. The cascade method of synthesis offers two practical advantages over the direct method as follows:

1) The tuning of the network is simplified.

2) A small number of universal sections can be designed which can realize a multitude of network specifications.

Finally, active synthesis methods can be classified according to the type of the active devices used such as finite-gain or infinite-gain controlled sources, negative immittance converters (NIC), gyrators, negative resistances, generalized immittance converters (GIC), etc. [1-4]

1.3 ACTIVE DEVICES

As mentioned in the preceding section, a wide variety of active devices has been reported in the literature. In this section, the current conversion type generalized immittance converters (CGIC) are discussed at length since they will be used as the building blocks of the design procedures presented in this thesis. As the CGIC can be realized using operational amplifiers (OA), it is worthwhile to look first into the properties of the OA.

1.3.1 The Operational Amplifier

Presently, the OA [33,34] is readily available in integrated form as an off-the-shelf component. It can be used to realize most other active devices. [4] Commercially available silicon monolithic integrated OA's are reliable, versatile, relatively inexpensive and have excellent properties. As an example, the Fairchild μA741OA is internally compensated and input-overvoltage and output-shortcircuit protected. It has an input impedance of 2MΩ, output resistance of 75Ω and gain-bandwidth product of 1MHz

(65 MHz for μA715OA). Its price is less than $1.00, compared with $70.00 for the μA709 in 1965, and there is a strong indication of OA prices going down even further. Presently, Motorola has put out four OA's on a single chip (MC3401) with a price of $1.75 only. The most commonly used OA, shown in Fig. 1.1, is a d.c. voltage amplifier with differential input and single output capabilities (Differential output OA's are also available but they are not widely

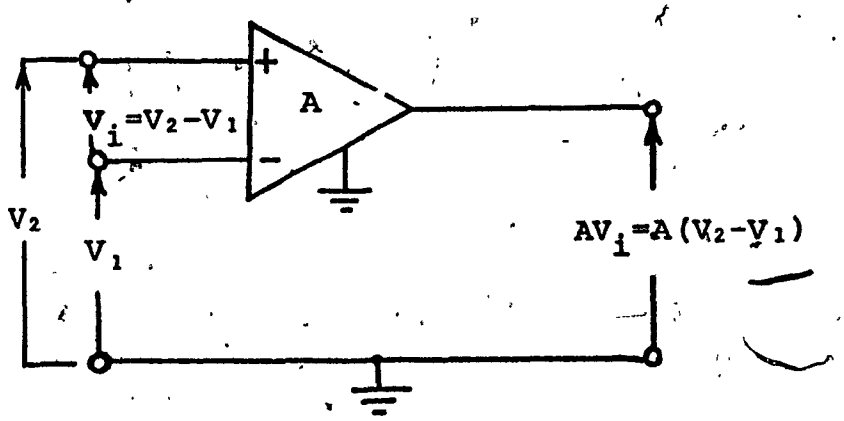

FIG. 1.1 THE OPERATIONAL AMPLIFIER

used at present). It is a non-reciprocal two-port, ideally characterized by a frequency independent infinite gain, infinite input-impedance and zero output-impedance. In practice, the OA has a frequency dependent finite gain, finite input and non-zero output impedances. The output voltage V_o is related to the input voltage V_i by

$$V_o = AV_i \qquad (1.1)$$

A is the differential open-loop gain which, for a frequency compensated OA, is given by

$$A = A_o\omega_c/(s + \omega_c) \qquad (1.2)$$

where A_o, ω_c and $B = A_o\omega_c$ are the d.c. gain, the cut-off frequency and the gain-bandwidth product, respectively.

A_o and ω_c have large manufacturability tolerances in addition to their dependence on the temperature and power-supply voltage. Hence, the characteristics of networks whose response is highly dependent on A_o and/or ω_c will be subject to undue variations with changing temperature and power supply voltage. Thus, one of the critical factors in comparing or evaluating OA networks is the dependency of the response on A_o and ω_c.

1.3.2 The Current Conversion Type Generalized Imittance Converter

The CGIC is an active two port which has a chain matrix [a] given by

$$[a] = \begin{bmatrix} 1 & 0 \\ 0 & h(s) \end{bmatrix} \qquad (1.3)$$

where h(s) is the admittance conversion function.

From (1.3), it is easy to show that

$$Y_i = h(s) Y_L \qquad (1.4)$$

where Y_i and Y_L are the input and load admittances respectively, connected to the input and output ports. Depending on the nature of $h(s)$, the CGIC's that have been reported so far, can be classified as belonging to one of the following two types. The first type of CGIC can be implemented using only one OA [4] and is shown in Fig. 1.2.

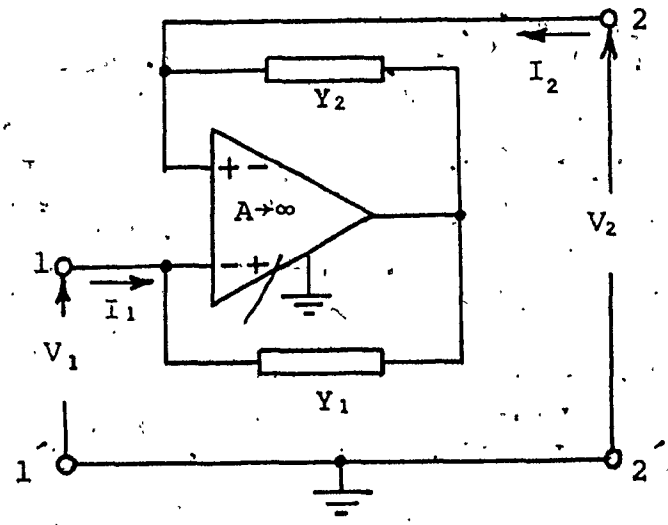

FIG. 1.2 THE CGICA

Its conversion function $h(s)$ is given by

$$h(s) = -Y_1/Y_2 \qquad (1.5)$$

This type of CGIC will be referred to as Type A in this thesis, and will be denoted CGICA. The other type of CGIC

can be implemented using two OA's [31,35], as shown in Fig. 1.3.

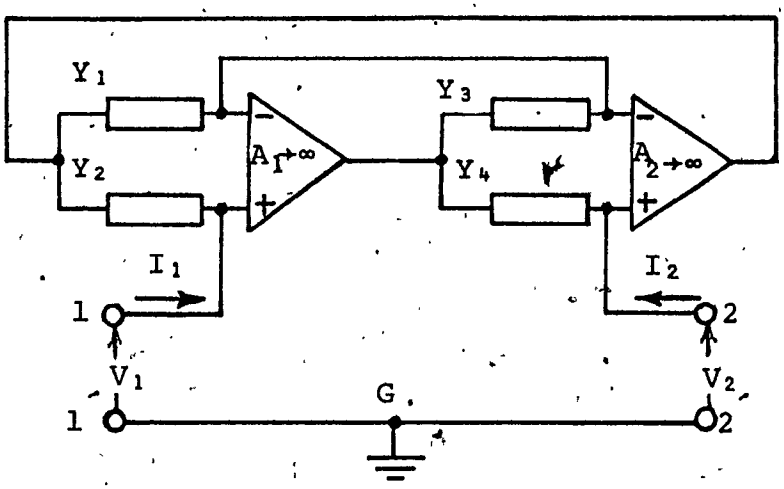

FIG. 1.3 THE CGICB

This will be referred to as Type B and denoted by CGICB. Its conversion function h(s) is given by

$$h(s) = Y_2Y_3/Y_1Y_4 \qquad (1.6)$$

Fig. 1.4 shows the symbolic representation for both types of CGIC's. The representation is derived from the fact that 1 mho connected across the output port will reflect an admittance of h(s) mhos across the input port. Both CGICA and CGICB are three terminal devices.

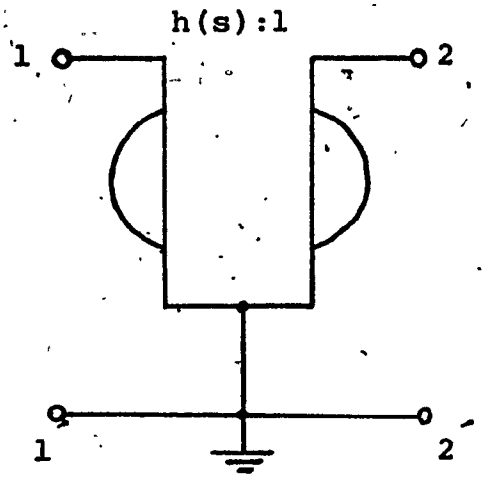

FIG. 1.4 THE SYMBOLIC REPRESENTATION OF THE CGIC

If Y_1 and Y_2 are conductances in the CGICA, it reduces to an NIC.

1.4 RECENT DESIGN CONSIDERATIONS IN ACTIVE FILTERS

In the earliest stage of active RC-network synthesis, the main objective was to demonstrate the potential of active networks as opposed to passive networks. Numerous techniques merely showed that any given rational function of s can always be synthesized as the driving point or transfer function of this or that RC-active networks [1-4]. In the next stage, minimizing the number of active elements was the major concern of active network designers. This, however, invariably resulted in extremely sensitive networks and their consequent poor performance caused the engineering

community to mistrust active networks. The efforts to reduce the sensitivity of single active element realizations were only partially successful in that they restricted the active filters to very low frequency and low Q applications. Recently, widespread application of integrated circuit technology to linear active devices has considerably eased earlier economic constraints. Now, the emphasis is often not so much on minimizing the number of active devices in a network but rather on improving the functional performance of the overall network at the expense, if necessary, of more active elements. From the point of view of reduced power consumption, size and cost, it is still preferable to use a lower number of active elements, if the network performance obtained is otherwise acceptable. For an active realization to be useful, it should be free from low frequency unstable modes of operation [36,37] and no instability should be introduced due to the frequency dependence of the active elements. The effect on the useful bandwidth of the overall realization due to the finite bandwidth of the active devices is an important consideration in active networks. High performance realizations should have as low a sensitivity as possible to the passive, as well as to the active element variations. Also, for the realizations to be suitable for the available microelectronic technology, attention should be given to the total resistance and more significantly, to the total capacitance, as well as to the spread in the values of the resistors and capacitors in the circuit.

Ideally, for integrated circuit implementation, the values for all these quantities should be as low as possible failing which, minimization of total capacitance in the circuit assumes importance. It may be of advantage for the capacitors to be minimum in number and also for them to have a common ground. It is essential that the filters be tunable in a simple manner, preferably by trimming only resistors. The designed filters should have a wide dynamic range of linear operation and a large signal to noise ratio.

1.5 SCOPE OF THE THESIS

The aim of the thesis is to develop new synthesis techniques for the realization of open circuit voltage transfer functions using CGIC's of Types A or B, as the basic active device. The proposed techniques are shown to yield realizations which have attractive features in comparison with the presently available high performance realizations from the point of view of design considerations discussed in the previous section. For this purpose, the thesis is divided into five main sections. The concern of the second Chapter of the thesis is to obtain direct synthesis procedures for any stable voltage transfer function. The first configuration developed uses CGICA's, while the second configuration presented uses CGICB's as the active elements. It is shown that by suitably choosing h(s)'s in configuration A, a new realization which is minimal, with respect to

the number of capacitors is obtained. Special cases of h(s) in configuration B lead to the realizations described in references [26;39]. The realizations obtained from configurations A and B have similar and low sensitivities to the different passive and active elements. Chapters 3 and 4 deal with realizations of a general biquadratic transfer function. These realizations are useful for the cascade synthesis procedure. The biquadratic sections, termed BIQUAD A and BIQUAD B in this thesis, are obtained from configurations A and B respectively. The commonly used second order sections are:

1) Low-pass (LP)
2) High-pass (HP)
3) Band-pass (BP)
4) Notch (N)
5) All-pass (AP)

Most practical filter specifications can be realized by a suitable cascade combination of these sections. All of these sections can be readily obtained from either BIQUAD A or BIQUAD B and are to have the following features:

1) Freedom from low frequency unstable modes of operation.

2) Low sensitivity to passive element variations.

3) Low sensitivity to d-c-gain variations.

4) Low dependence on the OA cutoff frequency.

5) With the exception of one configuration obtained from BIQUAD B, isolation amplifiers are not necessary. Thus second order sections can be cascaded directly.

6) Tuning can be achieved in a very simple manner by trimming only resistors.

BIQUAD A uses one more OA than BIQUAD B which uses only two OA's. However, BIQUAD A has less dependence on the parameters of the OA. Design and tuning procedures are described for both biquads. By using combinations of the various sections obtained from any of the biquads, Butterworth, Chebychev, Bessel, elliptic, all pass transfer functions, etc., can be realized. The theory is verified experimentally for each of the biquads. Finally, the performance of each of the biquads is compared with the currently available high performance similar second order realizations. Chapter 5 offers a comparison of BIQUAD A and BIQUAD B. The theoretical comparison given is based on approximate formulas derived in Chapters 3 and 4, and also on exact results obtained using digital computer simulation. The typical values of μA715 OA, which is one of the best OA's available at the time of writing this thesis, are

used in the simulation. Experimental results for both of the biquads are also assessed. The final Chapter, namely, Chapter 6, summarizes the results of the thesis and contains the conclusion.

CHAPTER II

DIRECT SYNTHESIS OF RC-ACTIVE FILTERS USING CURRENT CONVERSION TYPE GENERALIZED IMMITTANCE CONVERTERS

CHAPTER II

DIRECT SYNTHESIS OF RC-ACTIVE FILTERS USING CURRENT CONVERSION TYPE GENERALIZED IMMITTANCE CONVERTERS

2.1 INTRODUCTION

Two RC-active network configurations are proposed in this Chapter. Using either of these configurations, any stable open circuit voltage transfer function can be directly synthesized. The configurations, referred to as Structure A and Structure B in this thesis, employ CGICA and CGICB respectively, (Section 1.3.2), as the active device. One of the main purposes of presenting these direct realizations is to lay the foundation for the cascade synthesis procedures that will be considered in detail in Chapters 3 and 4.

2.2 STRUCTURE A - THE RC-ACTIVE NETWORK CONFIGURATION USING CGICA

Consider the two-port using CGIC's of the Type A and one port RC admittances as shown in Fig. 2.1. The open circuit voltage transfer function T(s) of the two-port is given by

$$T(s) = \frac{V_2(s)}{V_1(s)} = -\frac{y_{21}}{y_{22}} \qquad (2.1)$$

where y_{21} and y_{22} are, respectively, the transfer and output admittances of the two-port with terminals 2-2' and 1-1' short circuited.

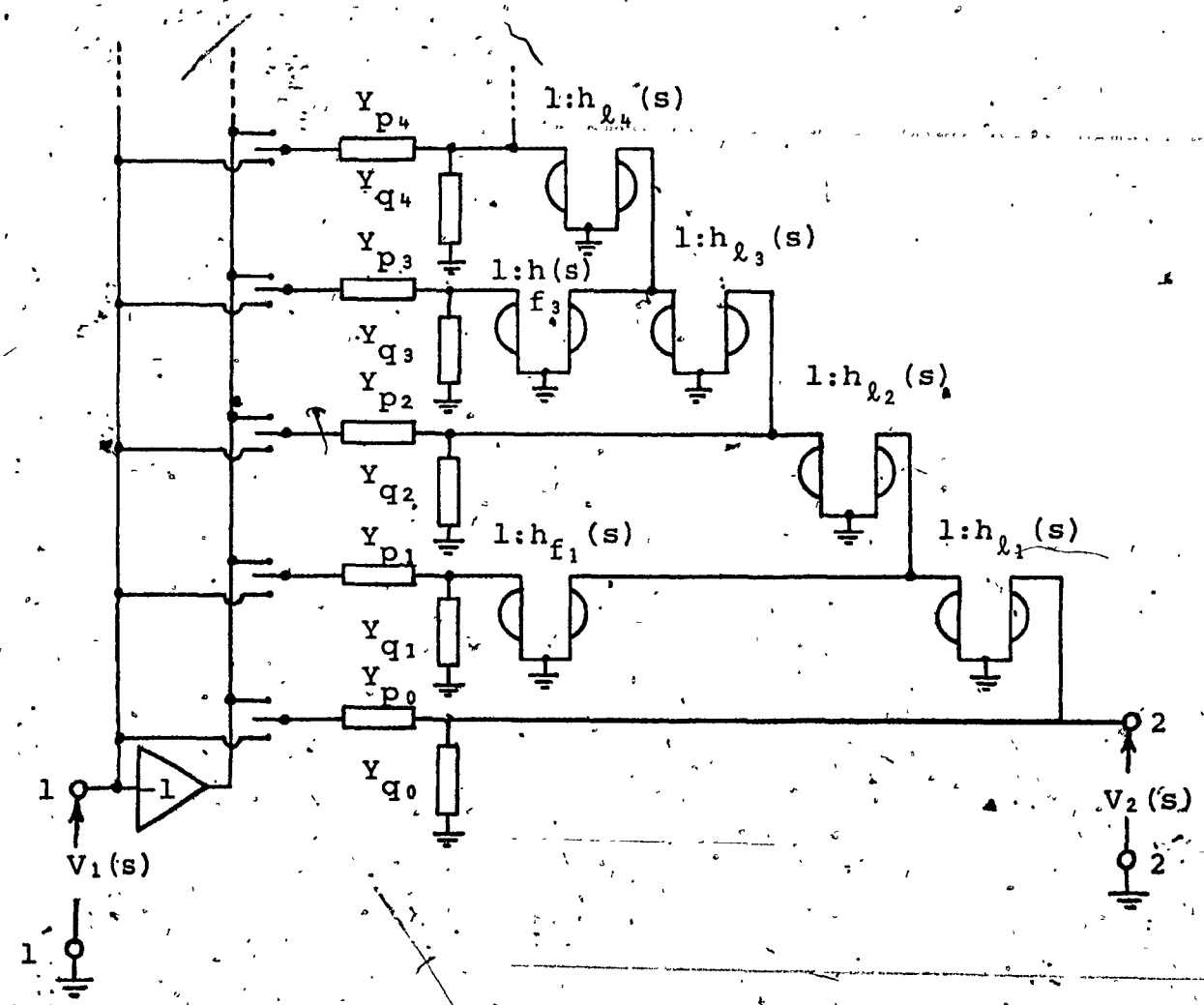

FIG. 2.1 STRUCTURE A - ACTIVE RC CONFIGURATION USING CGICA

A simple analysis of the two-port of Fig. 2.1 yields

$$-y_{21} = \pm Y_{po} \pm h_{f_1} h_{\ell_1} Y_{p_1} \pm h_{\ell_1} h_{\ell_2} Y_{p_2} \pm \ldots$$

$$= \pm Y_{po} + \sum_i \prod_{j=1}^{2i} h_{\ell j} (\pm Y_{p_2 i})$$

$$+ \sum_i (h_{f(2i+1)} \prod_{j=1}^{2i+1} h_{\ell j})(\pm Y_{p(2i+1)}) \quad (2.2a)$$

and

$$y_{22} = (Y_{po} + Y_{qo}) + h_{\ell_1} h_{f_1} (Y_{p_1} + Y_{q_1}) +$$

$$+ h_{\ell_1} h_{\ell_2} (Y_{p_2} + Y_{q_2}) + \ldots$$

$$= \sum_i (h_{f(2i+1)} \prod_{j=1}^{2i+1} h_{\ell j})(Y_{p(2i+1)} + Y_{q(2i+1)})$$

(2.2b)

Any stable open circuit voltage transfer function T(s) of a two-port can be described in the complex s-plane as

$$T(s) = \frac{\sum_{i=o}^{n} a_i s^i}{\sum_{i=o}^{n} b_i s^i} \quad (2.3)$$

where

$$b_i \geq |a_i| \ , \ b_i > 0, \ a_i \gtrless 0 \quad (2.4)$$

The condition $b_i > 0$ is automatically satisfied by a stable $T(s)$, while, to satisfy the condition $b_i \geq |a_i|$, the given $T(s)$ may have to be realized within a multiplying constant.

It is clear that, by choosing appropriately the admittances Y_{pi}'s, Y_{qi}'s and the conversion functions h_{fi}'s, $h_{\ell i}$'s in Structure A, any given $T(s)$ can be realized. In the following section, a new minimal capacitor low sensitivity realisation using Structure A is described.

2.3 NEW MINIMAL CAPACITOR LOW SENSITIVITY REALIZATION

Let

$$h_{f(2i+1)} = -\alpha_{2i+1} \tag{2.5a}$$

and

$$h_{\ell j} = \beta_j s \tag{2.5b}$$

These conversion functions can be readily realized by setting $Y_1 = G_{2i-1}$ and $Y_2 = G_{2i}$ ($i = 1, 2, \ldots$) or $Y_1 = sC_j$ and $Y_2 = G_{2j}$ ($j = 1, 2, \ldots$) in (1.5). Note that α's and β's are positive constants. It is also to be noted that CGICA with the conversion function as given by (2.5a) is the familiar current inversion type negative immittance converter (CNIC). [4] Let us also identify the different RC admittances in Structure A as follows:

$$Y_{pi} = G_{pi} \ , \ Y_{qi} = G_{qi} \qquad (2.6)$$

that is, the different admittances are taken as conductances. Structure A then reduces to the network of Fig. 2.2. From (2.2), (2.5) and (2.6), we obtain the following for even n:

$$-y_{21} = \pm G_{po} + \sum_{i=1}^{n/2} \left[\prod_{k=1}^{2i} \beta_k \right] [\pm G_{p_2 i}] s^{2i} + \sum_{j=0}^{(n/2)-1} \alpha_{2j+1} \left[\prod_{\ell=1}^{2j+1} \beta\ell \right] [\pm G_{p(2j+1)}] s^{2j+1} \qquad (2.7a)$$

$$y_{22} = (G_{po} + G_{qo}) + \sum_{i=1}^{n/2} \left[\prod_{k=1}^{2i} \beta_k \right] [G_{p(2i)} + G_{q(2i)}] s^{2i} + \sum_{j=0}^{(n/2)-1} \alpha_{2j+1} \left[\prod_{\ell=1}^{2j+1} \beta\ell \right] [G_{p(2j+1)} + G_{q(2j+1)}] s^{2j+1} \qquad (2.7b)$$

For odd n, (2.7) still holds excepting i and j both now run up to (n-1)/2.

It is seen that the two-port of Fig. 2.2 can realize any stable transfer function. Comparing the coefficients in (2.1) and (2.7) we have

$$G_{po} = |a_o| \ ; \ G_{qo} = b_o - |a_o| \qquad (2.8a)$$

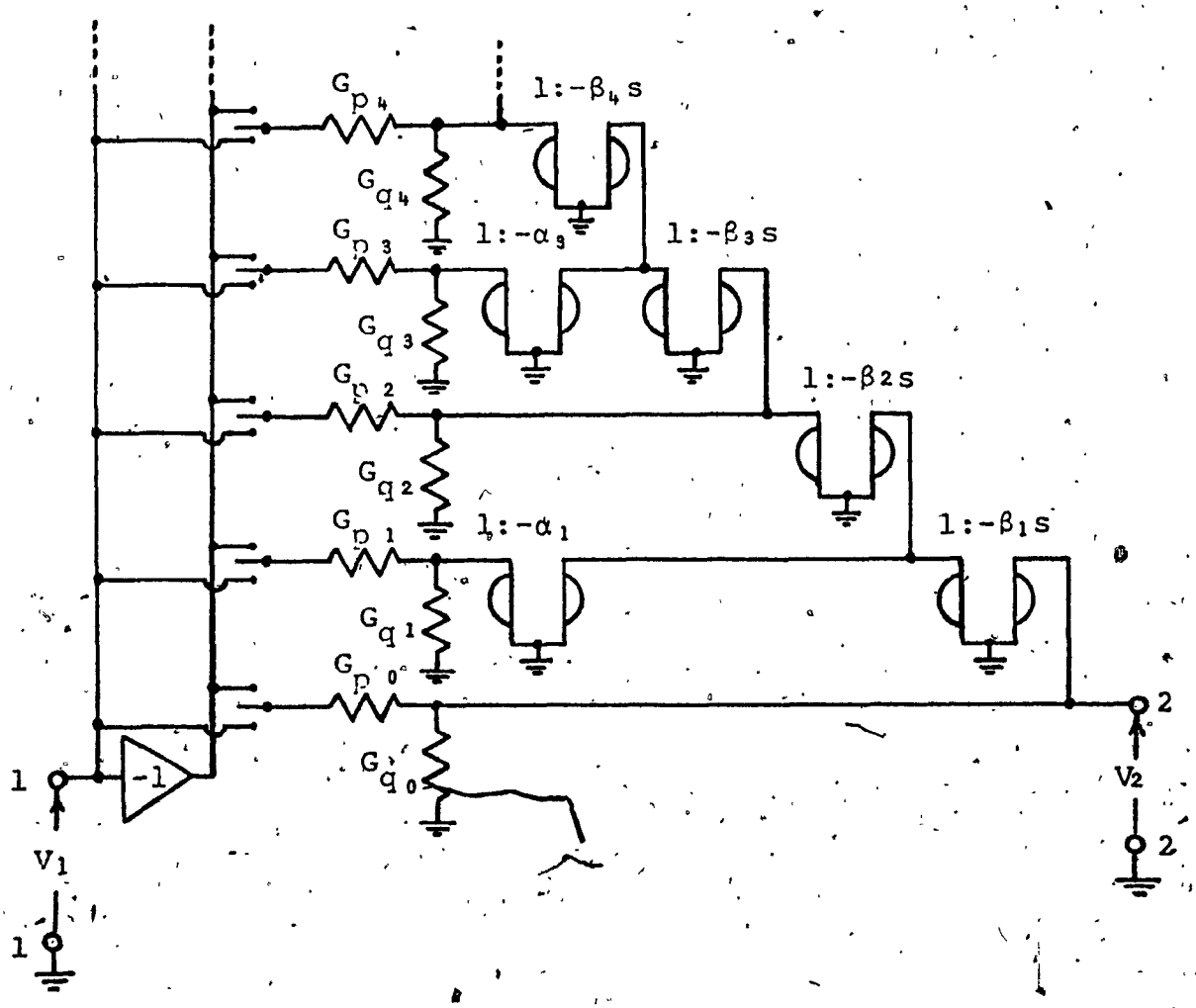

FIG. 2.2 NEW MINIMAL CAPACITOR REALIZATION

and for even m, $(m \leq n)$,

$$G_{pm} = |a_m| / \prod_{i=1}^{m} \beta_i, G_{qm} = (b_m - |a_m|) / \prod_{i=1}^{m} \beta_i \qquad (2.8b)$$

while for odd m, $(m \leq n)$,

$$G_{pm} = |a_m| / \alpha_m \prod_{i=1}^{m} \beta_i, G_{qm} = (b_m - |a_m|) / \alpha_m \prod_{i=1}^{m} \beta_i \qquad (2.8c)$$

It is clear from (2.7) that for a T(s) of a denominator polynomial of degree n, only n capacitors are required. These capacitors are all contained in the CGICA's. This is in fact, the minimum number of capacitors required in an RC-active realization for any given transfer function. [24,38]

2.3.1 Sensitivity Analysis

An important criterion of a realization is its sensitivity to element variations.

From (2.1), (2.3) and (2.7), we obtain

$$a_o = \pm G_{po}, \quad b_o = (G_{po} + G_{qo}) \qquad (2.9a)$$

and for even i $(i \leq n)$

$$a_i = \pm G_{pi} \prod_{j=1}^{i} \beta_j, \quad b_i = (G_{pi} + G_{qi}) \prod_{j=1}^{i} \beta_j \qquad (2.9b)$$

while for odd i $(i \leq n)$,

$$a_i = \pm \alpha_i G_{pi} \prod_{j=1}^{i} \beta_j, \quad b_i = \alpha_i (G_{pi} + G_{qi}) \prod_{j=1}^{i} \beta_j \qquad (2.9c)$$

The coefficient sensitivity is given by [4].

$$S_e^{a_i} = (e/a_i)(\partial a_i/\partial e) \qquad (2.10)$$

where e is any element, active or passive on which the coefficient a_i depends.

From (2.9) and (2.10) we obtain the various coefficient sensitivities with respect to α_i's, β_i's, G_{pi}'s, and G_{qi}'s as

$$|S_e^{a_i}| \leq 1, \quad |S_e^{b_i}| \leq 1 \qquad (2.11)$$

Considering now the more interesting case of a second order transfer function, the Q-factor Q_p, the undamped frequency of oscillation ω_p and their sensitivities to any element e, $S_e^{Q_p}$ and $S_e^{\omega_p}$, are given by

$$Q_p = \sqrt{(b_0 b_2)}/b_i, \quad \omega_p = \sqrt{b_0/b_2} \qquad (2.12a)$$

$$S_e^{Q_p} = (\partial Q_p/\partial e)(e/Q_p), \quad S_e^{\omega_p} = (\partial \omega_p/\partial e)(e/\omega_p) \qquad (2.12b)$$

where the b_i coefficients are as defined before. From (2.9) and (2.12a) we get

$$Q_p = \sqrt{\{(\beta_2/\beta_1)(G_{p_2} + G_{q_2})(G_{po} + G_{qo})\}}/\alpha_1(G_{p_1} + G_{q_1}) \quad (2.13)$$

and

$$\omega_p = \sqrt{(G_{po} + G_{qo})/\beta_1\beta_2(G_{p_2} + G_{q_2})} \quad (2.14)$$

The Q_p and ω_p sensitivities $S_e^{Q_p}$ and $S_e^{\omega_p}$ calculated from (2.12)-(2.14) are given in Table 2.1, from which we observe

$$|S_e^{Q_p}| \leq 1 \quad \text{and} \quad |S_e^{\omega_p}| \leq \tfrac{1}{2} \quad (2.15)$$

Note that the Q_p-sensitivity is independent of Q_p. Furthermore, it is much lower than the optimum sensitivity achieved in realizations using positive gain amplifiers or negative immittance converters [1-4] where the sensitivity is proportional to the Q-factor. However, this reduction in sensitivity is obtained at the expense of an increased number of active elements.

2.3.2 An Interesting Feature of the Realization

Consider the realization of the all pole or low-pass transfer function

$$\frac{V_2}{V_1} = T(s) = b_o / \sum_{i=o}^{n} b_i s^i \quad (2.16)$$

TABLE 2.1

SENSITIVITY TO ELEMENT VARIATIONS

e	$S_e^{Q_p}$	$S_e^{\omega_p}$
α_1	-1	0
β_1	$-\frac{1}{2}$	$-\frac{1}{2}$
β_2	$\frac{1}{2}$	$-\frac{1}{2}$
G_{po}	$G_{po}/2(G_{po}+G_{qo})$	$G_{po}/2(G_{po}+G_{qo})$
G_{qo}	$G_{qo}/2(G_{po}+G_{po})$	$G_{qo}/2(G_{po}+G_{qo})$
G_{p_1}	$-G_{p_1}/(G_{p_1}+G_{q_1})$	0
G_{q_1}	$-G_{q_1}/(G_{p_1}+G_{q_1})$	0
G_{p_2}	$G_{p_2}/2(G_{p_2}+G_{q_2})$	$-G_{p_2}/2(G_{p_2}+G_{q_2})$
G_{q_2}	$G_{q_2}/2(G_{p_2}+G_{q_2})$	$-G_{q_2}/2(G_{p_2}+G_{q_2})$

From (2.3), we have $G_{pm} = o$ for $m \neq o$ and $G_{qo} = o$; also the unity gain inverting amplifier is then not needed in Fig. 2.2.

If G_{po} is now connected to ground and V_1 inserted in series with $G_{q\ell}$ ($\ell = 1,2, \ldots, (n-1)$ or n), analysis shows that the numerator of the transfer function becomes $b_\ell s^\ell$ while the denominator remains the same. Thus, for the low-pass filter (2.16), the corresponding high pass filter is obtained simply by grounding G_{po} and inserting the input V_1 in series with G_{qn}. Also, as seen, a band pass response can be obtained directly from the corresponding low-pass response merely by connecting V_1 in series with $G_{q\ell}$ ($\ell < n$) and grounding G_{po}.

Example

The design of a second-order Butterworth low-pass filter with unity d.c. gain and a cut-off frequency $f_p = 1.59$ kHz ($\omega_p = 10^4$ rad./sec) is given in Fig. (2.3a). The corresponding high-pass filter with the same pole pair and unity multiplier constant at $f >> f_p$ is obtained from the low-pass filter by grounding G_{po} and inserting V_1 in series with G_{q_2}, as shown in Fig. (2.3b).

Also, to obtain the corresponding band-pass filter with the same pole pair and unity gain at $f = f_p$, then the realization in Fig. (2.3a) should be modified by grounding

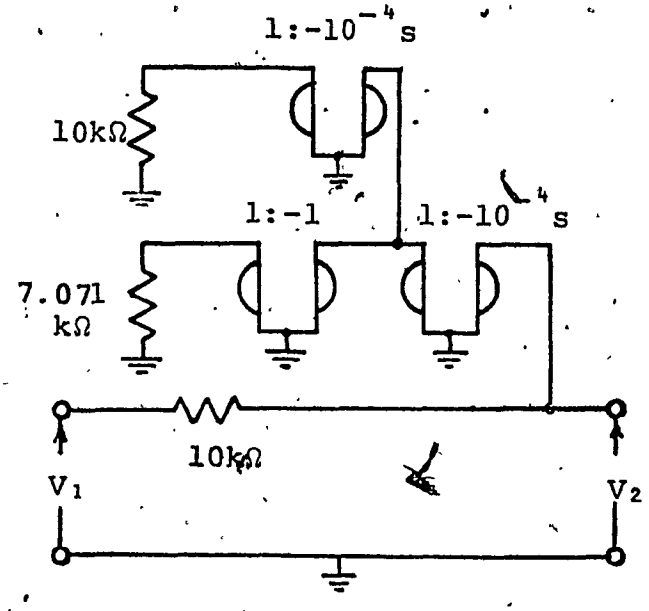

$$T(s) = \frac{1}{1+1.4142s+s^2}$$

(a)

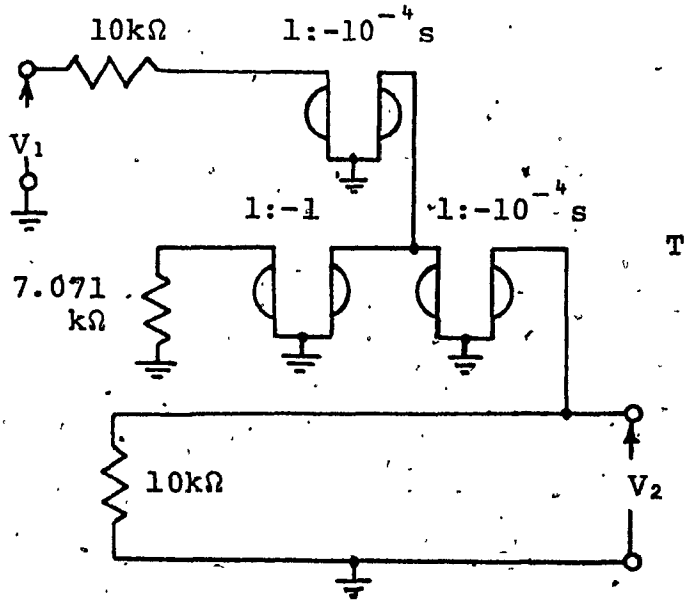

$$T(s) = \frac{s^2}{1+1.4142s+s^2}$$

(b)

FIG. 2.3 (a) REALIZATION OF A SECOND ORDER BUTTERWORTH LOW-PASS FILTER

(b) THE CORRESPONDING HIGH-PASS FILTER

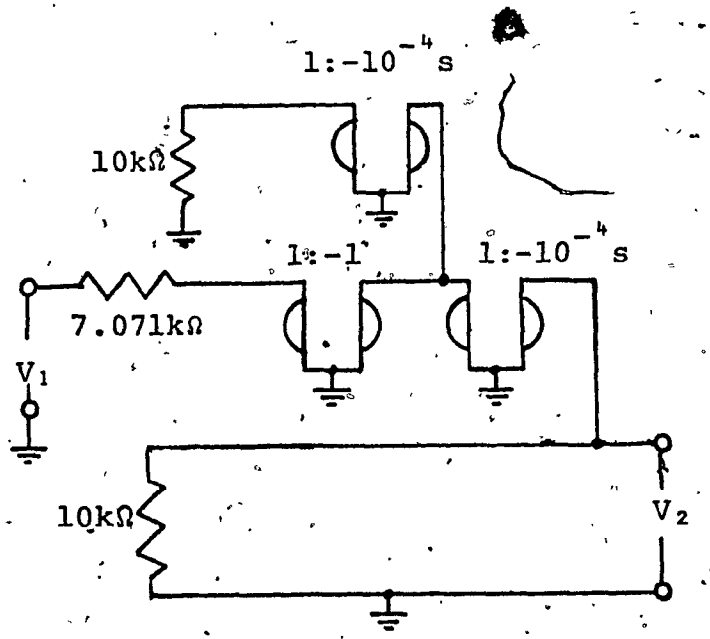

$$T(s) = \frac{1.4142s}{1+1.4142s+s^2}$$

(c)

FIG. 2.3a (c) THE CORRESPONDING BAND-PASS FILTER

G_{po} and inserting V_1 in series with G_{q_1}, as shown in Fig. (2.3c).

2.4 STRUCTURE B - THE RC-ACTIVE NETWORK CONFIGURATION USING CGICB

An RC-active configuration using CGICB is presented which is shown to include, as special cases, the low sensitivity realizations reported earlier by Antoniou [26], and Cobb and Su [39].

Consider the two port of Fig. (2.4). Analysis shows that

$$-Y_{21} = \pm Y_{po} \pm h_1 Y_{p_1} \pm h_1 h_2 Y_{p_2} \pm \ldots$$

$$= \pm Y_{po} + \sum_i \prod_{j=1}^{i} h_j (\pm Y_{pi}) \qquad (2.17a)$$

and

$$y_{22} \triangleq (Y_{po}+Y_{qo}) + h_1(Y_{p_1}+Y_{q_1}) + h_1 h_2 (Y_{p_2}+Y_{q_2}) + \ldots$$

$$= (Y_{po}+Y_{qo}) + \sum_i \prod_{j=1}^{i} h_j (Y_{pi}+Y_{qi}) \qquad (2.17b)$$

It is seen that by selecting appropriately Y's and h's in Structure B, any stable transfer function can be realized.

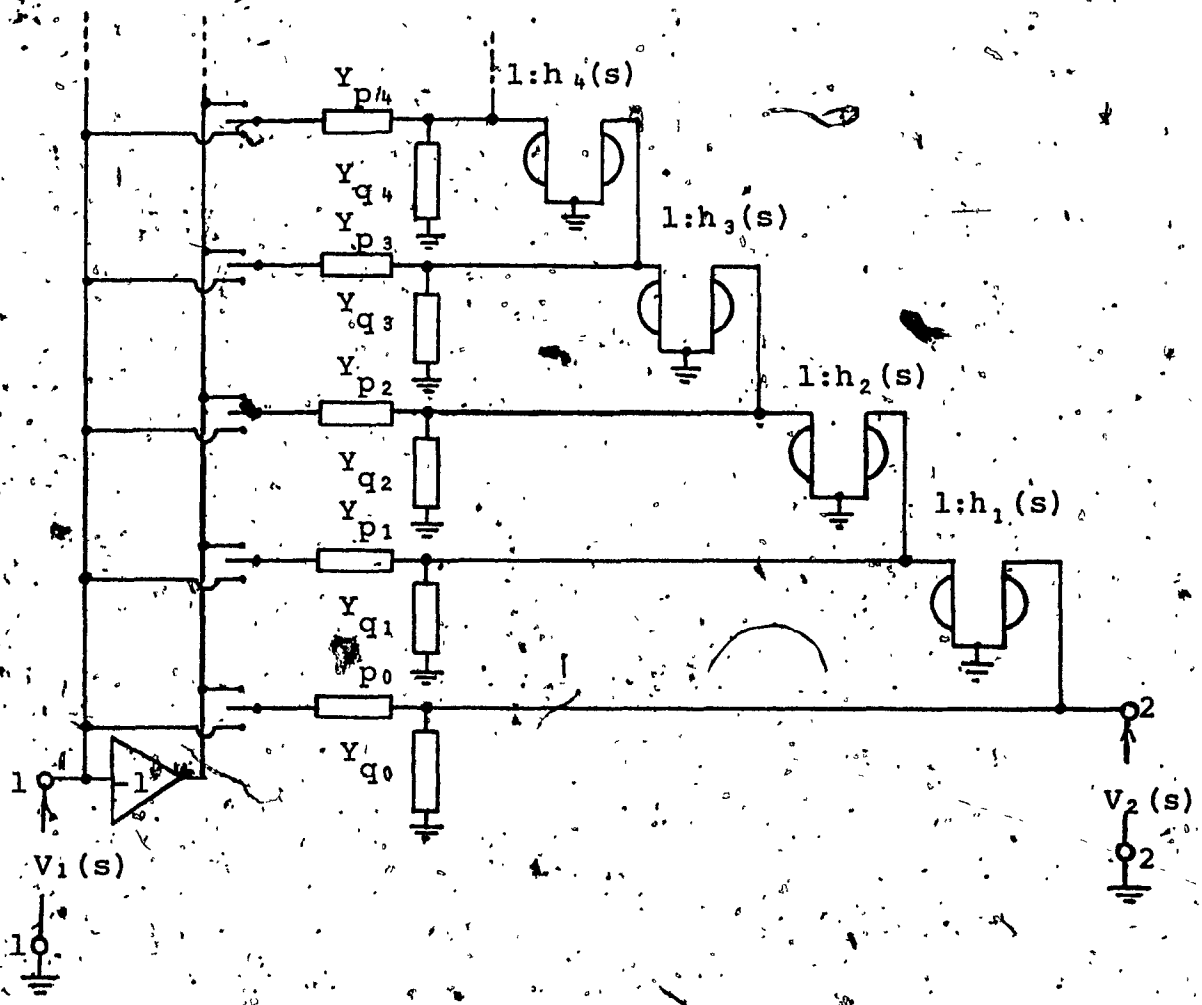

FIG. 2.4 STRUCTURE B - THE RC-ACTIVE CONFIGURATION USING CGICB

2.4.1 Antoniou's Realization

Set

$$Y_1 = G_j,\ Y_2 = sC_{2j},\ Y_3 = sC_{3j},\ Y_4 = G_{4j} \tag{2.18}$$

in (1.6). We then have

$$h_j(s) = K_j s^2 \tag{2.19}$$

where

$$K_j > 0$$

Also, choose in Structure B

$$Y_{pi} = G_{pi} + sC_{pi},\ Y_{qi} = G_{qi} + sC_{qi} \tag{2.20}$$

We then have, using (2.17), for even n

$$\frac{V_2}{V_1} = \frac{\pm G_{pr}\, s^{n} \prod_{m=o}^{n/2} K_m + \sum_{m=o}^{(n-2)/2} (\pm G_{pm} \pm sG_m)\, s^{2m} \prod_{j=o}^{m} K_j}{(G_{pr}+G_{qr})\, s^{n} \prod_{m=o}^{n/2} K_m + \sum_{m=o}^{(n-2)/2} \{(G_{pm}+G_{qm}) + (C_{pm}+C_{qm})s\}\, s^{2m} \prod_{j=o}^{m} K_j} \tag{2.21}$$

where $r = n/2$ and $K_o = 1$.

And for odd n

$$\frac{V_2}{V_1} = \frac{\sum_{m=o}^{(n-1)/2} (\pm G_{pm} \pm sC_{pm})\, s^{2m} \prod_{j=o}^{m} K_j}{\sum_{m=o}^{(n-1)/2} \{(G_{pm}+G_{qm}) + (C_{pm}+C_{qm})s\}\, s^{2m} \prod_{j=o}^{m} K_j} \tag{2.22}$$

where

$$K_o = 1$$

A comparison of (2.1), (2.21) and (2.22) shows that, for even i

$$a_i = \pm G_{pm} \prod_{j=o}^{m} K_j, \quad b_i = (G_{pm}+G_{qm}) \prod_{j=o}^{m} K_j \qquad (2.23)$$

where

$$m = i/2$$

and for odd i

$$a_i = \pm C_{pm} \prod_{j=o}^{m} K_j, \quad b_i = (C_{pm}+C_{qm}) \prod_{j=o}^{m} K_j \qquad (2.24)$$

where

$$m = (i-1)/2$$

From (2.10), (2.23) and (2.24), we have

$$|S_e^{a_i}| \leq 1 \quad , \quad |S_e^{b_i}| \leq 1 \qquad (2.25)$$

where e represents any one of the elements : G_{pm}, G_{qm}, C_{pm}, G_{qm}, $K_1, K_2, \ldots, K_m$.

By considering now the second order case, then from (2.12) and (2.21), it can be shown that

$$|S_e^{Q_p}| \leq 1 \quad , \quad |S_e^{\omega_p}| \leq 1 \qquad (2.26)$$

2.4.2 Cobb and Su's Realization

Choosing Y_2 or $Y_3 = sC_j$ and the rest of $Y_1 - Y_4$ as conductances in (1.6) yields $h_j(s) = K_j s$, where $K_j > 0$. Also choose

$$Y_{pi} = G_{pi} \quad , \quad Y_{qi} = G_{qi} \tag{2.27}$$

Analysis of Structure B then yields

$$\frac{V_2}{V_1} = \frac{\pm G_{po} \pm \sum_{m=1}^{n} [G_{pm} s^m \prod_{j=1}^{m} K_j]}{(G_{po}+G_{qo}) + \sum_{m=1}^{m} [(G_{pm}+G_{qm}) s^m \prod_{j=1}^{m} K_j]} \tag{2.28}$$

A comparison of (2.1) and (2.28) shows that

$$a_i = \pm G_{pi} \prod_{j=1}^{i} K_j \quad , \quad b_i = (G_{pi}+G_{qi}) \prod_{j=1}^{i} K_j \tag{2.29}$$

where

$$K_o = 1 \quad , \quad 0 \leq i \leq n$$

From (2.10) and (2.29), we have

$$|S_e^{a_i}| \leq 1 \quad , \quad |S_e^{b_i}| \leq 1 \tag{2.30}$$

where e represents any of the elements

$$G_{pi}, G_{qi} \text{ and } K_1, K_2, \ldots, K_i$$

Again considering the second-order case, then from (2.12) and (2.28), it can be shown that

$$|S_e^{Q_p}| \leq 1 \quad , \quad |S_e^{\omega_p}| \leq \tfrac{1}{2} \tag{2.31}$$

2.5 CONCLUSIONS

Two general configurations, Structure A and Structure B are given for the direct synthesis of a transfer function. It is shown that Structure A yields a minimal capacitor realization while Structure B contains, as special cases that due to Antoniou and the one due to Cobb and Su. A careful study of all the three techniques reveals that they possess the following attractive features:

1) No factorization of the transfer function is necessary.

2) The synthesis is simple, since the elements are directly related to the coefficients of the transfer function.

3) The numerator and denominator coefficients can be independently controlled by distinct elements and hence the alignment of the designed network is expected to be relatively simple.

4) Resulting realizations have very low sensitivity to element variations.

While Antoniou's technique requires the lowest number of OA's amongst the three techniques, the other two techniques realize a given T(s) with the minimum possible number of capacitors. The minimal capacitor realization described in this thesis while requiring 50% more OA's than in the one due to Antoniou, needs however, 50% less OA's than in Cobb and Su's technique.

At the present time, OA's are readily integrable. Capacitors, however, remain the most difficult of elements to integrate. The cost of OA's is also continually decreasing. On the other hand, in many applications, where chip capacitors may be needed, these capacitors may be costlier than OA's. Thus, situations may arise where a reduction in the number of capacitors may be desirable even at the cost of an increased number of OA's.

As has been pointed out in Chapter 1, integrated technology offers several attractive advantages to the filter manufacturers. One major advantage is the reduction of cost, if the filter is manufactured in large quantities. Unfortunately, this may not be possible in many applications where filters may be required to meet specific signal transmission characteristics. This problem can be avoided in the cascade synthesis approach where a small number of universal second-order sections can be designed for a given frequency range of interest. By using a combination of two or more of these sections, the desired transmission character-

istics may be obtained. The cascade technique is also attractive for post design adjustments as each section is isolated from the others. Therefore, in the following two chapters, second-order realizations with desirable properties will be sought from Structures A and B.

CHAPTER III

FIRST CASCADE REALIZATION

CHAPTER III

FIRST CASCADE REALIZATION

3.1 INTRODUCTION

The purpose of this Chapter is to develop a design procedure for realizing low sensitivity, very high Q second order sections. The design is derived from the direct synthesis procedure of the new minimal capacitor realization described in the previous Chapter. It is first shown that the second-order sections obtained from the minimal capacitor realization can attain low-frequency unstable modes of operation during activation (just after switching on the power supply). Using the theory of singular elements [31], two alternative circuits are then obtained which are free from low-frequency unstable modes of operation. These two circuits retain all the other attractive features of the original realization. One of these circuits, referred to as Biquad A in this thesis, is studied in more detail in this Chapter. It is shown that Biquad A has the following features which make it desirable for high Q-factor realization:

i) Low sensitivity to passive element variations.

ii) Low Q_p sensitivity to d.c. gain variations of the OA's.

iii) Zero ω_p sensitivity to d.c. gain variations of the OA's.

iv) Low dependence of Q_p and ω_p on the finite bandwidth of the OA's.

v) Only three OA's per section are needed. Since the output can always be located at one of the OA output terminals, direct cascading of second order blocks is possible without isolating amplifiers.

vi) There is no spread in the values of the capacitors while the spread* in the values of the resistors is at most, $2\ Q_p^{\frac{1}{2}}$.

vii) The filters use the minimum number of capacitors.

By using combinations of the various sections proposed, most of the practical filter specifications such as Butterworth, Chebychev, Bessel, elliptic, etc., can be realized.

3.2 Stability Properties of the Minimal Capacitor Realization

The realization of the second-order transfer function

---

* The expression "element spread" is used in this thesis to mean the ratio of the maximum value to the minimum value of an element in the circuit.

$$T(s) = \frac{V_o}{V_i} = \frac{N(s)}{D(s)} = \frac{a_2 s^2 + a_1 s + a_0}{b_2 s^2 + b_1 s + b_0} \qquad (3.1)$$

can be obtained readily from Fig. 2.2 and is shown in Fig. 3.1. The unity gain sign changing amplifier is omitted

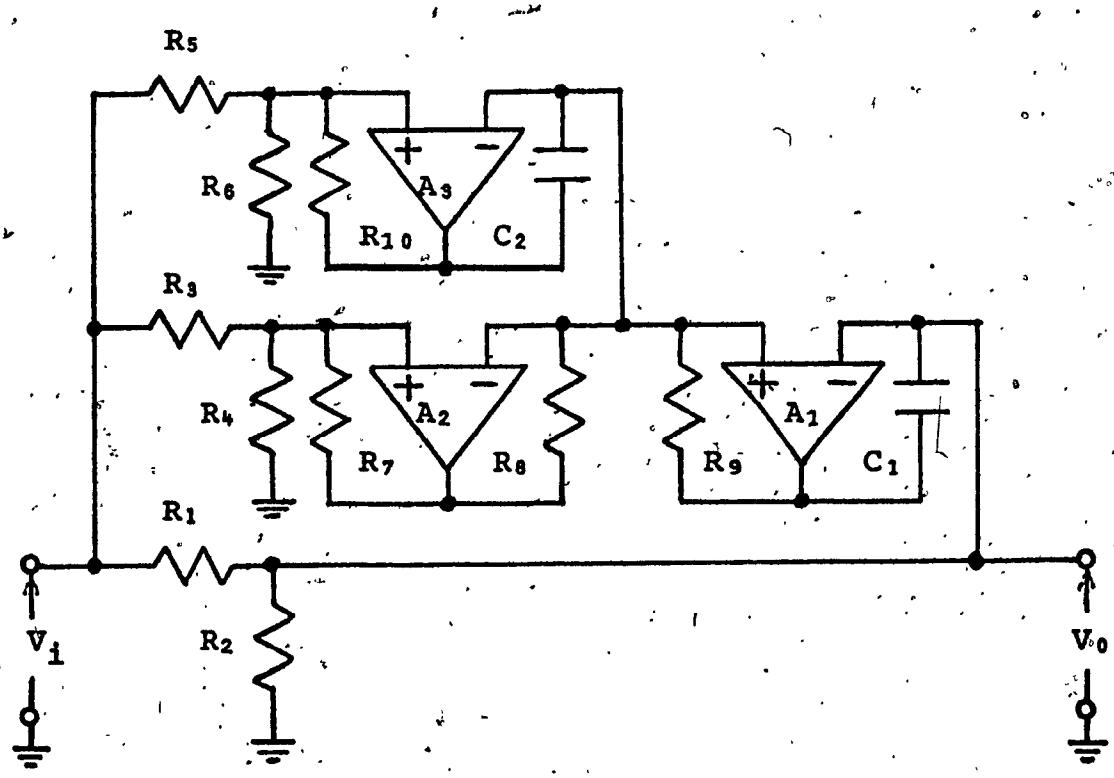

FIG. 3.1 CIRCUIT I - SECOND ORDER REALIZATION OBTAINED FROM SECTION 2.3

as it has no bearing on the stability of the circuit. In the rest of the discussion, this circuit will be referred to as Circuit I. Assuming ideal OA's, the characteristic polynomial, namely the denominator $D_I(s)$ of the voltage transfer function of Circuit I is given by

$$D_I(s) = (G_5+G_6)s^2 + \{(G_3+G_4)G_8G_{10}/(G_7C_2)\}s + (G_1+G_2)G_9G_{10}/C_1C_2 \quad (3.2)$$

For finite differential gains A_1, A_2 and A_3 the coefficients b_i of $D_I(s)$ can be shown to be

$$\left.\begin{aligned} b_0 &= K_1K_6(K_7-G_9)/C_1C_2 \\ b_1 &= K_1(K_2+K_3/A_3)/(C_1A_1)+K_6\{G_8+K_7/A_1+(K_4G_8)/K_5\}/C_2 \\ b_2 &= (1+1/A_1)(K_2+K_3/A_3) \end{aligned}\right\} \quad (3.3)$$

where

$$\left.\begin{aligned} K_1 &= G_1 + G_2,\ K_2 = G_5 + G_6,\ K_3 = G_5 + G_6 + G_{10} \\ K_4 &= G_3 + G_4 + G_7,\ K_5 = K_4/A_2 - G_7 \\ K_6 &= K_3/A_3 - G_{10},\ K_7 = (G_8 + G_9 + K_4G_8/K_5)/A_1 \end{aligned}\right\} \quad (3.4)$$

For infinite amplifier gains, b_i's as given by (3.3), reduce to those in (3.2).

In practice, the amplifier gains can assume values in the range

$$0 \leq (|A_1| \text{ or } |A_2| \text{ or } |A_3|) \leq |A_{max}|$$

where $|A_{max}| < \infty$, since these rise from zero just after activation (switching on the direct supply voltage). It will now be shown that attainable sets of amplifier gains exist which will make circuit I unstable.

The differential open loop gain of a frequency compensated OA is given by (1.2). Instability in the high frequency region of operation can always be controlled by proper compensation of the OA's [34]. Thus, the low frequency region, namely, $|s| << \omega_c$ of the s plane is of interest. Consequently, the gains $A_i (i = 1,2,3)$ can be assumed to be real in (3.3). Using this equation, the natural frequencies of Circuit I can be calculated for a series of amplifier gains in the range

$$0 \leq (A_1 \text{ or } A_2 \text{ or } A_3) \leq A_{max}$$

where $A_3 = \alpha A_2 = \beta A_1$ (α, β are arbitrary positive constants since the A_i's are uncorrelated while rising).

Eqn. (3.3) shows that some of the b_i's can become negative due to the presence of the difference terms. Thus, $D_I(s)$ may have roots in the right half of the s-plane when the amplifier gains are rising. As an example, suppose we are required to realize the following band-pass function

$$T(s) = s/(s^2 + s + 1) \qquad (3.5)$$

The element values may be chosen as follows

$G_1 = G_4 = G_5 = 0, G_2 = G_3 = G_6 = G_7 = G_8 = G_9 = G_{10} = G_{11} = 1$ mho

$C_1 = C_2 = 1$ Farad

Assuming now that the OA gains are related while rising from zero just after switching on the power supply as $A_1 = 2A_2 = 2A_3$, the root locus of $D_I(s)$ may be obtained and is shown in Fig. 3.2. The root locus shows that Circuit I can attain a zero frequency (d.c.) unstable mode.

We can associate eight possible combinations of amplifier polarities with Circuit I. It can be shown, by examining $D_I(s)$ for each of these cases, that Circuit I is potentially unstable.

An unstable mode may be attained in practice while the amplifier gains are rising from zero just after activation. The amplitude of oscillation during the unstable mode can rise to a sufficient level to saturate the amplifiers. Then the effective amplifier gains will cease to rise owing to the nonlinearity of the dynamic characteristics of the amplifiers, and consequently the circuit may lock in an unstable mode. Such behaviour has been observed in practice for Circuit I.

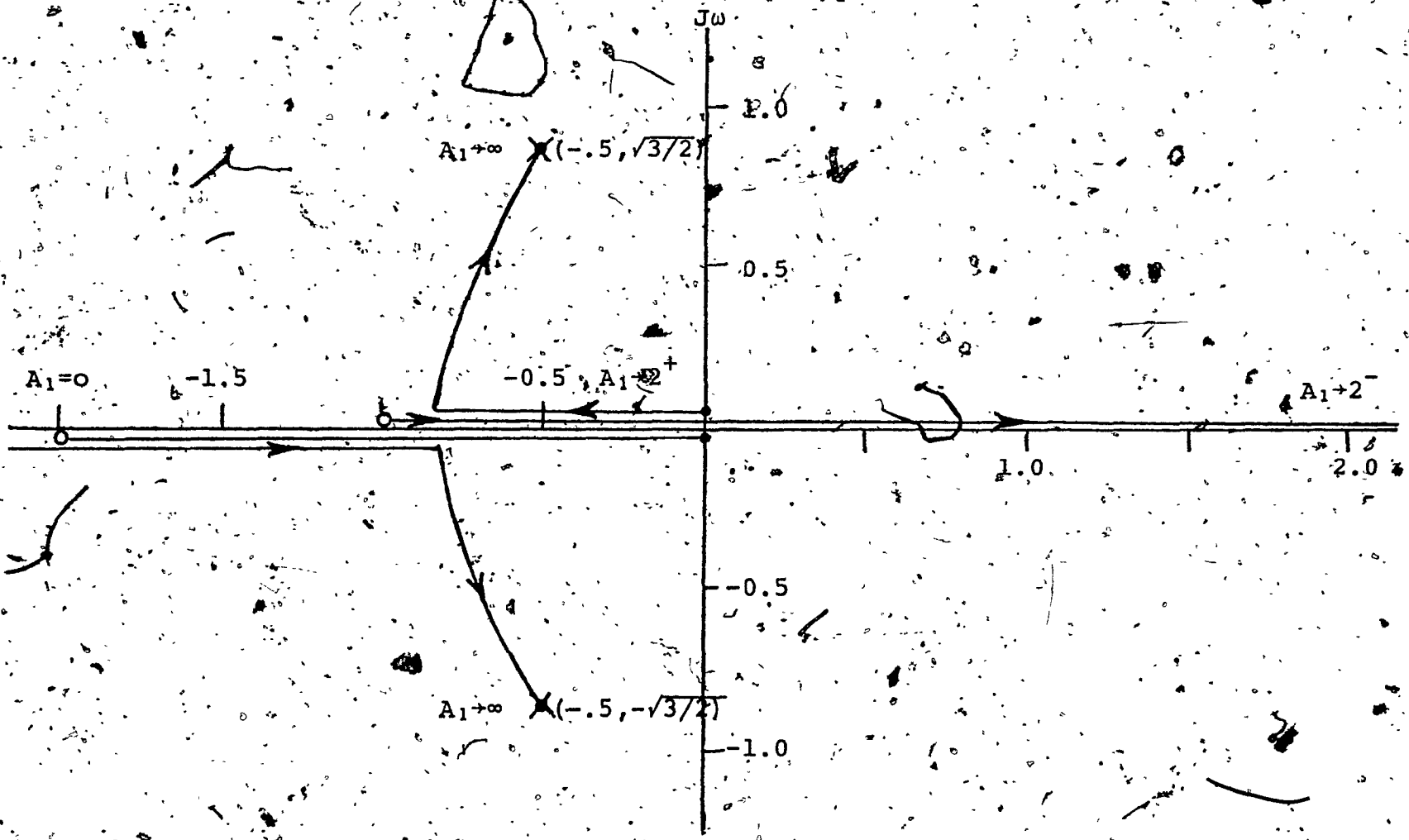

FIG. 3.2 NATURAL FREQUENCY LOCUS OF CIRCUIT I

3.3 NEW STRUCTURES

The singular elements, the nullator and the norator, were described by Carlin and Youla [40]. The nullator, shown in Fig. 3.3a, is a one-port which will neither

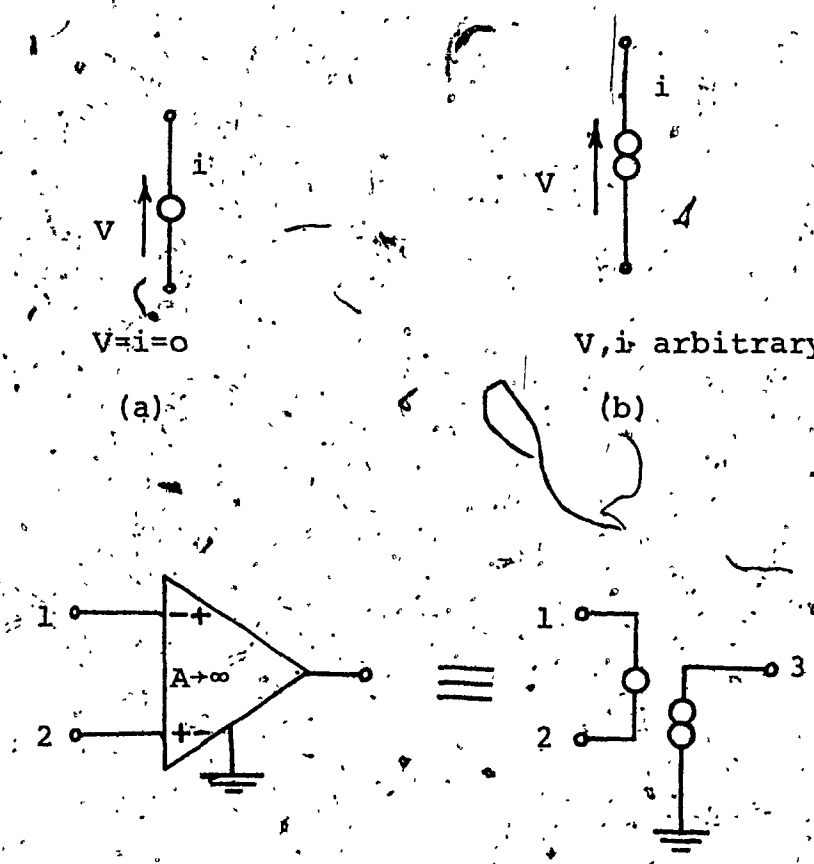

FIG. 3.3 SINGULAR ELEMENTS

sustain a voltage across nor pass a current through it (i.e. V = I = 0), while the norator, shown in Fig. 3.3b, is a one-port which will support an arbitrary voltage across and pass an arbitrary current through it. A two-port consisting of a nullator as port one, and a norator as port two, has been defined as a nullor [41]. Martinelli [42] has shown that an ideal transistor is equivalent to a nullor. Butler [43] and Davies [44] have also demonstrated, without a general proof, that an infinite gain voltage-controlled voltage source (such as an ideal OA) is also equivalent to a nullor, Fig. 3.3c. A proof of this equivalence has been given by Antoniou [31]. The nullor representation of an OA is shown in Fig. 3.3d.

Assuming the OA's in Circuit I to be ideal, they can be replaced by nullors, and a nullor equivalent network results. The nullors are then separated into nullators and norators to yield a nullator-norator equivalent network. The nullator-norator equivalent network contains three nullators and three norators. This yields 3! nullor equivalent networks, since nullators and norators can be paired into nullors in an arbitrary manner. Thus, by using the theory of nullator-norator pairing, five new circuits II, III, IV, V and VI may be derived from Circuit I. Figures 3.4 and 3.5 show Circuits II and V, respectively. Topologies for III and IV are the same as that of II, while the topology of VI is the same as that of V. The

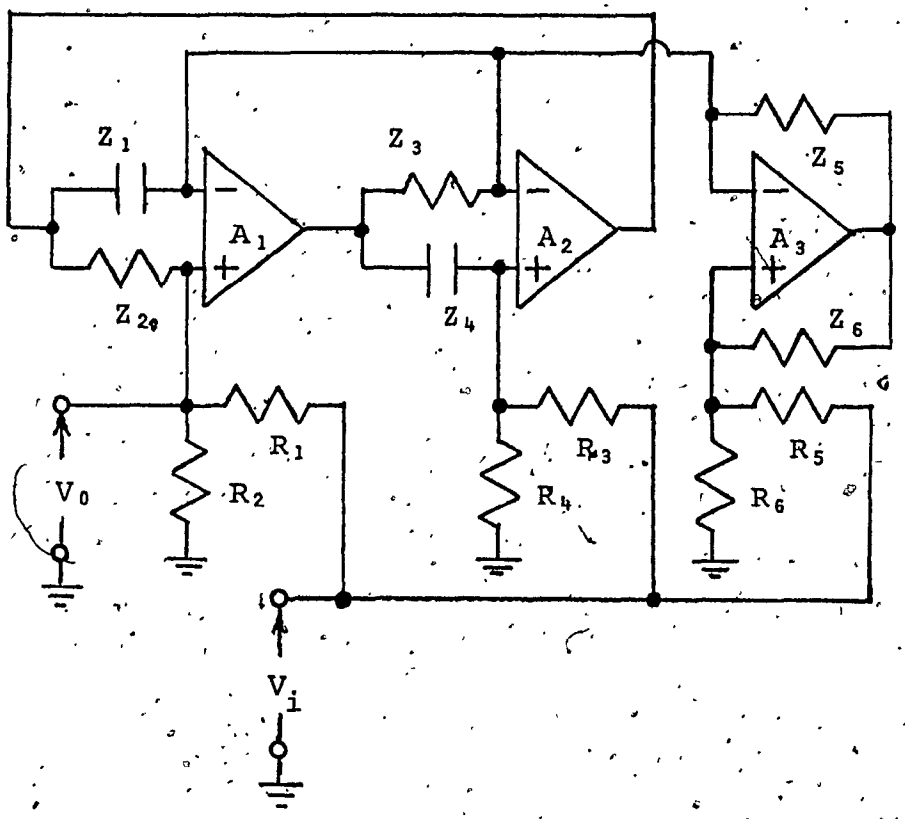

FIG. 3.4 CIRCUIT II OBTAINED BY NULLATOR-NORATOR PAIRING

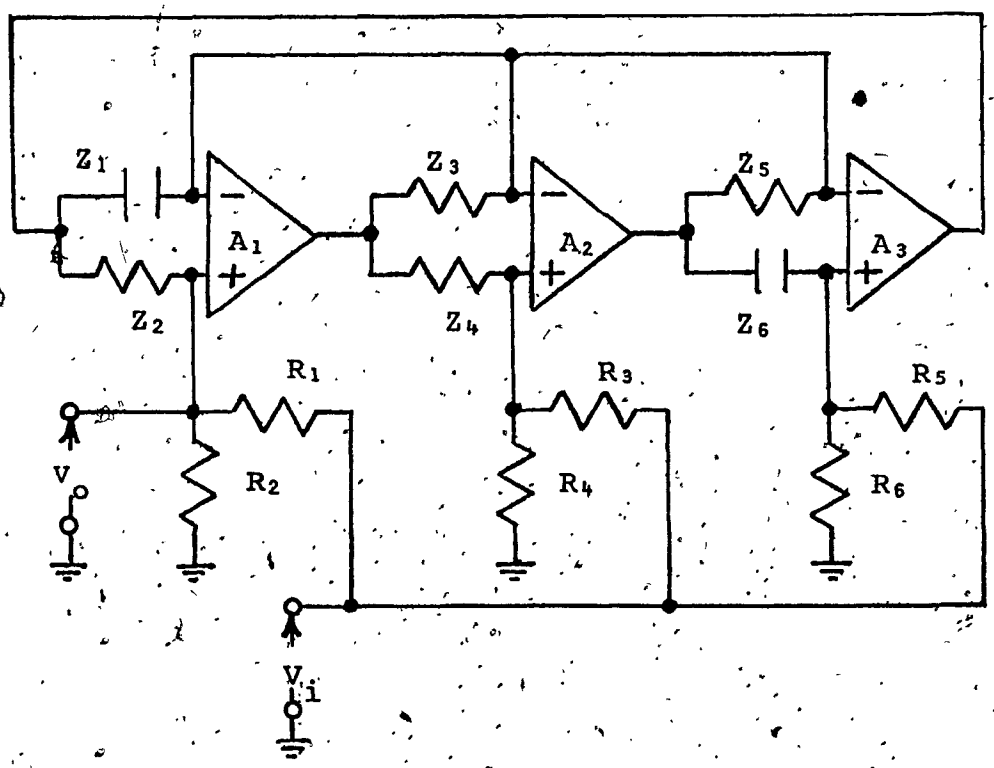

FIG. 3.5 CIRCUIT V OBTAINED BY NULLATOR-NORATOR PAIRING

elements R_1 to R_6 are the same in all the five circuits while the nature of the remaining elements Z_1 to Z_6 for Circuits III, IV and VI, are given in Table 3.1.

The Circuits II, III and IV have the same topology. Thus, for the indicated polarities of the amplifiers, the characteristic polynomials $D_{II,III,IV}$ for these circuits with appropriate Z_i's for Circuits II, III and IV are given by:

$$\begin{aligned} D_{II,III,IV} &= Y_2M_3 + (Y_2Y_3Y_6M_2)/(Y_4Y_5) + (Y_1Y_6M_1)/Y_5 \\ &+ [Y_2Q_4 - Y_2Y_3Q_2Q_3/Y_5 - Y_1Q_1Q_3/Y_5/A_3 \\ &+ (Y_1Y_6Q_1Q_2)/(A_1Y_5) + (Y_3Y_6Q_1Q_2)/(A_2Y_5) \\ &- (Y_1Q_1Q_2Q_3)/(A_1A_3Y_5) \\ &+ \{Y_6(Y_1+Y_3)Q_1Q_2\}/(A_1A_2Y_5) - (Y_3Q_1Q_2Q_3)/(A_2A_3Y_5) \\ &- (Q_1Q_2Q_4)/(A_1A_2A_3) \end{aligned} \qquad (3.6)$$

where

$$\begin{aligned} &M_1 = G_1 + G_2,\ M_2 = G_3 + G_4,\ M_3 = G_5 + G_6, \\ &Q_1 = M_1 + Y_2,\ Q_1 = 1 + M_2/Y_4,\ Q_3 = M_3 + Y_6, \\ &Q_4 = M_3(1+Y_1/Y_5+Y_3/Y_5) + Y_6(1+Y_1/Y_5) \end{aligned} \qquad (3.7)$$

As before, eight possible combinations of amplifier polarities can be associated with each of Circuits II, III and IV. By examining the characteristic polynomials $D_{II,III,IV}$, it can be shown that these circuits can attain low frequency unstable modes for all these cases.

TABLE 3.1

Z_1 TO Z_6 OF CIRCUITS III, IV AND VI

CIRCUIT	Z_1	Z_2	Z_3	Z_4	Z_5	Z_6
III	Capacitor	Resistor	Resistor	Resistor	Resistor	Capacitor
IV	Resistor	Capacitor	Resistor	Resistor	Capacitor	Resistor
VI	Capacitor	Resistor	Resistor	Capacitor	Resistor	Resistor

The Circuits V and VI have the same topology. Thus, for the indicated polarities of the amplifiers, the characteristic polynomials $D_{V,VI}(s)$ for both circuits (with appropriate Z_i's for Circuits V and VI) are given by

$$\begin{aligned} D_{V,VI}(s) = {} & Y_1Y_6\{(1+1/A_1)M_4M_5/(A_2A_3) + (M_4M_5)/A_3 + M_1\} \\ & + Y_2Y_3Y_6Z_4M_2 + \{M_4M_5/(A_2A_3)\}\{Y_1M_3(1+1/A_1) + Y_5Y_6/A_1\} \\ & + Y_6M_4M_5M_6/(A_1A_3) + Y_5Y_6M_5/A_1 + Y_3Y_6M_4M_7/A_2 \\ & + Y_5M_3M_4M_5/(A_1A_2A_3) + M_3M_7(Y_5+Y_3M_4/A_2) \\ & + M_3M_4M_5M_6/(A_1A_3) \end{aligned} \tag{3.8}$$

where

$$\begin{aligned} & M_1 = G_1 + G_2,\ M_2 = G_3 + G_4,\ M_3 = G_5 + G_6, \\ & M_4 = 1 + Z_4M_2,\ M_5 = M_1 + Y_2,\ M_6 = Y_5 + Y_3/A_2, \\ & M_7 = M_5/A_1 + Y_2 \end{aligned} \tag{3.9}$$

All the terms in (3.8) are positive. This guarantees that the coefficients of $D_{V,VI}(s)$ remain positive during activation for all the attainable values of the amplifier gains. Hence, the necessary and sufficient conditions for the stability of Circuits V and VI are satisfied.

The circuits of Fig. 3.5, is studied in more detail in the remaining part of this Chapter.

3.4 SYNTHESIS USING BIQUAD A

Consider the circuit of Fig. 3.5 redrawn in Fig. 3.6, where the output can now be taken to be either V_1 or V_2 or V_3. The configuration will be called Biquad A

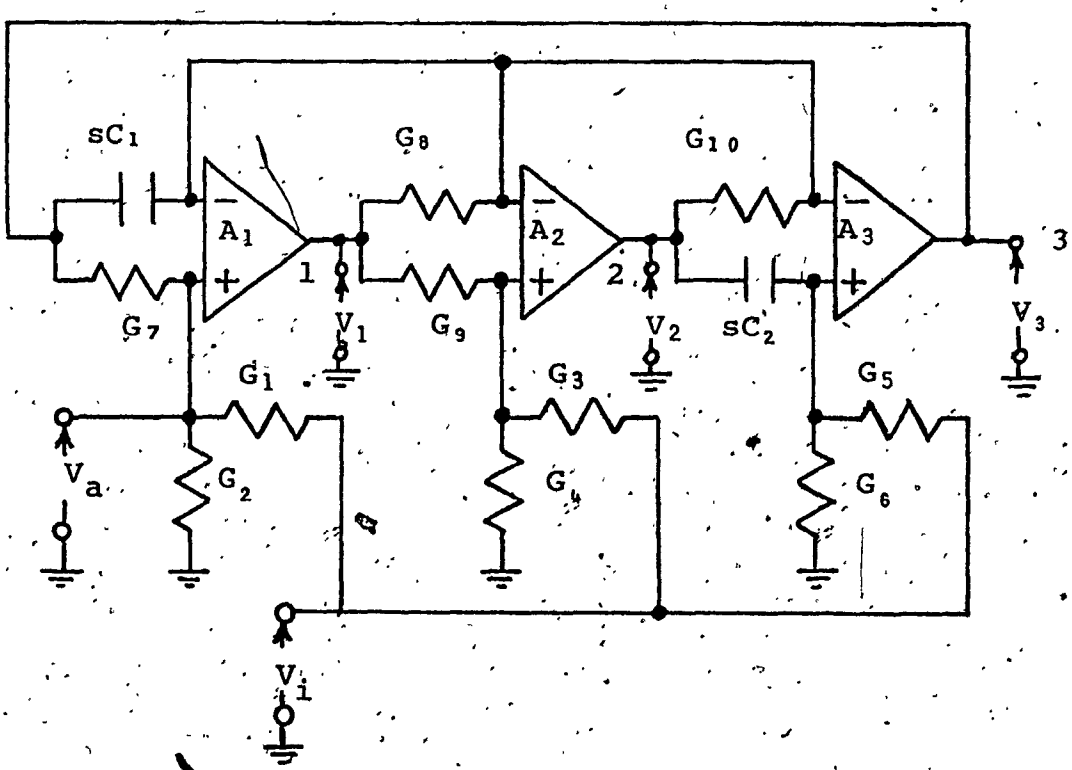

FIG. 3.6 BIQUAD A

and a synthesis procedure is now described which uses this configuration. The transfer functions between the input and output terminals 1,2,3 and a are readily obtained as

$$V_1/V_i = T_1 = \{s^2[G_1(1+R_9G_4) - R_9G_2G_3] + s\frac{G_3G_7G_8}{C_1G_9} + [(1+R_9G_4)G_5 - R_9G_3G_6]/(C_1C_2R_7R_{10})\}/D(s) \quad (3.10a)$$

$$V_2/V_i = T_2 = \{s^2G_1 + s[\frac{G_1G_6}{C_1} + \frac{G_3G_7G_8}{C_1G_9} - \frac{G_5G_6}{C_1}] + [\frac{G_3G_6}{C_1} - \frac{G_4G_5}{C_1}]G_7G_8/(C_1G_9) + G_5G_7G_{10}/(C_1C_2)\}/D(s) \quad (3.10b)$$

$$V_3/V_i = T_3 = \{s^2G_1 + s[(1+R_7G_2)G_3 - R_7G_1G_4]G_7G_8/(C_1G_9) + [(1+R_7G_2)G_5 - R_7G_1G_6]G_7G_{10}/(C_1C_2)\}/D(s) \quad (3.10c)$$

$$V_a/V_i = T_4 = [s^2G_1 + sG_3G_7G_8/(C_1G_9) + G_5G_7G_{10}/(C_1C_2)]/D(s) \quad (3.10d)$$

where

$$D(s) = s^2(G_1+G_2) + s(G_3+G_4)G_7G_8/(C_1G_9) + (G_5+G_6)G_7G_{10}/(C_1C_2) \quad (3.10e)$$

From (3.10a) - (3.10c), it is easily seen that second order transfer functions with any desirable zero locations can be realized by choosing the conductances G_1 to G_6 suitably.

Most frequently, filters are designed by using Butterworth, Chebychev, Bessel or elliptic approximations in which the transmission zeros are located at the origin, imaginary axis or at infinity. Consequently, the transfer function can be expressed as a product of second order transfer functions of the form given by (3.1), where $a_1 = a_2 = 0$, $a_0 = a_1 = 0$, $a_0 = a_2 = 0$ or $a_1 = 0$ for a low pass (LP), high pass (HP), band pass (BP), or a notch (N) section, respectively. The coefficients a_i's and b_i's of T(s) for these sections are all positive. These sections can be realized by choosing the conductances G_1 to G_5 in (3.10). By comparing (3.1) and (3.10), Circuits 1 to 4 in Table 3.2, can be obtained.

All-pass transfer functions are often needed for delay equalization and these can be realized by using second order transfer functions of the type given by (3.1) where $a_2 = b_2$, $a_1 = -b_1$ and $a_0 = b_0$. Second order sections of this class can be obtained from Circuit 5 of Table 3.2.

Figure 3.6 and Table 3.2 show that the response is always obtained from the output of an OA. Owing to the low output resistance of the amplifier, any number of sections can be cascaded without isolation amplifiers.

TABLE 3.2

ELEMENT IDENTIFICATION FOR REALIZING THE MOST COMMONLY USED TRANSFER FUNCTIONS

CIRCUIT NUMBER	G_1	G_2	G_3	G_4	G_5	G_6	TRANSFER FUNCTION	REMARKS
1	0	*	0			*	$T_3 = \dfrac{(1+G_2/G_7)G_5G_7G_{10}/(C_1C_2)}{s^2G_2+sG_4G_7G_8/(C_1G_9)+(G_5+G_6)G_7G_{10}/(C_1C_2)}$	LP
2		*	0		0		$T_1 = \dfrac{s^2G_1(1+G_4/G_9)}{s^2(G_1+G_2)+sG_4G_7G_8/(C_1G_9)+G_6G_7G_{10}/(C_1C_2)}$	HP
3	0			*	0		$T_3 = \dfrac{s(1+G_2/G_7)G_5G_7G_8/(C_1G_9)}{s^2G_2+s(G_5+G_4)G_7G_8/(C_1G_9)+G_6G_7G_{10}/(C_1C_2)}$	BP
4		*	0			*	$T_1 = G_1(1+G_4/G_9)\dfrac{s^2+G_5G_7G_{10}/(C_1C_2G_1)}{s^2(G_1+G_2)+sG_4G_7G_8/(C_1G_9)+(G_5+G_6)G_7G_{10}/(C_1C_2)}$	N
5		*	0			0	$T_3 = \dfrac{s^2G_1-sG_1G_4G_8/(C_1G_9)+(1+G_2/G_7)G_5G_7G_{10}/(C_1C_2)}{s^2(G_1+G_2)+sG_4G_7G_8/(C_1G_9)+G_5G_7G_{10}/(C_1C_2)}$	non-minimum phase †

NOTES:

1) $Y_2-Y_5 = G_7-G_{10}$ always

2) $Y_1 = sC_1, Y_6 = sC_2$

3) * These elements can be set to zero.

4) † For all pass $G_2 = 0$, $G_7 = G_1$

3.4.1 Sensitivity Analysis

The pole Q-factor, Q_p, and the undamped frequency of oscillation, ω_p, are defined by (2.12).

For a notch section, the notch frequency is defined by

$$\omega_n = (a_0/a_2)^{\frac{1}{2}} \tag{3.11}$$

and the multiplier constant can be taken to be

$$H_N = a_2/b_2 \tag{3.12}$$

Similarly, for the LP, HP and BP sections

$$H_{LP} = a_0/b_0 \ , \ H_{HP} = a_2/b_2 \ , H_{BP} = a_1/b_1 \tag{3.13}$$

For an all-pass section, let

$$Q_Z = (a_0a_2)^{\frac{1}{2}}/a_1 , \omega_Z = (a_0/a_2)^{\frac{1}{2}}, \ H_{AP} = a_2/b_2 \tag{3.14}$$

The sensitivity of a quantity x with respect to variations in an element e is given by

$$S_e^x = (\partial x/\partial e)(e/x) \tag{3.15}$$

For ideal amplifiers, the use of (2.10), (3.11-3.15) and Table 3.2 leads to

$$0 \leq |S_e^x| \leq 1 \qquad (3.16)$$

where x represents any one of the quantities defined by (2.10) and (3.11-3.14) and e represents any capacitance or conductance. This shows that the sensitivities to passive element variations are independent of the selectivity.

For amplifiers with a finite open-loop gain A, the circuit of Fig. 3.6 gives

$$V_k/V_i = N_k(s)/D(s) \qquad (3.17)$$

where $k = 1,2,3,a$ and

$$\begin{aligned} D(s) = {} & s^2[1 + \{1/A_3+1/(A_2A_3)+1/(A_1A_2A_3)\}M_4M_5/(C_1C_2M_1)] \\ & + s[G_7G_8M_2/(C_1G_9M_1)+\{C_1M_3+C_1M_3/A_1+C_2G_{10}/A_1\}M_4M_5/C_1C_2M_1A_2A_3 \\ & + M_4M_5M_6/(C_1M_1A_1A_3)+G_{10}M_5/(C_1M_1A_1)+G_8M_4M_7/(C_1M_1A_2)] \\ & + M_3M_7(G_{10}+G_8M_4/A_2)/(C_1C_2M_1) \\ & + M_3M_4M_5M_6/(C_1C_2M_1A_1A_3)+G_{10}M_3M_4M_5/(C_1C_2M_1A_1A_2A_3) \end{aligned} \qquad (3.18)$$

where

$$M_1 = G_1 + G_2,\ M_2 = G_3 + G_4,\ M_3 = G_5 + G_6,\ M_4 = 1 + M_2/G_9,$$
$$M_5 = M_1 + G_7,\ M_6 = G_{10} + G_8/A_1,\ M_7 = G_7 + M_5/A_1$$

For real amplifier gains such that

$A_1 = A_2 = A_3 = A_0$ (3.18) gives

$$D(s) = s^2[1 + (1/A_0+1/A_0^2+1/A_0^3)\{1+1/X_1+1/X_2+1/(X_1X_2)\}]$$
$$+ s(\omega_p/Q_p)[1 + (1/A_0)\{1+X_1+X_1X_3+X_1X_2X_3\}$$
$$+ (1/A_0^2)(1+X_1+X_2+X_1X_2)(1+X_2+C_1X_4/C_2)(1+1/A_0)]$$
$$+ \omega_p^2[1 + (1/A_0)\{1+X_2+1/X_3+1/(X_1X_3)$$
$$+ (1/A_0^2)(1+1/X_3)(1+X_2+X_2/X_1+1/X_1)(1+1/A_0)] \quad (3.19)$$

where

$$X_1 = G_9/M_2,\ X_2 = M_1/G_7,\ X_3 = G_{10}/G_8,\ X_4 = M_3/G_8,$$
$$\omega_p = [(G_7G_{10}M_3)/(C_1C_2M_1)]^{\frac{1}{2}}$$
$$Q_p = [G_9/(G_8M_2)][(G_1G_7C_1M_1M_3)/(G_7C_2)]^{\frac{1}{2}} \quad (3.20)$$

For $A_0 >> 1$, (3.19) can be simplified further as

$$D(s) = s^2[1 + \{(1+1/X_1+1/X_2+1/(X_1X_2)\}/A_0]$$
$$+ s(\omega_p/Q_p)[1 + (1+X_1+X_1X_3+X_1X_2X_3)/A_0]$$
$$+ \omega_p^2[1 + \{1+X_2+1/X_3+1/(X_1X_3)\}/A_0] \quad (3.21)$$

From (3.20) and (3.21), the actually realized Q-factor, and ω_p can be obtained as

$$Q_{pa} = Q_p[1 + \{1+X_2+1/X_3+1/(X_1X_3)\}/A_0]^{\frac{1}{2}} \times$$
$$[1 + \{1+1/X_1+1/X_2+1/(X_1X_2)\}/A_0]^{\frac{1}{2}} /$$
$$[1 + (1+X_1+X_1X_3+X_1X_2X_3)/A_0] \qquad (3.22)$$

$$\omega_{pa} = \omega_p[1 + \{1+X_2+1/X_3+1/(X_1X_3)\}/A_0]^{\frac{1}{2}} /$$
$$[1 + \{1+1/X_1+1/X_2+1/(X_1X_2)\}/A_0]^{\frac{1}{2}} \qquad (3.23)$$

The sensitivities of Q_{pa} and ω_{pa} with respect to the amplification A_0 can be written as

$$S_{A_0}^{Q_{pa}} = 0.5/[1 + (1/A_0)\{1+X_2+1/X_3+1/(X_1X_3)\}]$$
$$+ 0.5/[1 + (1/A_0)\{1+1/X_1+1/X_2+1/(X_1X_2)\}]$$
$$- 1/[1 + (1/A_0)\{1+X_1+X_1X_2+X_1X_2X_3\}]$$
$$\doteq -[X_2+1/X_3+1/(X_1X_3)+1/X_1+1/X_2+1/(X_1X_2)$$
$$+ 2X_1+2X_1X_3+2X_1X_2X_3]/(2A_0) \qquad (3.24)$$

$$S_{A_0}^{\omega_{pa}} = 0.5/[1 + (1/A_0)\{1+X_2+1/X_3+1/(X_1X_3)\}]$$
$$- 0.5/[1 + (1/A_0)\{1+1/X_1+1/X_2+1/(X_1X_2)\}]$$
$$\doteq -[X_2+1/X_3+1/(X_1X_3)+1/X_1+1/X_2+1/(X_1X_2)]/(2A_0)$$
$$(3.25)$$

At this stage, two sets of design values can be assigned to X_1, X_2 and X_3 in (3.24) and (3.25). The corresponding values of $S_{A_0}^{Q_{pa}}$ and $S_{A_0}^{\omega_{pa}}$ obtained are of practical interest. The first design has zero Q_{pa} and ω_{pa} sensitivities with respect to the amplification A_0. However, the spread in element values,

particularly of the capacitors is rather large and is of the order of Q_p. Further, we shall see later that the useful frequency range of operation of this design is limited. The second design yields a zero $S_{A_0}^{\omega_{pa}}$ while maintaining a low $S_{A_0}^{Q_{pa}}$. Further, there is no spread in capacitor values while the spread in resistor values is at most $2Q_p^{\frac{1}{2}}$. Thus, this design is particularly attractive for high Q realization†.

3.4.2 Design I - Zero $S_{A_0}^{Q_{pa}}$ and $S_{A_0}^{\omega_{pa}}$ design

From (3.24) and (3.25), $S_{A_0}^{Q_{pa}} = S_{A_0}^{\omega_{pa}} = 0$ if

$$X_2+1/X_3+1/(X_1X_3) = 1/X_1+1/X_2+1/(X_1X_2) = X_1(1+X_3+X_2X_3) \quad (3.26)$$

---

† If BW is the bandwidth of a bandpass filter and $\Delta\omega_p$ is the deviation in ω_p due to deviation in A_0, then it is easily shown that

$$\frac{\Delta\omega_p}{BW} = Q_p S_{A_0}^{\omega_{pa}} \frac{\Delta A_0}{A_0}.$$

Thus, for high Q realizations $S_{A_0}^{\omega_{pa}}$ should be as small as possible.

One possible choice of X_1, X_2 and X_3 which satisfies (3.26) is given by

$$X_1 = X_2 = X_3 = 1 \qquad (3.27)$$

Using (3.27), (3.20) becomes

$$Q_p^2 = (C_1M_3)/(C_2G_8), \quad \omega_p^2 = M_3G_8/(C_1C_2) \qquad (3.28)$$

Let

$$C_1/C_2 = Q_p/m \qquad (3.29a)$$

where $m \geq 1$

Using (3.28) and (3.29a) yields

$$X_4 = M_3/G_8 = mQ_p \qquad (3.29b)$$

Eqns. (3.27) to (3.29) and (3.29b) constitute the design equations. It is seen that the spread in capacitor values is Q_p/m, while that in resistor values is mQ_p. Thus, to keep the spread in resistor values reasonable, of the order of Q_p, the spread in the capacitor values that has to be accepted must be of the order of Q_p. For zero spread in capacitor values, the spread in resistor values is of the order of Q_p^2, which may be prohibitive in many applications.

3.4.3 Design II - Low Spread, Low $S_{A_0}^{Q_{pa}}$ and Zero $S_{A_0}^{\omega_{pa}}$ Design

Let

$$X_1 = Q_p^{\frac{1}{2}},\ X_2 = 1, X_3 = Q_p^{\frac{1}{2}}/\alpha,\ C_1 = C_2 \qquad (3.30a)$$

where α is determined later.

Using (3.20) and (3.30a) gives

$$X_4 = \alpha Q_p^{\frac{1}{2}} \qquad (3.30b)$$

Substituting from (3.30) in (3.24) and (3.25) yields

$$S_{A_0}^{Q_{pa}} = -[2+Q_p^{-\frac{1}{2}}(2+\alpha)+\alpha Q_p - 2Q_p^{\frac{1}{2}} - 4Q_p/\alpha]/(2A_0) \doteq 2Q_p/(\alpha A_0) \qquad (3.31)$$

and

$$S_{A_0}^{\omega_{pa}} = [\alpha - 2 + \alpha Q_p^{-\frac{1}{2}}]/(2Q_p^{\frac{1}{2}}A_0) \qquad (3.32)$$

Choosing

$$\alpha = 2Q_p^{\frac{1}{2}}/(1+Q_p^{\frac{1}{2}}) \qquad (3.33)$$

Hence

$$S_{A_0}^{Q_{pa}} \doteq Q_p/A_0 \quad \text{for} \quad Q_p \gg 1$$

and

$$S_{A_0}^{\omega_{pa}} = 0 \qquad (3.34)$$

The design equations are (3.30) and (3.33).

The spread in capacitor values is unity and that in resistors is approximately $2Q_p^{\frac{1}{2}}$.

3.4.4 The Influence of the Amplifier Pole on Biquad A Response

The finite bandwidth of active devices tends to impose limitations on the frequency response of active networks. Moreover, it may introduce instability problems. The effect of the amplifier pole on the stability, Q-factor and natural frequency of oscillation will now be studied.

Assuming equal amplifier gains and substituting from (1.2) in (3.18), D(s) can be written as

$$D(s) = a_5 s^5 + a_4 s^4 + a_3 s^3 + a_2 s^2 + a_1 s + a_0 \qquad (3.35a)$$

where

$$a_5 = d_1/B^3, \quad a_4 = (1+3/A_0)d_1/B^2 + \omega_p d_3/(Q_p B^3)$$

$$a_3 = (1+2/A_0+3/A_0^2)d_1/B + \omega_p d_3/(Q_p B^2) + 3\omega_p d_3/(Q_p A_0 B^2) + \omega_p^2 d_5/B^3$$

$$a_2 = 1 + (1+1/A_0+1/A_0^2)d_1/A_0 + \omega_p d_2/(Q_p B) + 2\omega_p d_3/(Q_p A_0 B) + 3\omega_p d_3/(Q_p A_0^2 B) + \omega_p^2 d_5/B^2 + 3\omega_p^2 d_5/(B^2 A_0)$$

$$a_1 = (1+d_2/A_0)\omega_p/Q_p + (1+1/A_0)\omega_p d_3/(Q_p A_0^2) + 2\omega_p^2 d_5/(A_0 B) + 3\omega_p^2 d_5/(B A_0^2) + \omega_p^2 d_4/B$$

$$a_0 = \omega_p^2 [1 + d_4/A_0 + (1+1/A_0)d_5/A_0^2] \qquad (3.35b)$$

$$d_1 = 1+1/X_1+1/X_2+1/(X_1X_2)$$

$$d_2 = 1+X_1+X_1X_3+X_1X_2X_3$$

$$d_3 = (1+X_1+X_2+X_1X_2)(1+X_3+X_4C_1/C_2)$$

$$d_4 = 1+X_2+1/X_3+1/(X_1X_3)$$

$$d_5 = (1+1/X_3)(1+X_2+1/X_1+X_2/X_1) \qquad (3.35b)\ (2)$$

and $B = A_0\omega_c$ is the gain-bandwidth product of the amplifier.

Eqn. (3.35) can be expressed in a factored form as

$$D(s) = a_5(s+p_1)(s+p_2)(s+p_3)[s^2+(\hat{\omega}_{pa}/\hat{Q}_{pa})s+\hat{\omega}_{pa}^2] \qquad (3.36)$$

By comparing the coefficients in (3.35) and (3.36), it can be shown that

$$a_0/(\hat{\omega}_{pa}\hat{Q}_{pa}) = a_1-a_3\hat{\omega}_{pa}^2+a_4\hat{\omega}_{pa}^3/\hat{Q}_{pa}+a_5\hat{\omega}_{pa}^4(1-1/\hat{Q}_{pa}^2) \qquad (3.37a)$$

and

$$a_0/\hat{\omega}_{pa}^2 = a_2-a_3\hat{\omega}_{pa}/\hat{Q}_{pa}-a_4\hat{\omega}_{pa}^2(1-1/\hat{Q}_{pa}^2)$$
$$+ a_5(2-1/\hat{Q}_{pa}^2)\hat{\omega}_{pa}^3/\hat{Q}_{pa} \qquad (3.37b)$$

To study the exact effect of A_0 and B on Q_p and ω_p for any particular filter using Biquad A, Design I, Eqns. (3.37) have to be simulated on a computer. However, as is shown in Appendix A.1, for $Q_p >> 1$, $A_0 >> 1$, and neglecting third and higher order terms of $(\frac{\omega_p}{B})$ and $(\frac{Q_p}{A_0})$, we can

simplify the above equations to

$$\frac{Q_p}{\hat{Q}_{pa}} = 1 + 4\left(\frac{Q_p}{A_0}\right)^2 - 4Q_p^2\left(\frac{\omega_p}{B}\right)^2 \qquad (3.38a)$$

and

$$\frac{\omega_p}{\hat{\omega}_{pa}} = 1 + 4\left(\frac{Q_p}{A_0}\right)\left(\frac{\omega_p}{B}\right) \qquad (3.38b)$$

Fig. 3.7 compares the exact values of $\hat{Q}_{pa}$ and $\hat{\omega}_{pa}$ computed from (3.37) with those of $\hat{Q}_{pa}$ and $\hat{\omega}_{pa}$ computed from (3.38). The computations were done using a digital computer [Appendix A.2]. Typical data values of μA741 OA($A_0 = 10^5$, B = 1.0M Hz) have been used. Fig. 3.7a shows plots of $\hat{Q}_{pa}$, as well as $\hat{Q}_{pa}$ (exact) versus f_p for two values of Q_p, namely, 20 and 100. For the same values of Q_p, $\hat{\omega}_{pa}$ and $\hat{\omega}_{pa}$ (exact) versus f_p are plotted in Fig. 3.7b. It is seen from Fig. 3.7 that $\hat{Q}_{pa}$ and $\hat{\omega}_{pa}$ can be obtained with a close degree of accuracy, using (3.38).

It is to be noted from (3.38) that $\hat{Q}_{pa}$ and $\hat{\omega}_{pa}$ are independent of the active parameters if second and higher order effects are neglected.

As mentioned before, to study the exact effect of A_0 and B on Q_p and ω_p of Biquad A - Design II, Eqn. (3.37)

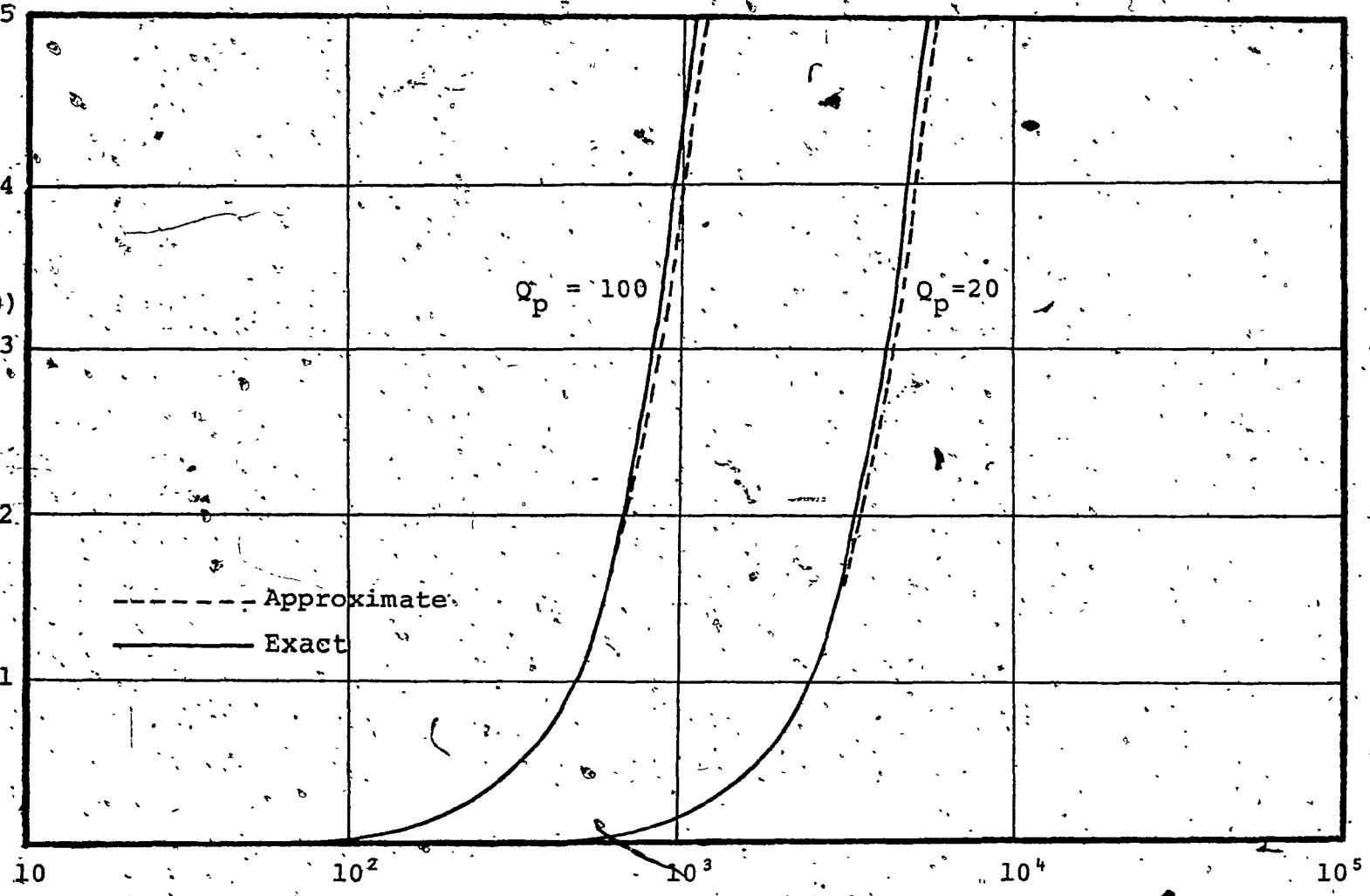

FIG. 3.7a ΔQ_n% VERSUS f_p FOR BIQUAD A - DESIGN I USING µA741 OA

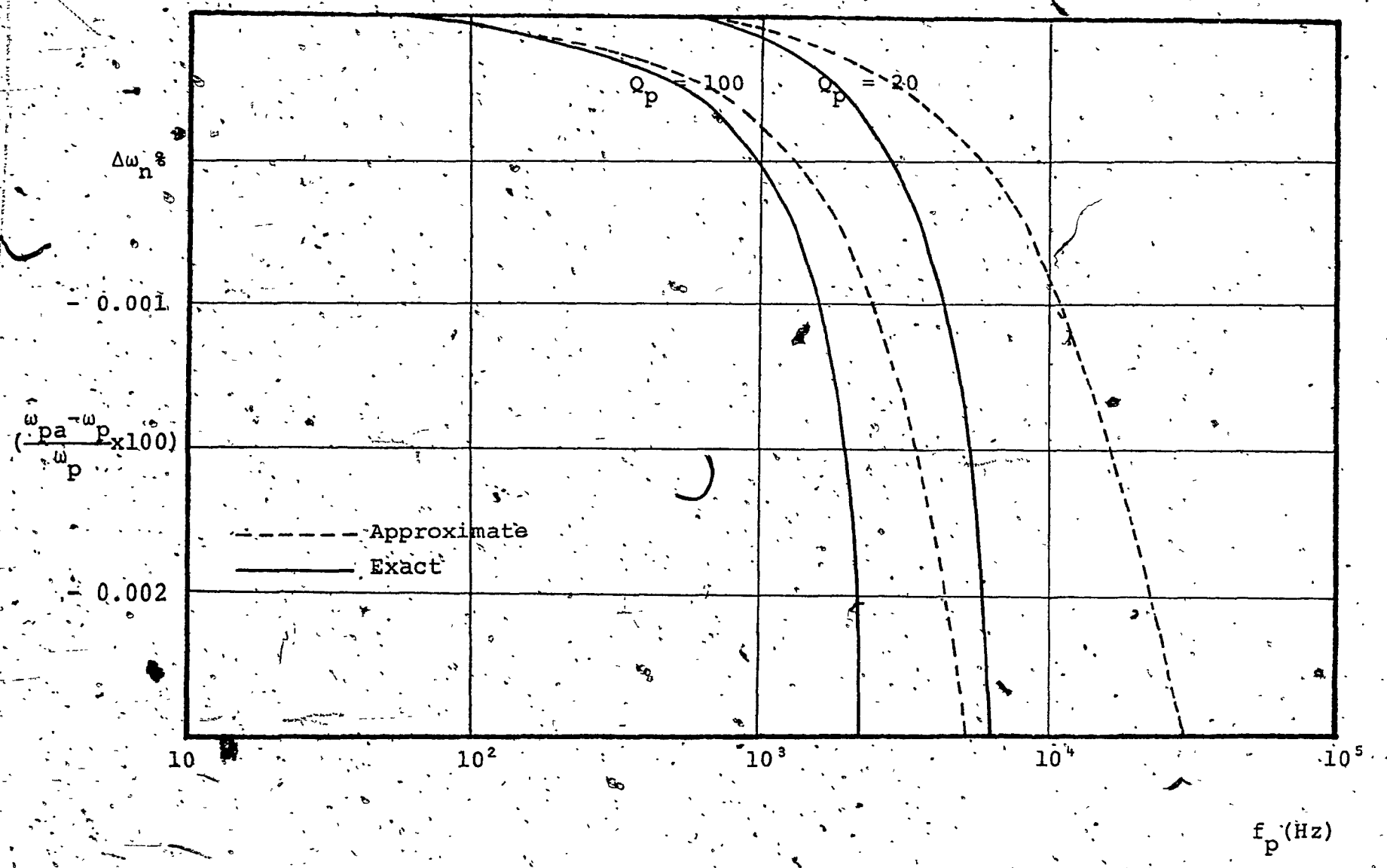

FIG. 3.7b $\Delta\omega_n$% VERSUS f_p FOR BIQUAD A - DESIGN I USING μA741 OA.

has to be simulated on a computer. However, under the same assumptions as those in the case of Design I, we can simplify the above equations to [Appendix B.1]

$$\frac{Q_p}{\hat{Q}_{pa}} \doteq 1+\left(\frac{Q_p}{A_0}\right)-\frac{1}{2}\left(\frac{\omega_p}{B}\right)+\frac{7}{2}\left(\frac{Q_p}{A_0}\right)\left(\frac{\omega_p}{B}\right)-3Q_p\left(\frac{\omega_p}{B}\right)^2 \qquad (3.39a)$$

$$\omega_p/\hat{\omega}_{pa} \doteq 1+\frac{1}{2}\frac{\omega_p}{B}-\frac{1}{8}\left(\frac{\omega_p}{B}\right)^2 \qquad (3.39b)$$

The accuracy of $\hat{Q}_{pa}$ and $\hat{\omega}_{pa}$ obtained from (3.39) is verified in the same manner as described above [Appendix B.2]. This is illustrated in Fig. 3.8, which shows that $\hat{Q}_{pa}$ and $\hat{\omega}_{pa}$ can be determined quite accurately from (3.39).

From (3.38) and (3.39), the presence of Q-enhancement at sufficiently high frequencies is observed in both the designs.

However, for the same OA's and Q_p, $\hat{Q}_{pa}$ versus f_p is seen to be enhanced faster in Design I than in Design II. This is also obvious from Figs. 3.7 and 3.8. Thus, Design II has a larger useful frequency range of operation than that of Design I.

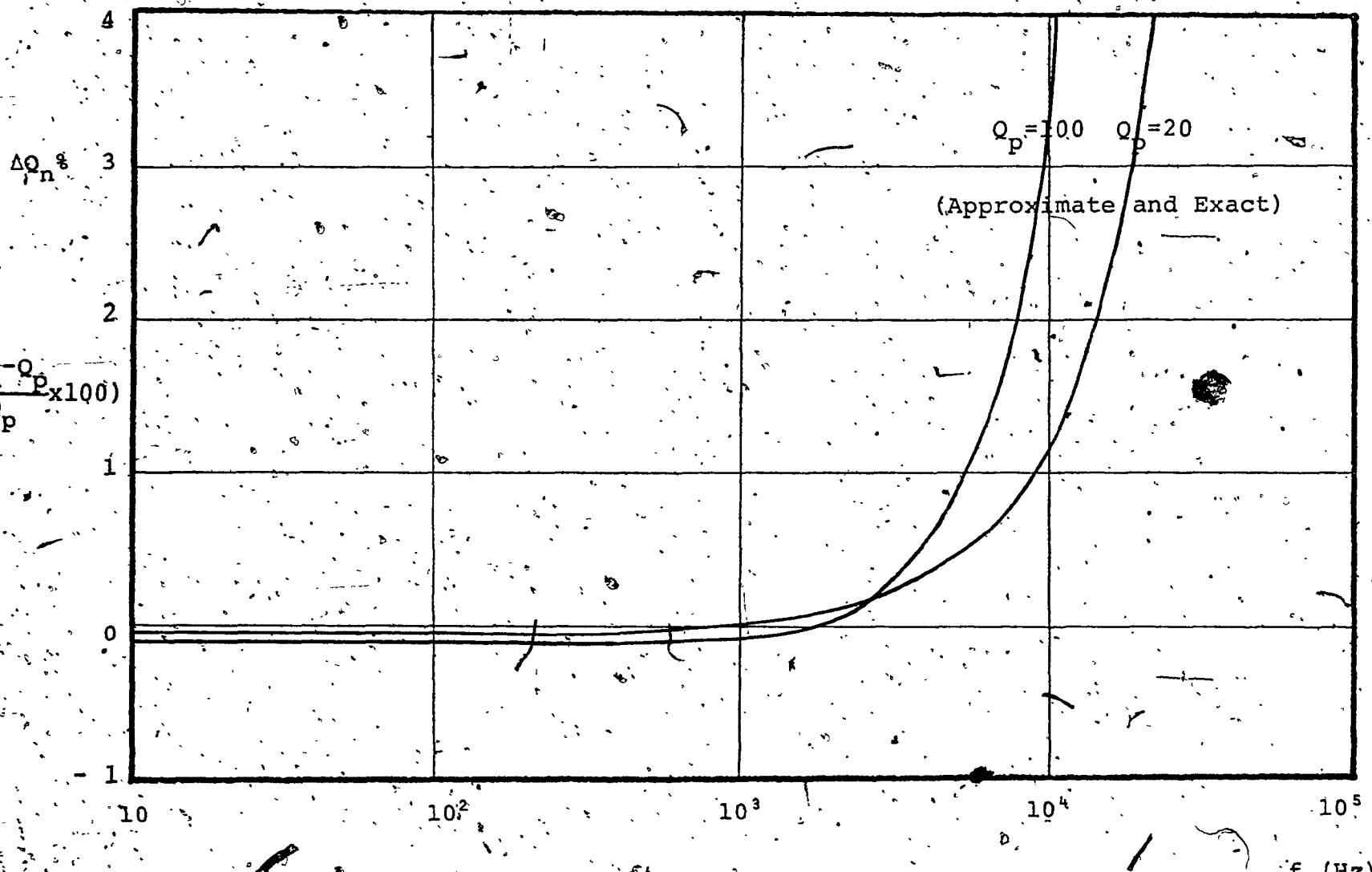

FIG. 3.8a ΔQ_n% VERSUS f_p FOR BIQUAD A -- DESIGN II USING μ741 OA

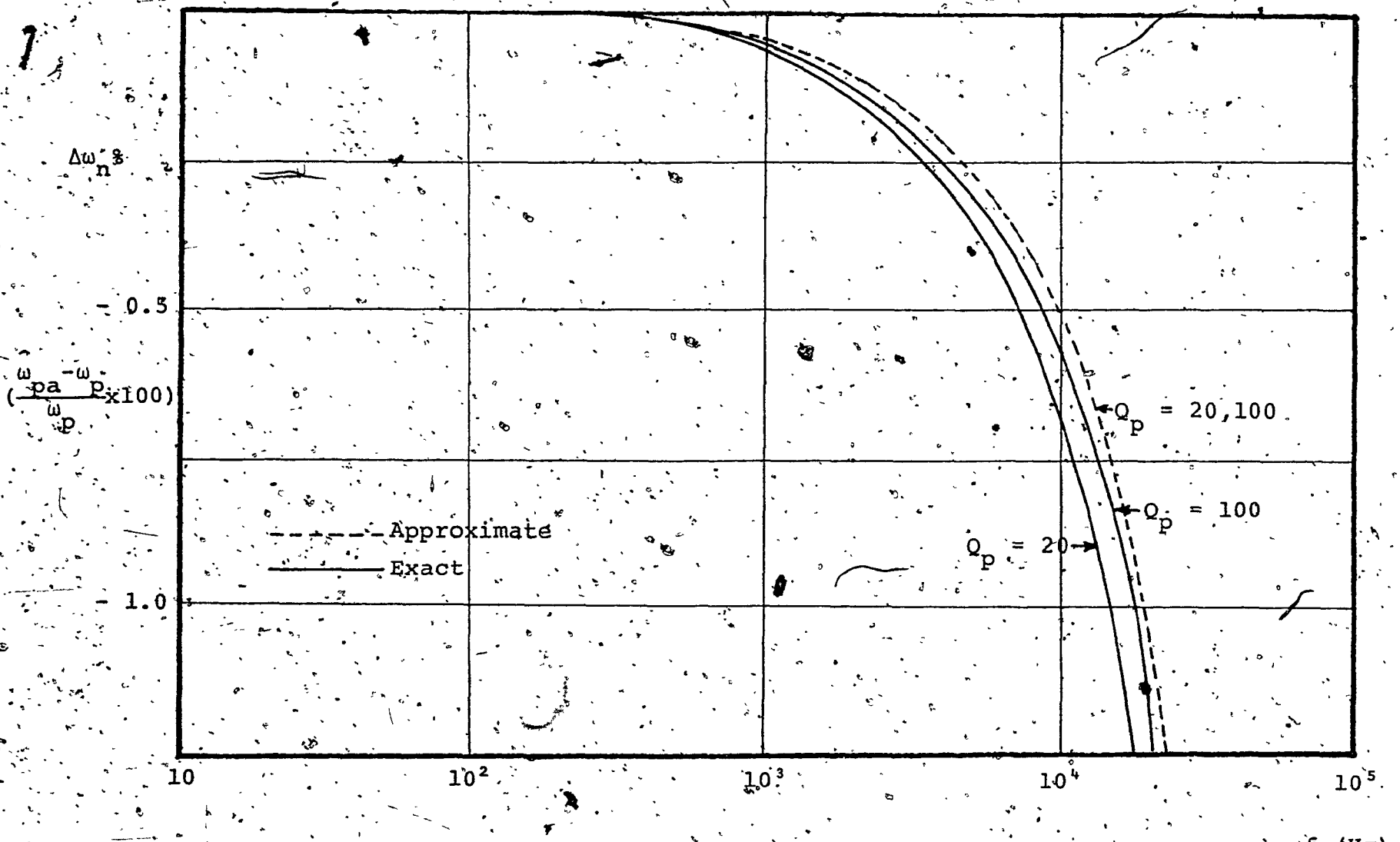

FIG. 3.8b $\Delta\omega_n$% VERSUS f_p FOR BIQUAD A - DESIGN II USING μA741OA

3.5 DESIGN PROCEDURE

Table 3.2 shows that there are several degrees of freedom in the choice of element values. These can be used to satisfy the constraints of Design I or Design II or some other consideration. By using the constraints of Design II, namely, those of low sensitivity and low element-spread design, in circuits 1 to 5 in Table 3.2, a possible design for LP, HP, BP, AP and N sections can be obtained, which is given in Table 3.3. It is seen that the quantities Q_p, ω_p, ω_n, Q_z and ω_z can be independently adjusted by trimming at most three resistors. A trimming sequence is also given in Table 3.3.

3.6 COMPARISON WITH KERWIN, HUELSMAN AND NEWCOMB, TARMI AND GHAUSI, AND THOMAS REALIZATIONS

The salient features of Design II are listed in Table 3.4, along with those of some well-known low sensitivity RC-active realizations, namely, the realizations proposed by Kerwin, Huelsman and Newcomb (KHN) [17], Tarmi and Ghausi (TG) [18], and Thomas (TH) [22]. The different properties have been derived under the assumption that all the realizations use identical OA's. The first six columns of the Table give the low frequency sensitivities, that is, in the frequency range for which $\omega_p << B$. The effects of the finite OA bandwidth are

TABLE 3.3

DESIGN VALUES AND TUNING PROCEDURES

CIRCUIT NUMBER	DESIGN VALUES	TRANSFER FUNCTION REALIZED	TUNING SEQUENCE			
			ω_n	ω_p	Q_p	Q_z
1	$R_2 = R, R_4 = RQ_p^{\frac{1}{2}}, R_5 = 2R/(\alpha H_{LP})$, $R_6 = R/[\alpha(1-H_{LP}/2)], H_{LP} \leq 2$	$T_3 = H_{LP} \dfrac{\omega_p^2}{D(s)}$	-	R_5	R_4	-
2	$R_1 = R(1+Q_p^{\frac{1}{2}})/H_{HP}$, $R_2 = R(1+Q_p^{\frac{1}{2}})/[1+Q_p^{\frac{1}{2}}-H_{HP}], R_4 = RQ_p^{\frac{1}{2}}$, $R_6 = R/\alpha$, $H_{HP} \leq 1+Q_p^{\frac{1}{2}}$	$T_1 = H_{HP} \dfrac{s^2}{D(s)}$	-	R_6	R_4	-
3	$R_2 = R$, $R_3 = 2RQ_p^{\frac{1}{2}}/H_{BP}$, $R_4 = RQ_p^{\frac{1}{2}}/(1-H_{BP}/2)$, $R_6 = R/\alpha$, $H_{BP} \leq 2$	$T_3 = H_{BP} \dfrac{s\omega_p/Q_p}{D(s)}$	-	R_6	R_3	-
4	$R_1 = R(1+Q_p^{\frac{1}{2}})/H_N$, $R_2 = 1/(G-G_1)$, $R_4 = RQ_p^{\frac{1}{2}}$, $R_6 = 1/(\alpha G-G_5)$, $R_5 = R\omega_p^2(1+Q_p^{\frac{1}{2}})/(\alpha H_N \omega_n^2)$, $H_N \leq (1+Q_p^{\frac{1}{2}})$, $H_N \leq \omega_p^2(1+Q_p^{\frac{1}{2}})/\omega_n^2$ for $\omega_n > \omega_p$	$T_1 = H_N \dfrac{(s^2+\omega_n^2)}{D(s)}$	R_5	R_6	R_4	-
5	For all-pass: $R_1 = R$, $R_4 = RQ_p^{\frac{1}{2}}$, $R_5 = R/\alpha$, $R_1 = R_7$, $R_2 = \infty$, $H_{AP} = 1$	$T_3 = H_{AP} \dfrac{s^2-(\omega_z/Q_z)s+\omega_z^2}{D(s)}$	R_5		R_4	

$D(s) = s^2+(\omega_p/Q_p)s+\omega_p^2$, $\alpha = 2Q_p^{\frac{1}{2}}/(1+Q_p^{\frac{1}{2}})$,

$C_1 = C_2 = C = 1/(\omega_p R)$, $R_{10} = \alpha R$, $R_8 = RQ_p^{\frac{1}{2}}$, $R_7 = R_9 = R$.

studied by neglecting second and higher order terms such as $(Q_p/A_0)^2$ or $(\omega_p/B)^2$. This is a reasonable assumption in the usual frequency range of applications of active RC-filters.

The Table shows that the passive element sensitivities are about the same for all the realizations, of the order of unity. However, amongst the four, the proposed design has the lowest dependence of Q_p on the finite d.c. gain (A_0) and the finite bandwidth (B) of the OA's. It is also observed that in the proposed design ω_p is least affected by the finite bandwidth of the OA.

For the same total capacitance 2C, where $C = 1/\omega_p R$, the highest resistor value required in the proposed realization is $RQ_p^{\frac{1}{2}}$, while that in the other realizations is RQ_p. This makes the proposed technique attractive for implementation of high Q_p realizations. The maximum resistance values in the circuit may have to be limited either due to technological considerations such as those in integrated circuit (IC) fabrication [1] or to minimize interactions with the imperfections of the OA's [34]. If the maximum resistance is the same for all the realizations, the present technique requires the lowest total capacitance. This is an attractive feature for IC implementation since capacitors occupy by far, the largest substrate area. Finally, the proposed technique results in a low element spread, namely, $2Q_p^{\frac{1}{2}}$, as compared to Q_p in other realizations. This again, is

TABLE 3.4

COMPARISON WITH KHN, TG AND TH

REALIZATION	$\omega_p \ll B$						EFFECT OF FINITE O A / S. BANDWIDTH		$\frac{C_{max}}{C_{min}}$	$\frac{R_{max}}{R_{min}}$	R_{max}	NO. OF O A / S. REQUIRED				
	$\lvert S^{Q_p}_{R,C}\rvert$	$\lvert S^{\omega_p}_{R,C}\rvert$	$\lvert S^{\omega_z}_{R,C}\rvert$	$\lvert S^{Q_z}_{R,C}\rvert$	$\lvert S^{\omega_p}_{A_0}\rvert$	$\lvert S^{Q_p}_{A_0}\rvert$	$Q_p/Q_{pa} \approx$	$\omega_p^2/\omega_{pa}^2 \approx$				LP	HP	BP	N	AP
PROPOSED DESIGN	≤ 1	≤ 1	≤ 1	≤ 1	0	$\frac{Q_p}{A_0}$	$1+\frac{Q_p}{A_0}-\frac{\omega_p}{2B}$	$1+\frac{\omega_p}{B}$	1	$2Q_p$	RQ_p	3	3	3	3	3
STATE VARIABLE (KHN)	≤ 1	≤ 1	≤ 1	≤ 1	0	$\frac{2Q_p}{A_0}$	$1+\frac{2Q_p}{A_0}-\frac{4Q_p\omega_p}{B}$	$1+\frac{2\omega_p}{B}$	1	$2Q_p$	RQ_p	3	4	3	4	4
TARMI AND GHAUSI (TG)	≤ 2	≤ 1	≥ 1	≥ 1	0	$\frac{3Q_p}{A_0}$	$1+\frac{3Q_p}{A_0}-\frac{3\omega_p}{2B}$	$1+\frac{3\omega_p}{B}$	1	Q_p	RQ_p	4	4	4	4	4
BIQUAD (TH)	≤ 1	≤ 1	≥ 1	≥ 1	0	$\frac{2Q_p}{A_0}$	$1+\frac{2Q_p}{A_0}-\frac{4Q_p\omega_p}{B}$	$1+\frac{2\omega_p}{B}$	1	Q_p	RQ_p	3	4	3	4	4

NOTE: Each of the realizations uses the minimum number of capacitors, namely, two.

desirable in IC implementation since, even in the permissible range for element values, a low spread will lead to low fabrication tolerances [1,5].

3.7 Experimental Results

A sixth-order Chebychev low-pass filter and a sixth order elliptic band-pass filter were designed and built using the proposed procedure.

The low-pass filter has a maximum passband attenuation of 1.0 dB, bandwidth = 3979 Hz. The band-pass filter has the following specifications:

Centre frequency = 1500 Hz

Passband = 60 Hz

Maximum passband attenuation = 0.3 dB

Minimum stopband attenuation outside the frequency range 1408 - 1595 Hz = 38 dB

Resistors (temperature coefficient = 250 p.p.m/^{o}C, tolerance ≤1%), capacitors (temperature coefficient = -140±40 p.p.m/^{o}C, tolerance ≤ 2%), and μA741C OA's (fixed internal frequency compensation) were used.

3.7.1 Low-Pass Filter

The realization is shown in Fig. 3.9a. The realization uses three cascaded sections of the Type No. 1, in Table 3.2. The element design values are given in Table 3.3. The measured frequency response (input level = 50 mv), shown in Figs. 3.9b and 3.9c, agrees with the theoretical response. The effect of the d.c. supply variations is illustrated in Fig. 3.9d. The deviation in the passband ripple is about 0.03 dB for supply voltages in the range ± 5V to ± 15V. The effect of temperature variations is illustrated in Fig. 3.9e, which shows the frequency response at -10^{o}C (right-hand curve), 20^{o}C and 70^{o}C (left-hand curve). The last peak has been displaced horizontally by 47 Hz, which corresponds to a change of 149 p.p.m/^{o}C. The frequency displacement is due to passive element variations and is within the predicted value.

3.7.2 Band-Pass Filter

The realization is shown in Fig. 3.10a which uses cascaded sections of the Types 3 and 4 in Table 3.3. The measured frequency response is shown in Figs. 3.10b and 3.10c, and it is in agreement with the theoretical response. Fig. 3.10d shows the frequency response for supply voltages of ± 7.5V(lower curve), and ± 15V (upper curve), the input voltage is 0.3V. The passband ripple remains less than 0.34 dB and the deviation in the stopband is negligible. Figs. 3.10e and 3.10f illustrate the effect of temperature

SECTION NO.	R_1	R_2	R_3	R_4	R_5	R_6	R_7	R_8	R_9	R_{10}	C_1	C_2
1	7.5	∞	6.542	∞	∞	8.049	7.5	7.5	6.542	6.988	15.103	15.103
2	4.99	∞	7.398	∞	∞	4.178	4.99	4.99	7.398	5.960	10.734	10.734
3	2	∞	5.658	∞	∞	1.353	2	2	5.658	2.955	20.093	20.093

Resistors in Kilo ohms and capacitors in Nanofarads.

(a)

FIG. 3.9(a) REALIZATION OF THE SIXTH ORDER CHEBYCHEV LOW-PASS FILTER (ELEMENT VALUES)

$$T(s) = \frac{2x0.12470686}{s^2+0.4641254s+0.12470686} \cdot \frac{2x0.55771963}{s^2+0.3397634s+0.55771963} \cdot \frac{2x0.99073288}{s^2+0.124362s+0.99073288}$$

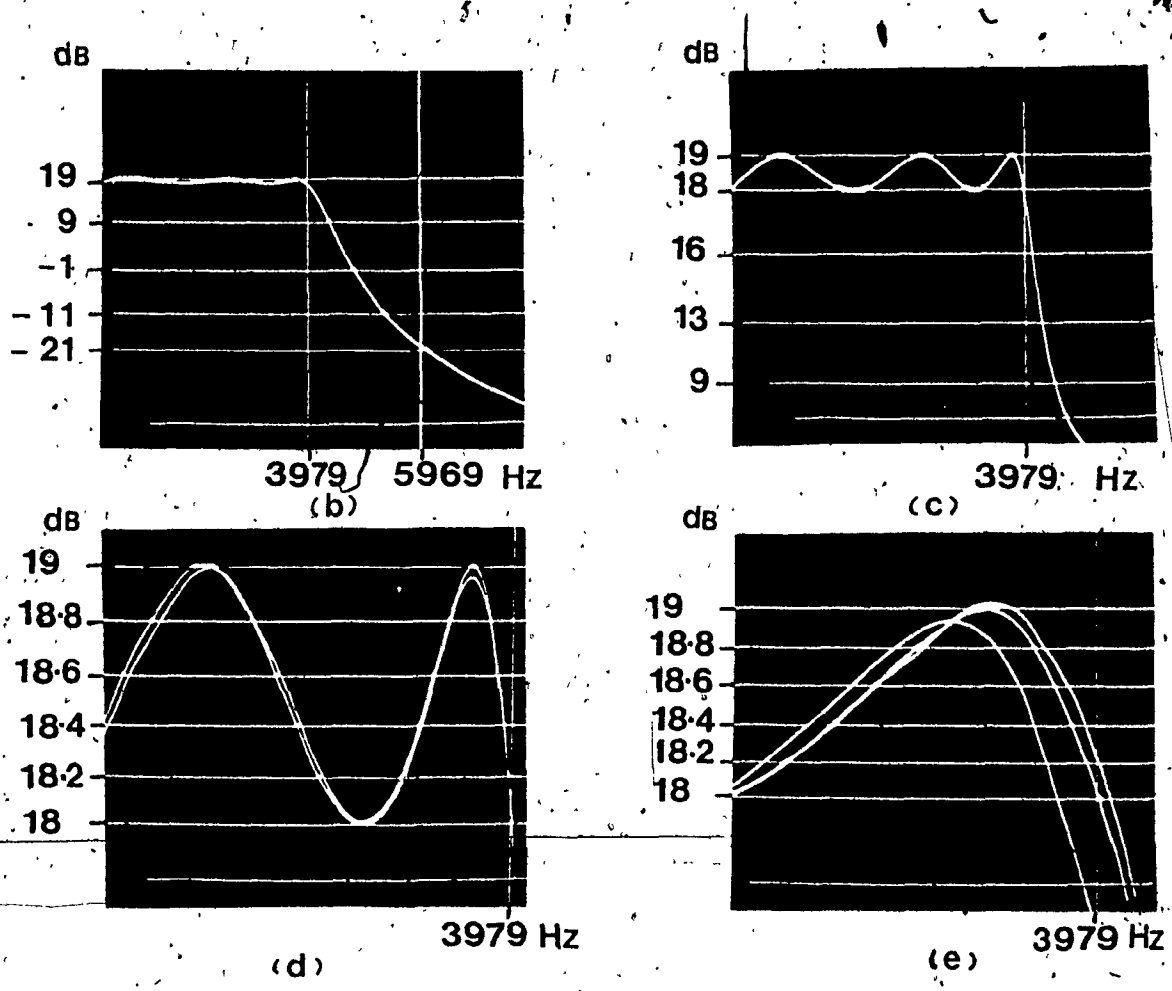

FIG. 3.9(b)-3.9(e) FREQUENCY RESPONSE

3.9(b)	LOGARITHMIC GAIN AND LINEAR FREQUENCY SCALES
3.9(c)	LINEAR GAIN AND FREQUENCY SCALES
3.9(d)	FREQUENCY RESPONSE FOR SUPPLY VOLTAGES ± 5v(LOWER CURVE) and ± 15v, INPUT LEVEL = 0.05v
3.9(e)	FREQUENCY RESPONSE AT TEMPERATURES - 10°C(RIGHT-HAND CURVE), 20°C AND 70°C(LEFT-HAND CURVE)

SECTION NO.	R_1	R_2	R_3	R_4	R_5	R_6	R_7	R_8	R_9	R_{10}	C_1	C_2
1	2	∞	∞	11.396	1.175	∞	2	2	11.396	3.403	53.052	53.052
2	2.576	8.939	17.273	∞	1.426	4.592	2	2	17.273	3.585	51.917	51.917
3	3.732	4.309	17.273	∞	1.948	2.611	2	2	17.273	3.585	54.211	54.211

Resistors in Kilo ohms and capacitors in Nanofarads

(a)

FIG. 10(a) REALIZATION OF THE SIXTH ORDER ELLIPTIC BAND-PASS FILTER (ELEMENT VALUES)

$$T(s) = \frac{2\times0.0308s}{s^2+0.0308s+1} \cdot \frac{0.249648(s^2+1.1341)}{s^2+0.0137s+1.0442} \cdot \frac{0.517835(s^2+0.8818)}{s^2+0.01312s+0.9577}$$

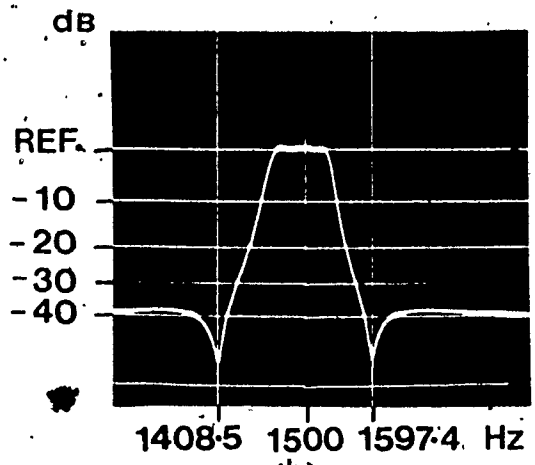

(b)

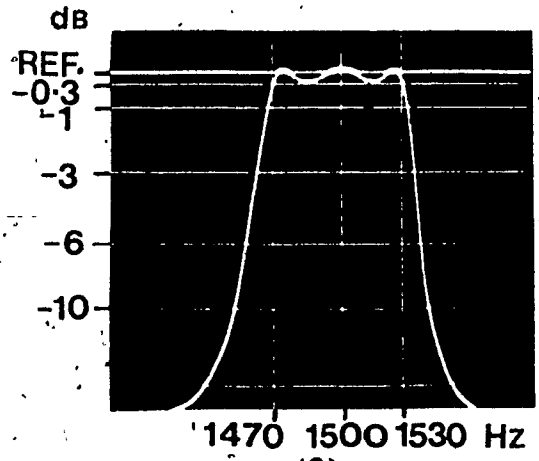

(c)

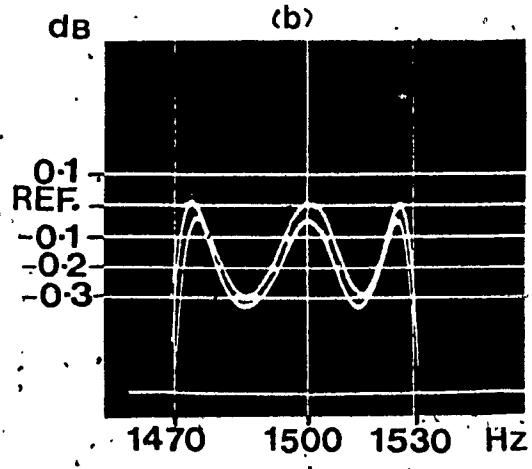

(d)

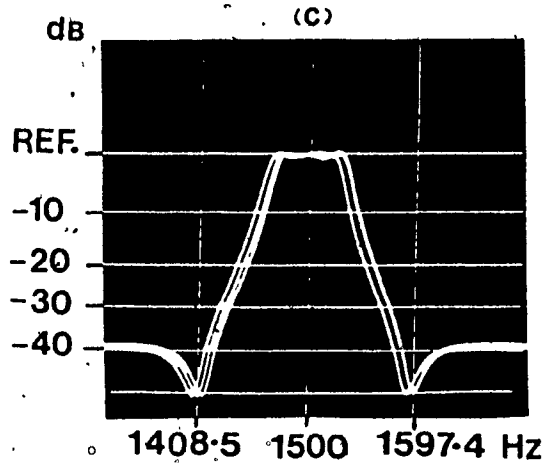

(e)

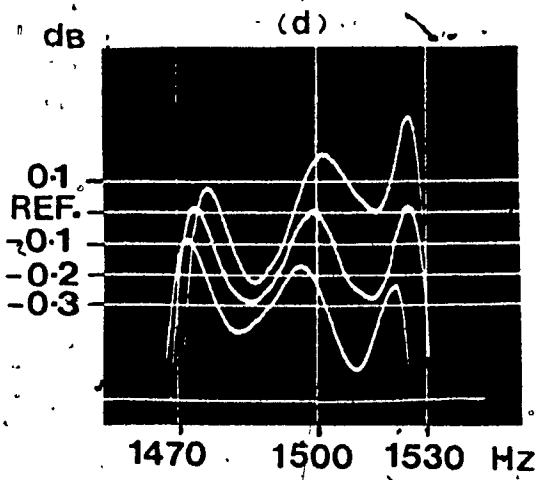

(f)

FIG.3.10(b) LOGARITHMIC GAIN AND LINEAR FREQUENCY SCALES

3.10(c) LINEAR GAIN AND FREQUENCY SCALES

3.10(d) FREQUENCY RESPONSE FOR SUPPLY VOLTAGES OF ± 7.5v (LOWER CURVE) AND ± 15v, INPUT LEVEL OF 0.3v.

3.10(e) FREQUENCY RESPONSE
3.10(f) AT TEMPERATURES OF $-10^{\circ}C$ (RIGHT-HAND CURVE), $20^{\circ}C$ AND $70^{\circ}C$ (LEFT-HAND CURVE)

FIG.3.10(b)-3.10(f) FREQUENCY RESPONSE

variations. The passband ripple remains less than 0.5 dB in the temperature range - 10°C to 70°C. A center frequency displacement of 9 Hz has been measured which corresponds to a change of 75 p.p.m/°C.

3.8 CONCLUSIONS

The stability of the minimal capacitor realization presented in Chapter 2 has been examined. It is found that the realization can attain low-frequency unstable modes of operation during activation. By using the theory of singular elements (nullator-norator pairing), two alternate circuits that are free from low frequency unstable modes during activation and which retain all the attractive features of the original realization are derived. A new configuration has been proposed for the synthesis of RC-active filters by using one of these stable circuits. This has been used to design a number of second-order sections such as low-pass, high-pass, band-pass, notch and all-pass sections. By using these sections, most of the practical filter specifications can be realized. Each section employs three OA's and the output can always be located at one of the OA output terminals. Consequently, these sections can be cascaded without isolating amplifiers. The sensitivities of Q_p, ω_p, Q_z, ω_z and also the multiplier constant of the realizations have been found to be low with respect to the passive and active element variations. An attractive design procedure, capable

of realizing very high Q_p's, has been given. In this procedure, the spread in capacitor values is unity, while that in resistors is at most $2Q_p^2$. The Q_p-sensitivity is very low, while the ω_p-sensitivity is zero to the variations in d.c. gain. The filters can be tuned easily by adjusting only three resistors. The influence of the amplifier pole has been examined and found to be negligible provided $B = A_0\omega_c >> \omega_p$. The proposed realization has been compared with the ones due to Kerwin, Heulsman and Newcomb, Tarmi and Ghausi, and Thomas. Several of the properties of the new realization are found to be attractive, as compared to these realizations. Experimental results show close agreement between theory and practice. Further, these results indicate that these realizations are insensitive to temperature and power supply variations.

There are many applications for which neither Q_p's required are very high, nor the specifications are very stringent. In such cases, the high performance obtained from Biquad A may not be necessary and one may be willing to accept a reduced performance from a network provided it offers other advantages. The purpose of the next Chapter is to describe another biquadratic realization. This realization, while sacrificing the performance for high Q_p and ω_p slightly, uses a lower number of OA's and results in a simpler network.

CHAPTER IV

SECOND CASCADE REALIZATION

CHAPTER IV

SECOND CASCADE REALIZATION

4.1 INTRODUCTION

It has been shown in Chapter 2, that the direct realization procedure described by Antoniou [26] can be derived from Structure B. This direct synthesis procedure can be used as a cascade method by realizing second order sections [45]. However, in such a case, isolating amplifiers are invariably required between individual sections. In addition, an inverting amplifier may also be required in general.

In this Chapter, a new cascade synthesis procedure is proposed. This procedure is also derived from Structure B and uses CGICB as the active element. The proposed realization is shown to result in realizations, comparable for many applications to those due to Kerwin, Huelsman and Newcomb (KHN) [17], Tarmi and Ghausi (TG) [18], and Thomas (TH) [22] while requiring only two OA's per second order section and resulting in simpler networks.

4.2 BIQUAD B - A NEW RC-ACTIVE NETWORK CONFIGURATION

Consider the network of Fig. 4.1, which is a special case of Structure B without the inverting amplifier. Consider also the network of Fig. 4.2, which is simply the

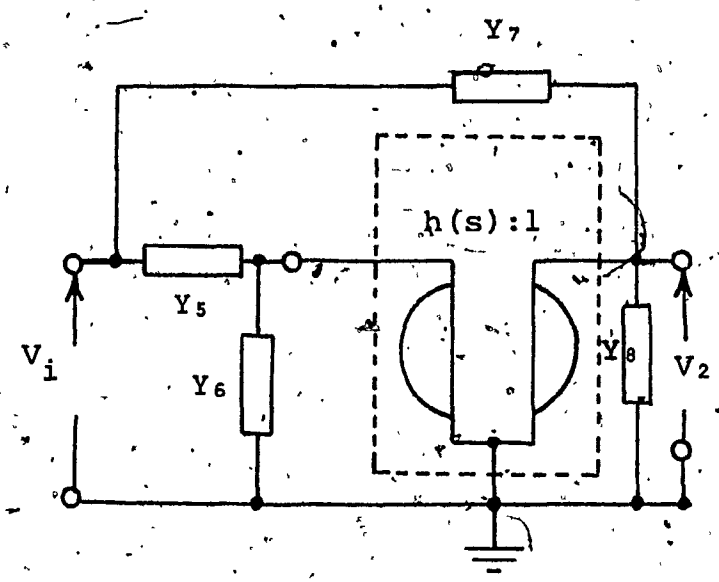

FIG. 4.1 SPECIAL CASE OF STRUCTURE B

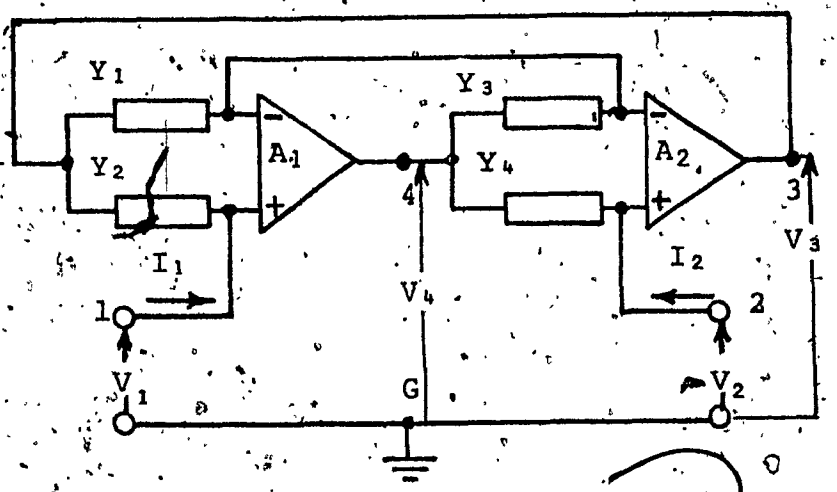

FIG. 4.2 THE CGICB WITH ADDITIONAL PORTS 3G AND 4G

CGICB described in Section 1.2, with two new ports created across 3-G and 4-G. This is symbolically shown in Fig. 4.3.

A new configuration is now obtained, as shown in Fig. 4.4, by combining the networks of Fig. 4.1 and Fig. 4.3. A synthesis procedure is described which uses the configuration of Fig. 4.4. The transfer functions between the input and output terminals 2,3 and 4, assuming ideal OA's, are readily obtained as

$$\frac{V_3}{V_i} = T_1 = [Y_5+h(s)\{Y_7(1+Y_6/Y_2)-Y_5Y_8/Y_2\}]/D(s) \qquad (4.1a)$$

$$\frac{V_4}{V_i} = T_2 = \{Y_5(1+Y_8/Y_4)-Y_6Y_7/Y_4+h(s)Y_7\}/D(s) \qquad (4.1b)$$

$$\frac{V_2}{V_i} = T_3 = \{Y_5+h(s)Y_7\}/D(s) \qquad (4.1c)$$

where

$$h(s) = Y_2Y_3/Y_1Y_4$$

$$D(s) = (Y_5+Y_6)+h(s)(Y_7+Y_8) \qquad (4.1d)$$

The conversion function $h(s)$ and Y_5 to Y_8 can be selected in many different ways and it is clear that any stable second-order transfer function with any desired zero and pole locations can be realized.

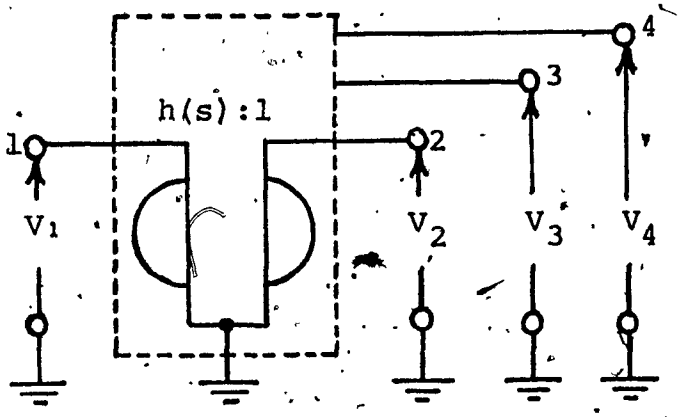

FIG. 4.3 SYMBOLIC REPRESENTATION OF THE CGICB IN FIG. 4.2

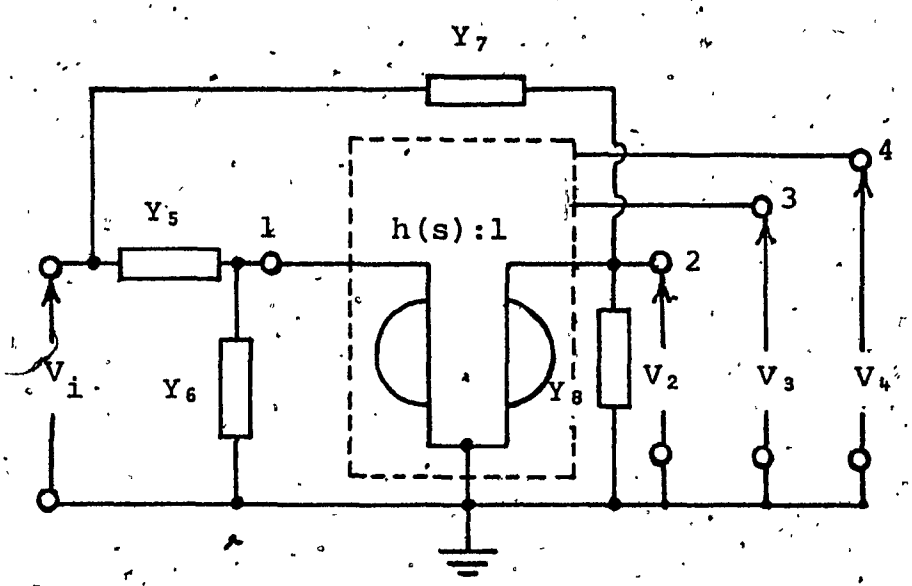

FIG. 4.4 THE BASIC CONFIGURATION

Letting

$$Y_i = sC_i + G_i \qquad (4.2)$$

where i = 1 to 4, we have from (4.1)

$$h(s) = (sC_2+G_2)(sC_3+G_3)/(sC_1+G_1)(sC_4+G_4) \qquad (4.3)$$

Clearly, by omitting one or more conductances and/or capacitances, a number of specific conversion functions can be generated.

The most frequently used second-order transfer functions have already been described in Section 3.4. Realizations of these functions using Biquad B are given in Table 4.1. LP, HP, BP and N sections are realized by choosing h(s) in a simple manner such as K_1s, K_2s^2, $K_3s + K_4s^2$ or their reciprocals. By comparing (4.1) with (3.1), circuits 1 to 10 in Table 4.1 can be obtained. Circuits 3,4 and 7 can be regarded as realizations of simple RLC networks [31,46]. Second-order AP sections can be obtained from circuits 11 and 12 of Table 4.1.

Figures 4.2 and 4.3 and Table 4.1 show that, with the exception of circuit 10, the response is obtained from the output of an OA. Owing to the low output resistance of the amplifier, any number of sections can be cascaded without isolation amplifiers.

TABLE 4.1

ELEMENT IDENTIFICATION FOR REALIZING THE MOST COMMONLY USED TRANSFER FUNCTIONS

CIRCUIT NUMBER	h(s)	Y_1	Y_2	Y_3	Y_4	Y_5	Y_6	Y_7	Y_8	TRANSFER FUNCTION	REMARKS
1	$\frac{sC_2(sC_3+G_3)}{G_1G_4}$	G_1	sC_2	sC_3+G_3	G_4	G_5	0	0	G_8	$T_2 = \frac{G_1G_5(G_4+G_8)}{G_1G_5G_4+sC_2G_3G_8+s^2C_2C_3G_8}$	LP
2	$\frac{G_2G_3}{sC_1(sC_4+G_4)}$	sC_1	G_2	G_3	sC_4+G_4	0	G_6	G_7	sC_8+G_8	$T_1 = \frac{G_2G_3G_7(1+\frac{G_6}{G_2})}{G_2G_3(G_7+G_8)+s(C_1G_4G_8+C_8G_2G_3)+s^2C_1C_4G_8}$	LP
3	$\frac{sC_3G_2}{G_1G_4}$	G_1	G_2	sC_3	G_4	0	G_6	sC_7	sC_8+G_8	$T_1 = \frac{s^2C_1C_7(G_2+G_6)}{G_6G_1G_4+sC_3G_2G_8+s^2(C_7+C_8)G_2C_3}$	HP
4	$\frac{sC_3G_2}{G_1G_4}$	G_1	G_2	sC_3	G_4	0	G_6	$\frac{sC_7}{1+sC_7R_7}$	0	$T_1 = \frac{s^2C_1C_7(G_2+G_6)}{G_6G_1G_4+sC_7G_1G_4G_6R_7+s^2C_3C_7G_2}$	HP
5	$\frac{s^2C_2C_3}{G_1G_4}$	G_1	sC_2	sC_3	G_4	sC_5	G_6	0	G_8	$T_2 = \frac{sC_5(1+\frac{G_6}{G_4})G_1G_4}{G_1G_4G_6+sC_5G_1G_4+s^2C_2C_3G_8}$	BP
6	$\frac{G_2G_3}{sC_1(sC_4+G_4)}$	sC_1	G_2	G_3	sC_4+G_4	0	G_6	sC_7	G_8	$T_1 = \frac{sC_7G_2G_3(1+\frac{G_6}{G_2})}{G_2G_3G_8+s(C_7G_2G_3+C_1G_4G_6)+s^2C_1C_4G_6}$	BP
7	$\frac{sC_3G_2}{G_1G_4}$	G_1	G_2	sC_3	G_4	0	G_6	G_7	sC_8+G_8	$T_1 = \frac{sC_3G_7(G_2+G_6)}{G_1G_4G_6+sC_3G_2(G_7+G_8)+s^2C_3C_8G_2}$	BP

TABLE 4.1 (Continued)

ELEMENT IDENTIFICATION FOR REALIZING THE MOST COMMONLY USED TRANSFER FUNCTIONS

CIRCUIT NUMBER	h(s)	Y_1	Y_2	Y_3	Y_4	Y_5	Y_6	Y_7	Y_8	TRANSFER FUNCTION	REMARKS
8	$\frac{G_2G_3}{s^2C_1C_4}$	sC_1	G_2	G_3	sC_4	G_5	0	G_7	sC_8^*	$T_2 = \frac{s^2C_1G_5(C_4+C_8)+G_2G_3G_7}{s^2C_1G_5C_4+sC_8G_2G_3+G_2G_3G_4}$	N
9	$\frac{sG_2C_3}{G_1G_4}$	G_1	G_2	sC_3	G_4	G_5	0	sC_7	G_8	$T_2 = \frac{s^2C_3C_7G_2+G_1G_5(G_4+G_8)}{s^2C_3C_7G_2+sC_3G_2G_8+G_1G_4G_5}$	N
10	$\frac{sG_2C_3}{G_1G_4}$	G_1	G_2	sC_3	G_4	G_5	G_6^*	sC_7	$sC_8^*+G_8$	$T_2 = \frac{(s^2+\frac{G_1G_4G_5}{C_3C_7G_2})(\frac{C_7}{C_7+C_8})}{s^2+s\frac{G_8}{C_7+C_8}+\frac{G_1G_4(G_5+G_6)}{C_3G_2(C_7+C_8)}}$	N
11	$\frac{G_2G_3}{s^2C_1C_4}$	sC_1	G_2	G_3	sC_4	G_5	G_6^*	G_7	sC_8	$T_1 = \frac{s^2C_1C_4G_5-sG_5C_8G_3+G_3G_7(G_2+G_6)}{s^2C_1C_4(G_5+G_6)+sC_8G_2G_3+G_2G_3G_7}$	Non minimum phase For all pass: $G_6=0$ $G_5=G_2$
12†	$\frac{sG_2C_3}{G_1G_4}$	G_1	G_2	sC_3	G_4	G_5	G_6	sC_7	G_8	$T_1 = \frac{s^2C_3C_7(G_2+G_6)-sC_3G_5G_8+G_1G_4G_5}{s^2C_3C_7G_2+sC_3G_2G_8+(G_5+G_6)G_1G_4}$	Non minimum phase For all pass: $G_6=0$ $G_2=G_5$

* These elements can be set equal to zero.

† A special case of Circuit #12, namely, the all pass case, has also been independently proposed by J.T. Lim, Bell Northern Research, Canada, as communicated privately by him to Dr. A. Antoniou.

4.3 STABILITY PROPERTIES

It has been shown in Section 3.2 and elsewhere [37] that some networks using CGIC's can be conditionally stable where a circuit can lock in an unstable mode during activation (just after switching on the power supply). In this section, the stability properties of the configuration shown in Fig. 4.4 are examined.

For amplifiers with a finite open loop gain A, the circuit of Fig. 4.4 gives

$$V_k/V_i' = N_k(s)/D(s)$$

where K = 2,3,4 and

$$D(s) = M_1Y_1+M_2Y_3+(1+M_1)(1+M_2)\left[Y_1/A_1+Y_3/A_2 + Y_1/A_1A_2+Y_3/A_1A_2\right] \qquad (4.4)$$

$$M_1 = (Y_5+Y_6)/Y_2$$

$$M_2 = (Y_7+Y_8)/Y_4$$

The natural frequencies of the circuit in Fig. 4.4 are the zeros of the characteristic polynomial D(s) given by (4.4). As previously explained in Section 3.2, the frequency range $\omega << \omega_c$ is of interest and the amplifier gains A_1 and A_2 can be assumed to be real. For any second-order transfer function the coefficients of D(s) are seen to remain

positive for any attainable pair of A_1 and A_2. This is due to the absence of negative terms in D(s). Therefore the zeros of D(s) will remain in the left-half s-plane and low frequency unstable modes cannot arise during activation.

4.4 SENSITIVITY ANALYSIS

The pole Q factor Q_p, the undamped frequency of oscillation ω_p, the notch frequency ω_n, the multiplier constants $H_N, H_{LP}, H_{HP}, H_{BP}$, as well as Q_Z, ω_Z and H_{AP} have been previously defined by (2.10), (3.11-3.14). The sensitivity of a quantity x with respect to variations in an element e is given by (3.15). For ideal amplifiers, the use of (2.10), (3.11-3.15) and Table 4.1 leads to

$$0 \leq |S_e^x| \leq 1 \qquad (4.5)$$

where x represents any one of the quantities defined by (2.10) and (3.11-3.14) and e represents any capacitance or conductance.

Consider realizations in which $h(s) = K_1 s$, such as the circuits 3(HP), 7(BP), 9,10(N) where

$$Y_1 = G_1, Y_2 = G_2, Y_3 = SC_3, Y_4 = G_4,$$
$$Y_5 = G_5, Y_6 = G_6, Y_7 = SC_7+G_7, Y_8 = SC_8+G_8 \qquad (4.6)$$

For real amplifier gains such that

$A_1 = A_2 = A_0$ and $A_0 >> 1$, (4.1) gives

$$D(s) = M_1Y_1+M_2Y_3+(1+M_1)(1+M_2)(Y_1+Y_3)/A_0 \qquad (4.7)$$

From (2.10), (4.6) and (4.7), the Q-factor and the undamped frequency of oscillation can be obtained as

$$Q_{pa} = Q_p\{1+\frac{x_4}{x_1A_0}\}^{\frac{1}{2}}\{1+\frac{x_5G_4}{(C_7+C_8)A_0}\}^{\frac{1}{2}}/\{1+\frac{C_3x_4+G_1x_5}{C_3x_2A_0}\}$$

$$\omega_{pa} = \omega_p\{(1+\frac{x_4}{x_1A_0})/(1+\frac{x_5G_4}{(C_7+C_8)A_0})\}^{\frac{1}{2}} \qquad (4.8)$$

where

$$Q_p = \{(G_5+G_6)(C_7+C_8)G_1G_4/(G_7+G_8)^2G_2C_3\}$$

$$\omega_p = \{(G_5+G_6)(G_1G_4/(C_7+G_8)G_2C_3\}^{\frac{1}{2}}$$

$$x_1 = (G_5+G_6)/G_2, x_2 = (G_7+G_8)/G_4 \qquad (4.9)$$

$$x_3 = (C_7+C_8)/G_4, x_4 = (1+x_1)(1+x_2),$$

$$x_5 = (1+x_1)x_3$$

The sensitivities of Q_{pa} and ω_{pa} with respect to the amplification A_0 can be written as

$$S^{Q_{pa}}_{A_0} \doteq -\frac{1}{2A_0}\left[\frac{x_4}{x_1} + \frac{x_5}{x_3} - \frac{2x_4}{x_2} - \frac{2G_1}{C_3}\frac{x_5}{x_2}\right]$$

$$S^{\omega_{pa}}_{A_0} \doteq \frac{1}{2A_0}\left[\frac{x_5}{x_3} - \frac{x_4}{x_1}\right] \qquad (4.10)$$

The use of (4.9) and (4.10) leads to

$$S^{Q_{pa}}_{A_0} \doteq -\frac{1}{2A_0}\left[\left(1+\frac{1}{x_1}\right)(1+x_2)+(1+x_1)\left\{1-2\left(1+\frac{1}{x_2}\right)-\frac{2Q_p^2x_2}{x_1}\right\}\right] \qquad (4.11)$$

By assuming that

$$\left(1+\frac{1}{x_1}\right) - x_1 \ll 2x_2(1+x_1) + 2Q_p^2x_2(1+1/x_1) \qquad (4.12)$$

Equation (4.11) reduces to

$$S^{Q_{pa}}_{A_0} \doteq \frac{Q_p}{A_0}\left[Q_px_2(1+1/x_1) + (1+x_1)/(Q_px_2)\right] \qquad (4.13)$$

Straightforward differentiation shows that

$S^{Q_{pa}}_{A_0}$ is minimum when

$$x_1 = 1, x_2 = 1/Q_p \qquad (4.14)$$

From (4.12) and (4.14), the analysis is valid provided that

$$4Q_p + 4/Q_p >> 1$$

which is clearly satisfied in practise.

From (4.13) and (4.14), the minimum sensitivity to variations in A_0 is derived as

$$S_{A_0}^{Q_{pa}} \doteq 4Q_p/A_0 \qquad (4.15)$$

The corresponding value of $S_{A_0}^{\omega_{pa}}$ is given by

$$S_{A_0}^{\omega_{pa}} \doteq -1/A_0Q_p \qquad (4.16)$$

LP realizations as circuits 1 and 2 can be obtained by using a conversion function of the form $K_3s^2 + K_4s$ or its reciprocals. The admittances Y_1 to Y_8 are chosen as

$$Y_1 = G_1, Y_2 = sC_2, Y_3 = sC_3+G_3, Y_4 = G_4,$$

$$Y_5 = G_5, Y_6 = 0, \quad Y_7 = 0, \quad Y_8 = G_8 \qquad (4.17)$$

to obtain a conversion function of the form

$$K_3s^2 + K_4s$$

Now Q_{pa} and ω_{pa} are obtained as

$$Q_{pa} = \frac{Q_p\{1+(1+G_8/G_4)(1+G_3/G_1)/A_0\}^{\frac{1}{2}}\{1+(1+G_4/G_8)/A_0\}^{\frac{1}{2}}}{1+(1+G_4/G_8)(1+G_3/G_1)/A_0+(1+G_4/G_8)C_3G_5/(C_2G_3A_0)}$$

$$\omega_{pa} = \omega_p\{1+(1+G_8/G_4)(1+G_3/G_1)/A_0\}^{\frac{1}{2}}/\{1+(1+G_4/G_8)/A_0\}^{\frac{1}{2}} \qquad (4.18)$$

where

$$Q_p = \{C_3G_1G_4G_5/(C_2G_3^2G_8)\}^{\frac{1}{2}}$$

$$\omega_p = \{G_1G_4G_5/(C_2C_3G_8)\}^{\frac{1}{2}} \qquad (4.19)$$

The sensitivity of Q_{pa} with respect to variations in A_0 can be minimized following the approach used earlier. It is found that for minimum sensitivity

$$G_4 = G_8, \quad G_1 = Q_p G_3 \qquad (4.20)$$

The minimum value of $S_{A_0}^{Q_{pa}}$ can be shown to be

$$S_{A_0}^{Q_{pa}} \doteq 4Q_p/A_0 \qquad (4.21)$$

and the corresponding value of $S_{A_0}^{\omega_{pa}}$ is given by

$$S_{A_0}^{\omega_{pa}} \doteq -1/(A_0Q_p) \qquad (4.22)$$

The above sensitivity analysis can be extended to realizations using any other type of conversion function.

Eq. (4.5) shows that the sensitivities to passive element variations are independent of the selectivity. Furthermore, the sensitivities with respect to variations in the amplifier gains are low.

4.5 THE INFLUENCE OF THE AMPLIFIER POLE

The effect of the amplifier pole on the stability, pole Q-factor and natural frequency of oscillation will now be examined.

Let $A_1 = A_2 = A$. By assuming that $A_0 >> 1$ and using (1.2), (4.1) can be written as

$$D \doteq M_1Y_1+M_2Y_3+(1+M_1)(1+M_2)(Y_1+Y_3)(1/A_0+S/B+S^2/B^2) \quad (4.23)$$

where

$$B = A_0\omega_c$$

is the gain-bandwidth product of the amplifier.

Consider a realization using a CGICB in which $h(s) = K_1s$ and satisfying the constraints for minimum $S_{A_0}^{Q_{pa}}$. From (4.6), (4.9) and (4.14), (4.23) can be written as $D = K_1D'$ where K_1 is a constant and

$$D' = a_4 s^4 + a_3 s^3 + a_2 s^2 + a_1 s + a_0 \qquad (4.24)$$

where

$$a_4 = 2/(\omega_p^2 B^2)$$

$$a_3 = 2(1/\omega_p + Q_1/Q_p B)/(\omega_p B)$$

$$a_2 = 1/\omega_p^2 + 2d/B^2 + 2Q_1/(\omega_p Q_p B) + 2/(\omega_p^2 A_0)$$

$$a_1 = 1/(\omega_p Q_p) + 2d/B + 2Q_1/(\omega_p Q_p A_0)$$

$$a_0 = 1 + 2d/A_0$$

$$d = 1 + 1/Q_p \quad , \quad Q_1 = 1 + 2Q_p$$

Similarly for a realization using a CGICB in which $h(s) = K_3 s^2 + K_4 s$ and satisfying the constraints for minimum $S^{Q_{pa}}_{A_0}$, (4.17) and (4.23) give $D(s) = K_2 D'(s)$ where K_2 is a constant and $D'(s)$ is given by (4.24).

By applying the Routh-Hurwitz stability criterion, it is found that

$$b = a_2 a_3 - a_1 a_4 > 0$$

$$a_1 b - a_0 a_3^2 > 0 \qquad (4.25)$$

and hence $D'(s)$ has roots in the left-half of the s-plane. Consequently, the amplifier poles cannot cause instability.

Equation (4.24) can be expressed in a factored form as

$$D' = (S+\frac{1}{P_1})(S+\frac{1}{P_2})(S^2/\hat{\omega}^2_{pa} + s/(\hat{\omega}_{pa}\hat{Q}_{pa}) + 1) \qquad (4.26)$$

By comparing the coefficients in (4.24) and (4.26) yields

$$\frac{P_1P_2}{\omega^2_{pa}} = \frac{2}{\omega^2_p B^2 X} \qquad (4.27a)$$

$$\frac{P_1P_2}{\hat{\omega}_{pa}\hat{Q}_{pa}} + \frac{P_1+P_2}{\hat{\omega}^2_{pa}} = \frac{2}{\omega^2_p BX} + \frac{4}{\omega_p B^2 X} \qquad (4.27b)$$

$$P_1P_2 + \frac{P_1+P_2}{\hat{Q}_{pa}\hat{\omega}_{pa}} + \frac{1}{\hat{\omega}^2_{pa}} = \frac{2}{\omega^2_p A_0 X} + \frac{4}{\omega_p BX} + \frac{2}{B^2X} + \frac{1}{\omega^2_p X} \qquad (4.27c)$$

$$(P_1+P_2) + \frac{1}{\hat{\omega}_{pa}\hat{Q}_{pa}} = \frac{1}{\omega_p Q_p X} + \frac{2}{BX} + \frac{4}{\omega_p A_0 X} \qquad (4.27d)$$

where

$$X = 1 + 2(1+1/Q_p)/A_0$$

Substituting for P_1P_2 from (4.27a) and (P_1+P_2) from (4.27d) in (4.27b) and (4.27c) yields

$$\frac{Q_p}{\hat{Q}_{pa}} = \frac{1}{X}\left\{\frac{\hat{\omega}_{pa}}{\omega_p} + \frac{\hat{\omega}_{pa}}{\omega_p}\frac{Q_p}{A_0} + \frac{2Q_p\hat{\omega}_{pa}}{B}\left(1 - \frac{\hat{\omega}^2_{pa}}{\omega^2_p}\right) + \right.$$

$$+ \frac{\hat{\omega}_{pa}^3}{B^2\omega_p}\left(\frac{2Q_p}{\hat{Q}_{pa}}\frac{\hat{\omega}_{pa}}{\omega_p} - 4Q_p\right)\Big\} \qquad (4.28a)$$

and

$$\frac{\omega_p^2}{\hat{\omega}_{pa}^2} = \frac{1}{X} + \frac{4\omega_p}{BX}\left(1 - \frac{\omega_p}{2\hat{\omega}_{pa}\hat{Q}_{pa}}\right) - \frac{1}{Q_p\hat{Q}_{pa}}\frac{\omega_p}{\hat{\omega}_{pa}}\left(\frac{1}{X} - \frac{\omega_p}{\hat{\omega}_{pa}}\frac{Q_p}{\hat{Q}_{pa}}\right)$$

$$+ \frac{2}{A_0X}\left(1 - \frac{2\omega_p}{\hat{\omega}_{pa}}\frac{1}{\hat{Q}_{pa}}\right) + \frac{2\hat{\omega}_{pa}^2}{XB^2}\left(\frac{\omega_p^2}{\hat{\omega}_{pa}^2} - 1\right) \qquad (4.28b)$$

Assume $A_0 >> 1$ and $Q_p >> 1$, then from Appendix C.1, we get

$$\frac{Q_p}{\hat{Q}_{pa}} = 1 + 4\frac{Q_p}{A_0} - 2\frac{\omega_p}{B}\left(1 - 2Q_p\frac{\omega_p}{B} + 4\frac{Q_p}{A_0}\right) \qquad (4.29a)$$

and

$$\frac{\omega_p}{\hat{\omega}_{pa}} = 1 + 2\frac{\omega_p}{B} \qquad (4.29b)$$

It is to be noted here, that $\hat{Q}_{pa}$ is relatively independent of the amplifier pole, at least as far as first order effects are concerned, provided $\omega_p << B$.

Using a digital computer, the values of $\hat{Q}_{pa}$ and $\hat{\omega}_{pa}$ obtained from (4.29) are compared with those of $\hat{Q}_{pa}$ (exact) and $\hat{\omega}_{pa}$ (exact) obtained from the exact formula (4.28) at different values of ω_p (Appendix C.2). Typical data values of μA7410A have been used. Figure 4.5a shows plots of $\hat{Q}_{pa}$, as well as $\hat{Q}_{pa}$ (exact) versus f_p for Q_p values of 200 and 100, respectively. Similarly, Figure 4.5b compared $\hat{\omega}_{pa}$ with $\hat{\omega}_{pa}$ (exact) for the same values of Q_p. It is seen from Fig. 4.5 that $\hat{Q}_{pa}$ and $\hat{\omega}_{pa}$ can be obtained quite accurately from (4.29) over the useful frequency range of operation, that is, the frequency range over which the deviations of $\hat{Q}_{pa}$ and $\hat{\omega}_{pa}$ from their ideal values are acceptable.

From (4.27a) and (4.27c) we obtain

$$P_1 P_2 \doteq \frac{2}{B^2} \qquad (4.30a)$$

and

$$P_1 + P_2 \doteq \frac{2}{B} \qquad (4.30b)$$

From (4.30), the location of the parasitic poles $S_1 = \frac{1}{P_1}$ and $S_2 = \frac{1}{P_2}$, in the S-plane, is given by

$$S_1 = S_2^* = -\frac{B(1-J)}{2} \qquad (4.31)$$

Hence, the effect of the OA finite gain-bandwidth product is seen to introduce a complex conjugate pole pair in the left-half of the S-plane. Its magnitude = $B/\sqrt{2}$ and

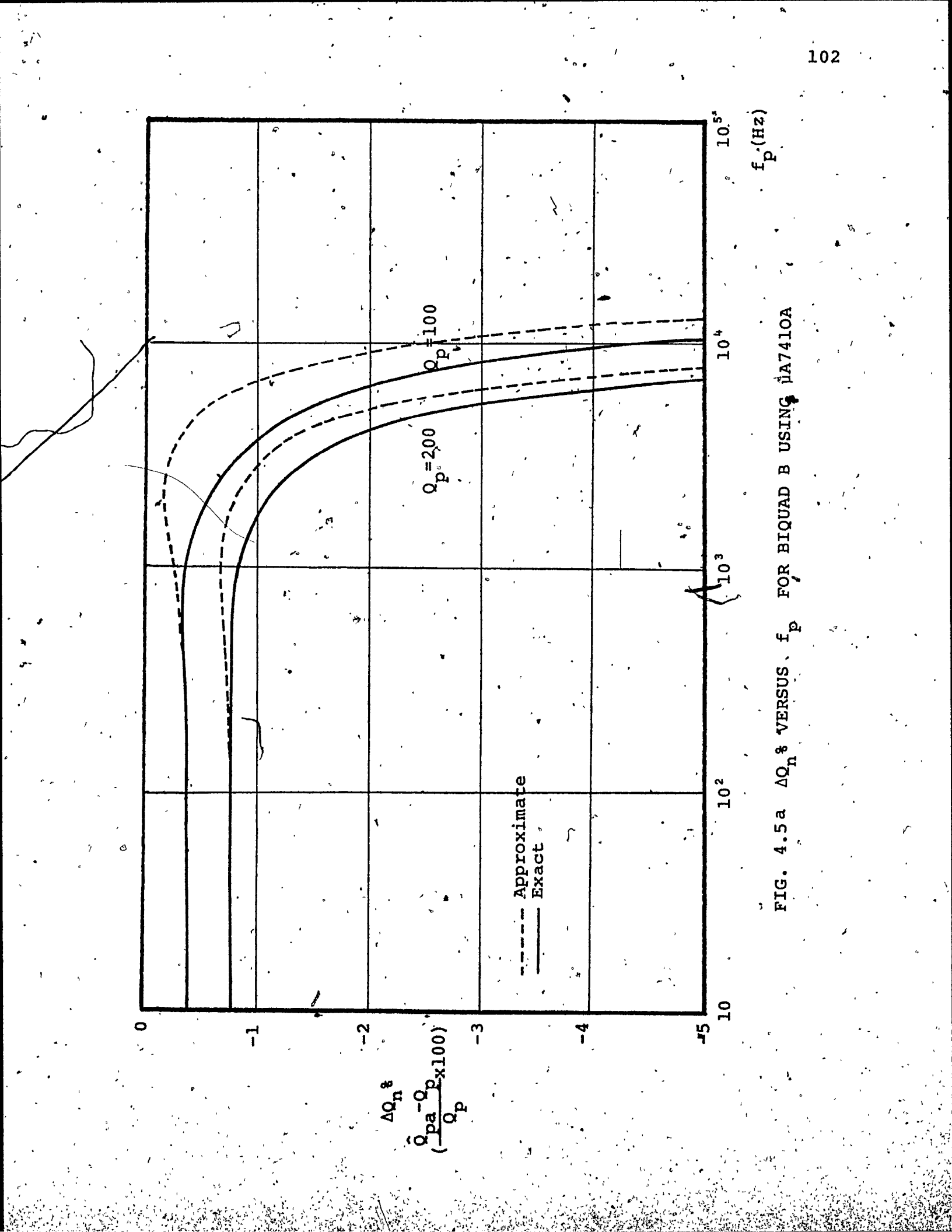

FIG. 4.5a $\Delta Q_n\%$ VERSUS f_p FOR BIQUAD B USING µA741OA

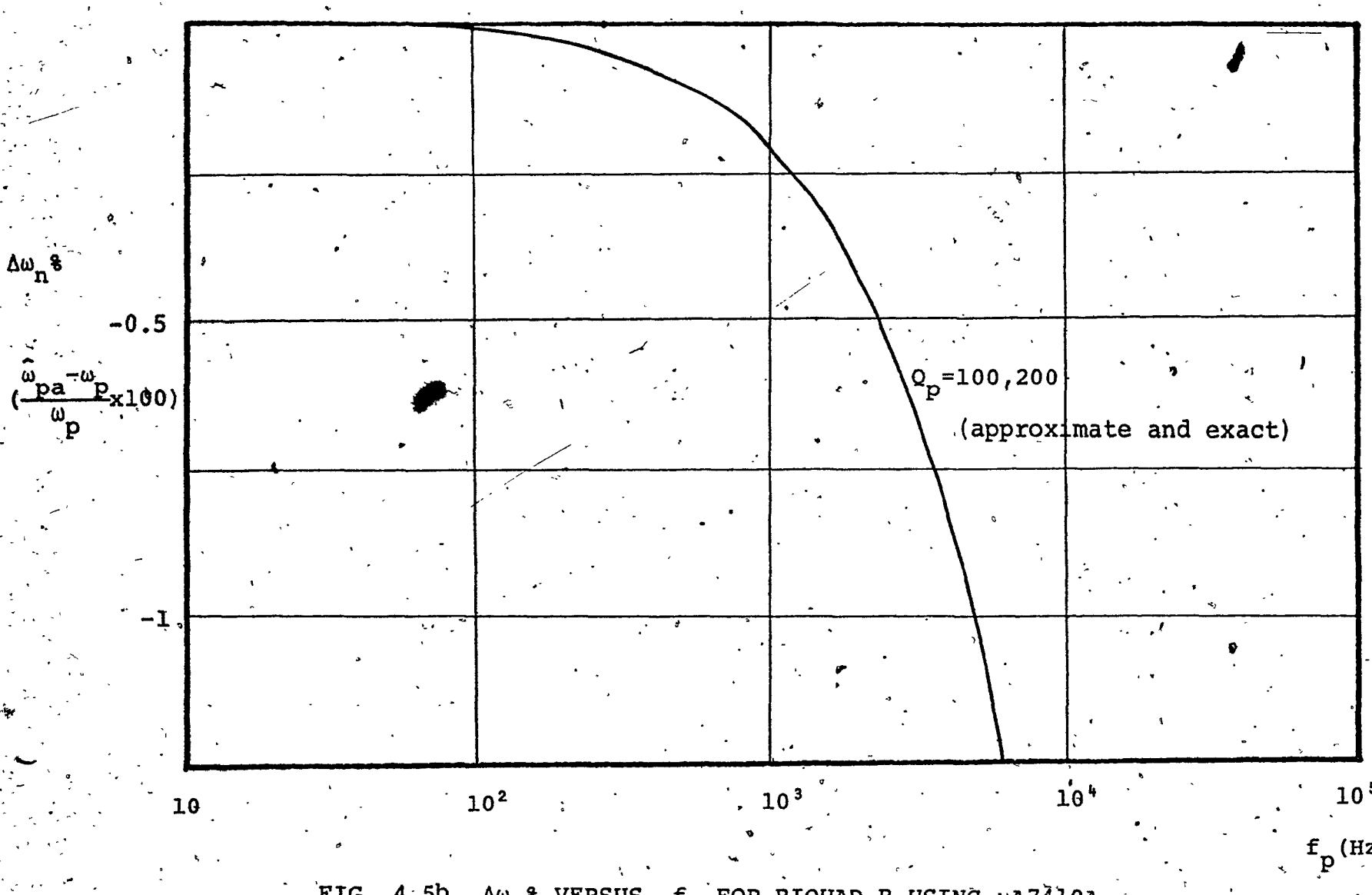

FIG. 4.5b $\Delta\omega_n$% VERSUS f_p FOR BIQUAD B USING μA7410A

phase = $\pm 3\pi/4$. The effect of this pole pair on the frequency response is weakened as B/ω_p is increased, i.e.

$$\omega_p << B \qquad (4.32)$$

Thus, the effects of the parasitic poles will be negligible provided $B >> \omega_p$.

4.6 DESIGN PROCEDURE

A design procedure is now described. Table 4.1 shows that there are several degrees of freedom in the choice of element values. These may be used to minimize $S_{A_0}^{Q_{pa}}$ or the spread of element values. By using the minimum sensitivity constraints of (4.14) and (4.20) in circuits 1,3,7 and 10, possible sets of element values for LP,HP,BP,N and AP sections have been obtained,as shown in Table 4.2. It follows from Section 4.5, that this choice of elements does not introduce parasitic poles in the right-half of the s-plane. It is seen that the notch frequency ω_n, the undamped frequency of oscillation ω_p and the Q-factor Q_p can be easily adjusted by trimming three distinct resistors. A tuning sequence is also given in Table 4.2.

It is to be noted from Table 4.2, for the design of N sections, that

$$\omega_n^2 = \omega_p G_5/C_7 \qquad (4.33)$$

TABLE 4.2

DESIGN VALUES AND TUNING PROCEDURE

CIRCUIT NUMBER (from Table 1)	DESIGN VALUES	TRANSFER FUNCTION REALIZED	TUNING SEQUENCE		
			ω_n	ω_p	Q_p
1	$G_1=G_4=G_5=G_8=G$, $G_3=G/Q_p$, $C_2=C_3=C$ where $C=\frac{G}{\omega_p}$	$T_2 = \frac{2\omega_p^2}{D(s)}$	—	G_8	G_3
3	$G_1=G_2=G_4=G_6=G$, $G_8=G/Q_p$, $C_8=0$, $C_3=C_7=C$ where $C=G/\omega_p$	$T_1 = \frac{2s^2}{D(s)}$	—	G_4	G_8
7	$G_1=G_2=G_4=G_6=G$, $G_7=G/Q_p$, $G_8=0$, $C_2=C_8=C$ where $C=G/\omega_p$	$T_1 = \frac{\frac{2\omega_p}{Q_p}s}{D(s)}$	—	G_2	G_7
10	$G_1=G_2=G_4=G_5+G_6=G$, $G_8=G/Q_p$, $C_3=C_7+C_8=C$ where $\omega_p = \frac{G}{C}$ and $\omega_n^2 = \omega_p \frac{G_5}{C_7}$	$T_3 = \frac{C_7}{C}\frac{(s^2+\omega_n^2)}{D(s)}$	G_2	G_6	G_8
12	$G_1=G_2=G_4=G_5=G$, $G_6=0$, $C_3=C_7=C$, $G_8=G/Q_p$ where $\omega_p=G/C$	$T_1 = \frac{D(-s)}{D(s)}$	G_4		G_8

$D(s) = s^2 + (\omega_p/Q_p)s + \omega_p^2$

where $G_5+G_6 = G, C_7+C_8 = C$ and $\omega_p = \frac{G}{C}$.

Hence

$$\frac{\omega_n^2}{\omega_p^2} = \frac{G_5}{G} \cdot \frac{C}{C_7} \qquad (4.34)$$

where

$$\frac{G_5}{G} \text{ is always } \leq 1$$

and

$$\frac{C}{C_7} \text{ is always } \geq 1$$

It is seen from (4.34) that for $\omega_n \leq \omega_p$, C_8 can be set to zero ($C_7 = C$) and only two capacitors per section are used. For $\omega_n > \omega_p$, three capacitors are required. In all cases, irrespective of the choice of C_7 and C_8, the total capacitance per section is always the same and equals 2C.

In most applications, where notch sections are used, $\frac{\omega_n}{\omega_p}$ is close to unity and care should be taken when choosing G_5 and C_7 in (4.34). A suitable choice of G_5, G_6, C_7 and C_8 values may be obtained by letting $\frac{G_5}{G} = \frac{1}{K}$ and $\frac{C}{C_7} = 2$. Thus, K is approximately equal to 2($K < 2$ for $\omega_n > \omega_p$ and $K > 2$ for $\omega_n \leq \omega_p$). The suggested choice yields a capacitor spread = 2 and each of R_5 and R_6 is approximately equal to 2R.

4.7 COMPARISON WITH KHN, TG AND TH REALIZATIONS

The salient features of the design, Biquad B, are listed in Table 4.3 along with those of KHN, TG and TH designs. These properties are derived under the same assumptions as those made in deriving similar properties in Table 3.4.

The Table shows that the passive element sensitivities are about the same for all the realizations, of the order of unity. However, amongst the four, the proposed design has a slightly higher dependence of Q_p on the finite d.c. gain (A_0) of the OA's. However, Q_p is relatively independent of the amplifier bandwidth as in the case of the realization due to TG. It is also observed that the finite bandwidth affects ω_p slightly more in Biquad B compared to the others. For the same total capacitance 2C, where $C = \frac{1}{\omega_p R}$, all the realizations have the same value for the maximum resistance, namely, RQ_p. For the same value of R, all the realizations use the same total capacitance 2C. The LP, HP, BP and AP sections use the minimal number of capacitors (two) in all the methods and the capacitors are equal. The N section in the proposed design (circuit No. 10', Table 4.1) uses three capacitors for $\omega_n > \omega_p$ and has a spread in capacitors of 2, while the total capacitance is 2C. For $\omega_n \leq \omega_p$ the section can be designed with two capacitors of equal value. An isolation amplifier is required if this section is connected to a low impedance load. If Sections 8

TABLE 4.3

COMPARISON WITH KHN, TG AND TH

REALIZATION	$\omega_p << B$						EFFECT OF FINITE OA'S BANDWIDTH		$\frac{C_{max}}{C_{min}}$	$\frac{R_{max}}{R_{min}}$	R_{max}	NO. OF OA'S REQUIRED				
	$\lvert S^{Q_p}_{R,C}\rvert$	$\lvert S^{\omega_p}_{R,C}\rvert$	$\lvert S^{\omega_z}_{R,C}\rvert$	$\lvert S^{Q_z}_{R,C}\rvert$	$\lvert S^{\omega_p}_{A_0}\rvert$	$\lvert S^{Q_p}_{A_0}\rvert$	$Q_p/Q_{pa} =$	$\omega_p^2/\omega_{pa}^2 =$				LP	HP	BP	N	AP
PROPOSED DESIGN	≤ 1	≤ 1	≤ 1	≤ 1	$\frac{-1}{A_0 Q_p} = 0$	$\frac{4Q_p}{A_0}$	$1 + \frac{4Q_p}{A_0} - \frac{2\omega_p}{B}$	$1 + \frac{4\omega_p}{B}$	1	Q_p	RQ_p	2	2	2	2	2
STATE VARIABLE (KHN)	≤ 1	≤ 1	≤ 1	≤ 1	0	$\frac{2Q_p}{A_0}$	$1 + \frac{2Q_p}{A_0} - \frac{4Q_p\omega_p}{B}$	$1 + \frac{2\omega_p}{B}$	1	$2Q_p$	RQ_p	3	4	3	4	4
TARMI AND GHAUSI (TG)	$\leq \frac{1}{2}$	≤ 1	≥ 1	≥ 1	0	$\frac{3Q_p}{A_0}$	$1 + \frac{3Q_p}{A_0} - \frac{3\omega_p}{2B}$	$1 + \frac{3\omega_p}{B}$	1	Q_p	RQ_p	4	4	4	4	4
BIQUAD (Th)	≤ 1	≤ 1	≥ 1	≥ 1	0	$\frac{2Q_p}{A_0}$	$1 + \frac{2Q_p}{A_0} - \frac{4Q_p\omega_p}{B}$	$1 \quad \frac{2\omega_p}{B}$	1	Q_p	RQ_p	3	4	3	4	4

or 9 in Table 4.1 are used as N sections, the isolation amplifier is not necessary. Tuning, however, has to be achieved through capacitors. The advantage of Circuit No. 10 is that it can be tuned easily using resistors. This facility may frequently outweigh the price paid for an additional amplifier.

Thus, we observe from Table 4.3, that Biquad B has comparable performance to that of the realizations due to KHN, TG and TH, while at the same time, requiring only two OA's and a simpler network.

Although the prices of OA's are low and still decreasing, reducing the number of OA's without sacrificing the performance unduly is desirable, since this will mean a reduction in power supply and heat dissipation requirements which, in turn, will lead to more compact sizes of the filters. These advantages will be more fully realized for large volume applications.

4.8 EXPERIMENTAL RESULTS

Using Table 4.2, resistors, capacitors and OA's similar to those described in Section 3.10, the two filter-specifications realized previously in Section 3.10 using Biquad A, were designed and built.

4.8.1 Low-Pass Filter

The realization uses cascaded sections of Type No. 1, in Table 4.2, as shown in Fig. 4.6a. The measured frequency response (input level = 50 mv) shown in Figs. 4.6b and 4.6c agrees with the theoretical response. The effect of d.c. - supply variations is illustrated in Fig. 4.6d. The deviation in the passband ripple is about 0.1 dB for supply voltages in the range ±5V to ±15V. The effect of temperature variations is illustrated in Fig. 4.6e, which shows the frequency response at -10°C (right-hand curve, 20°C and 70°C (left-hand curve). The last peak has been displaced horizontally by 42 Hz which corresponds to a change of 133 p.p.m. per deg. C. The frequency displacement is due to passive-element variations, and is within the predicted value.

4.8.2 Band-Pass Filter

The realization uses cascaded sections of the types 3 and 10, in Table 4.2 and is shown in Fig. 4.7a. The measured frequency response is shown in Figs. 4.7b and 4.7c, and it is in agreement with the theoretical response. Fig. 4.7d shows the frequency response for supply voltages of ±7.5V (lower curve) and ± 15V, the input is 0.3V. The passband ripple remains less than 0.39 dB and the deviation in the stopband is negligible. Figs. 4.7e and 4.7f illustrate the effect of temperature variations. The passband ripple

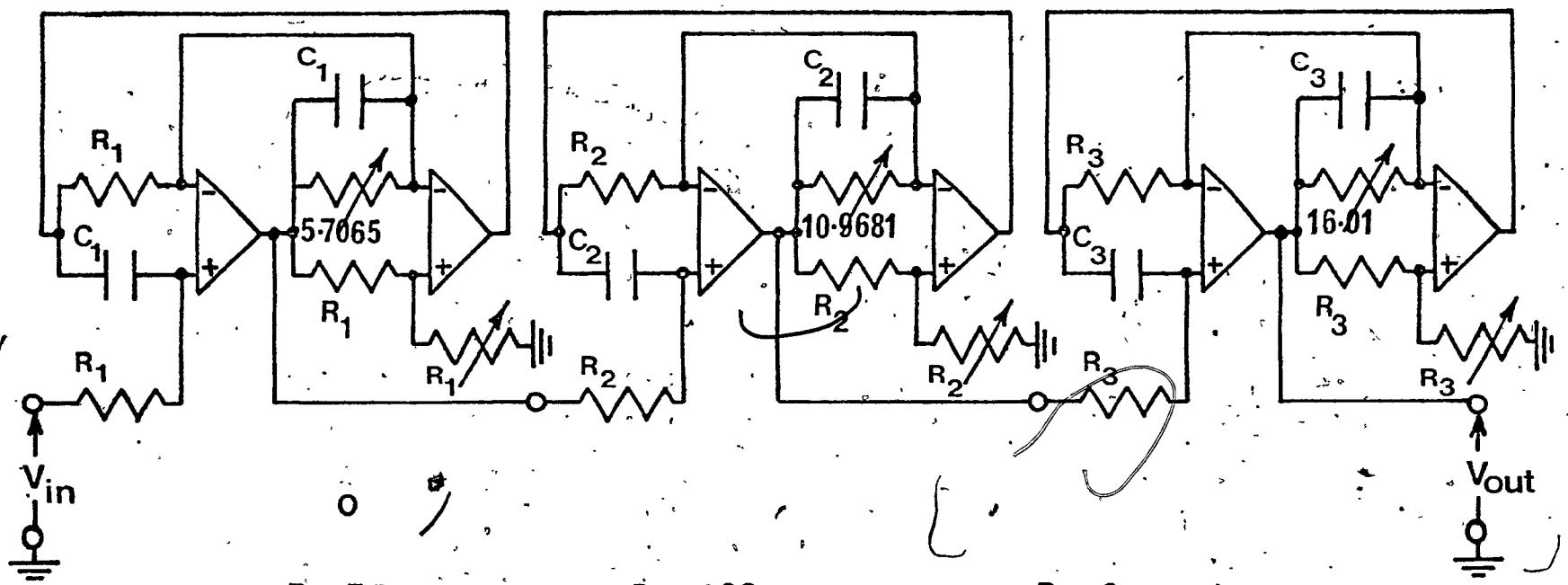

$R_1 = 7{\cdot}5$, $R_2 = 4{\cdot}99$, $R_3 = 2$

$C_1 = 15{\cdot}103$, $C_2 = 10{\cdot}734$, $C_3 = 20{\cdot}093$

(R's in kilo ohms, C's in nano farads)

$$T(s) = \frac{2 \times 0{\cdot}12470686}{s^2 + 0{\cdot}4641254\,s + 0{\cdot}12470686} \times \frac{2 \times 0{\cdot}55771963}{s^2 + 0{\cdot}3397634\,s + 0{\cdot}55771963} \times \frac{2 \times 0{\cdot}99073288}{s^2 + 0{\cdot}1243620\,s + 0{\cdot}99073288}$$

(a)

FIG. 4.6a REALIZATION OF THE SIXTH ORDER CHEBYCHEV LOW-PASS FILTER

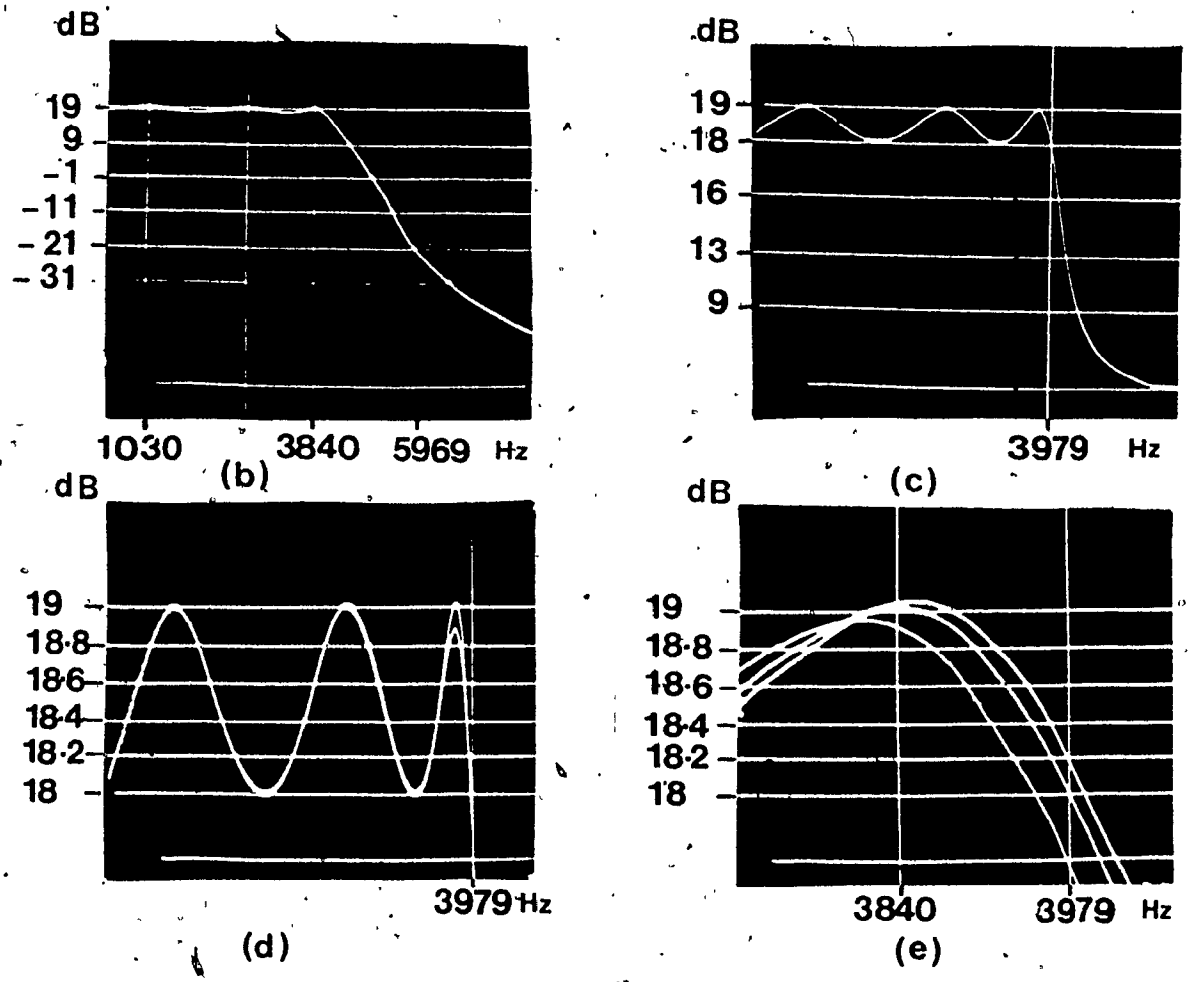

FIG. 4.6b-4.6e FREQUENCY RESPONSE:

4.6b LOGARITHMIC GAIN SCALE AND LINEAR FREQUENCY SCALE

4.6c LINEAR GAIN AND FREQUENCY SCALES

4.6d FREQUENCY RESPONSE FOR SUPPLY VOLTAGES ±5v(LOWER CURVE) AND ±15v, INPUT LEVEL = 0.05v

4.6e FREQUENCY RESPONSE AT TEMPERATURES -10°C(RIGHT-HAND CURVE),20°C AND 70°C (LEFT-HAND CURVE)

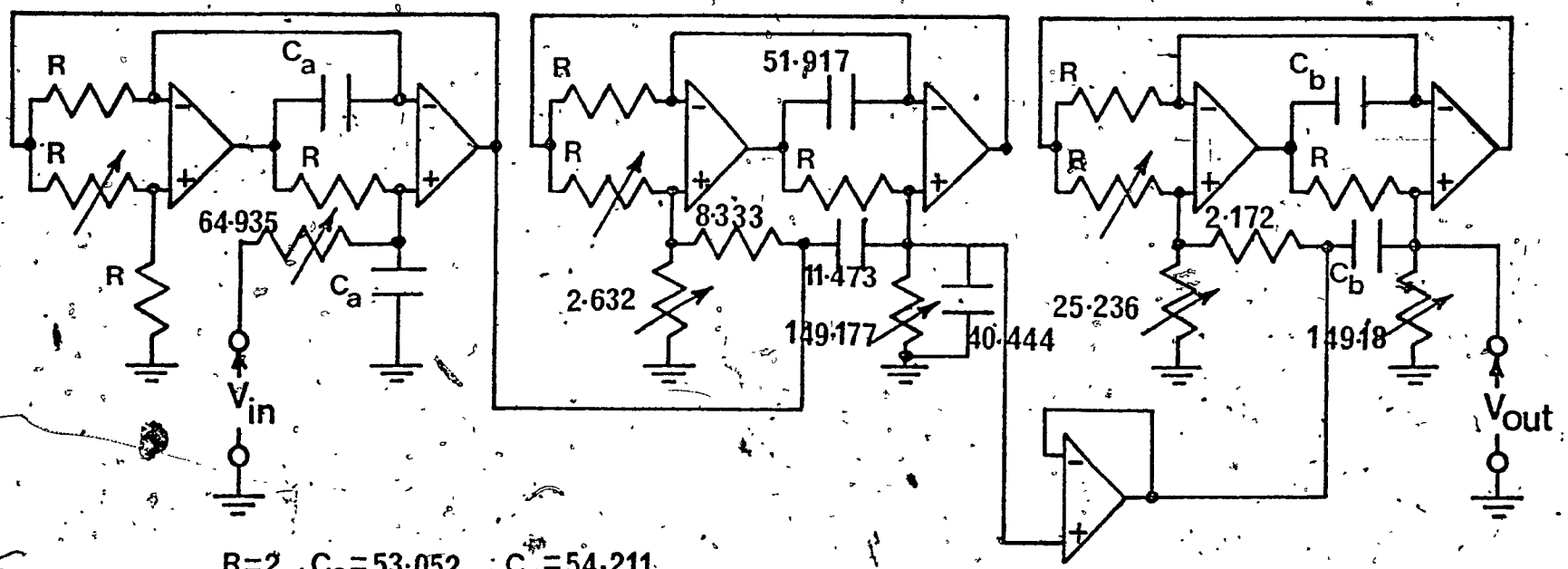

$R=2$, $C_a=53{\cdot}052$; $C_b=54{\cdot}211$

(R's in kilo ohms, C's in nano farads)

$$T(s)=\frac{2\times 0{\cdot}03080\ s}{s^2+0{\cdot}03080\,s+1}\times\frac{0{\cdot}220974\,(s^2+1{\cdot}1341)}{s^2+0{\cdot}01370\,s+1{\cdot}0442}\times\frac{s^2+0{\cdot}8818}{s^2+0{\cdot}01312\,s+0{\cdot}9577}$$

(a)

FIG. 4.7a REALIZATION OF THE SIXTH-ORDER ELLIPTIC BAND-PASS FILTER

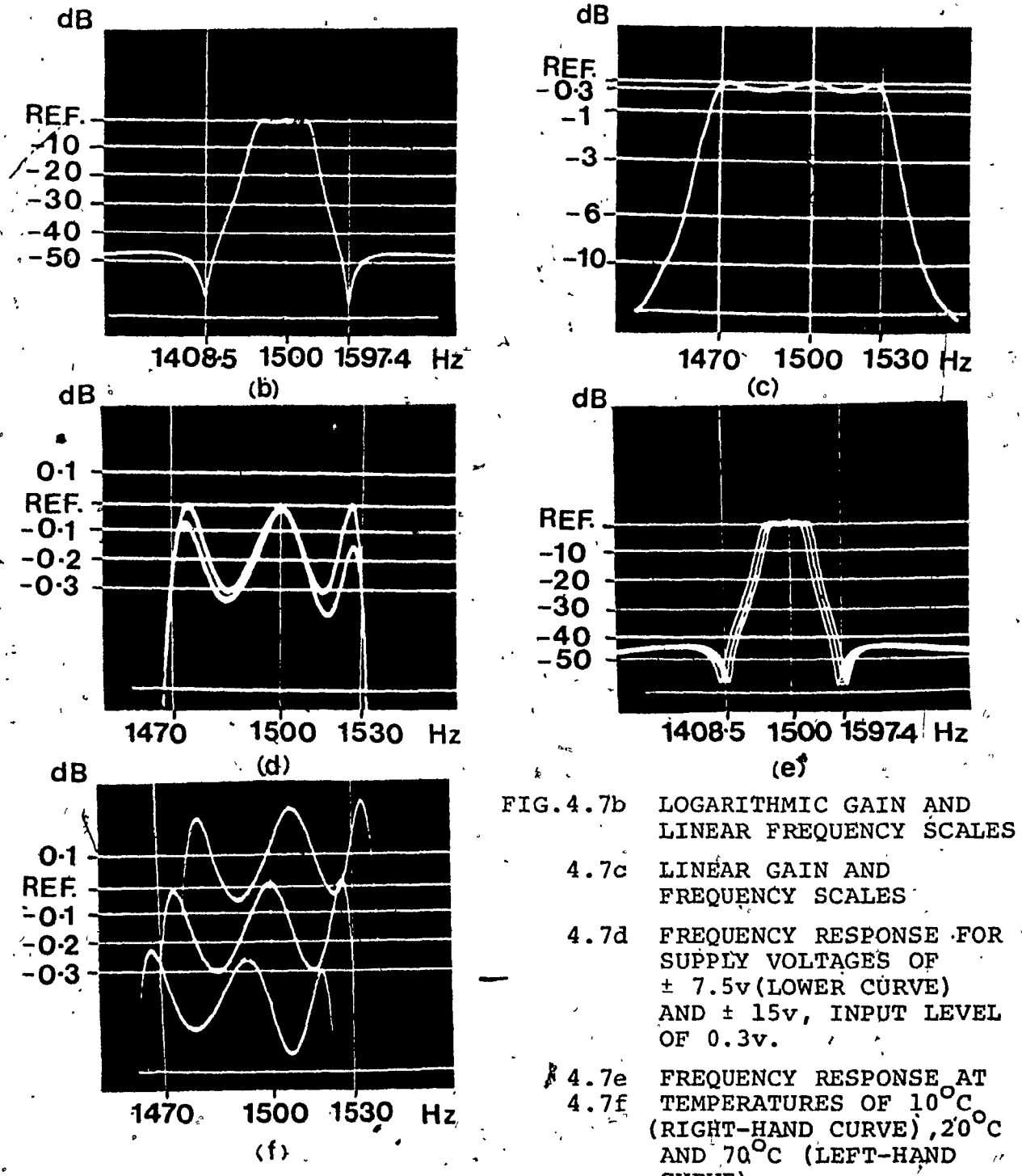

FIG.4.7b LOGARITHMIC GAIN AND LINEAR FREQUENCY SCALES

4.7c LINEAR GAIN AND FREQUENCY SCALES

4.7d FREQUENCY RESPONSE FOR SUPPLY VOLTAGES OF ± 7.5v(LOWER CURVE) AND ± 15v, INPUT LEVEL OF 0.3v.

4.7e 4.7f FREQUENCY RESPONSE AT TEMPERATURES OF 10°C (RIGHT-HAND CURVE), 20°C AND 70°C (LEFT-HAND CURVE)

FIG. 4.7b-4.7f FREQUENCY RESPONSE

remains less than 0.35 dB in the temperature range -10°C to 70°C. A centre frequency displacement of 15 Hz has been measured which corresponds to a change of 125 p.p.m. per deg. C.

4.9 CONCLUSIONS

A new configuration has been proposed for the synthesis of RC-active networks. This has been used to design a number of universal second-order sections such as low-pass, high-pass, band-pass and notch sections. By using these sections most of the practical filter specifications can be realized. Each section employs a CGICB which can be implemented by using only two op.amps. The sensitivities of $Q_p, \omega_p, Q_z, \omega_z$ and also the multiplier constant of the realization has been found to be low with respect to the passive and active element variations. A simple tuning sequence by adjusting only resistors has been described for circuits 1,3,7 and 10. With the exception of one of the notch sections in the twelve circuits considered, the output can be located at one of the op.amp. output terminals. Consequently, these sections can be cascaded without isolating amplifiers. It is found that the realizations are free from low frequency unstable modes of operation. Furthermore, the amplifier pole does not introduce any high frequency unstable mode. Also, Q_p is not affected by the amplifier pole ω_c, provided $A_0\omega_c >> \omega_p$. Experimental results show close agreement between theory and practice. Further, these results

indicate that these realizations are insensitive to temperature and power supply variations. The design procedure has been compared with those due to KHN, TG and TH and has been found to have comparable properties as observed from Table 4.3.

CHAPTER V

COMPARISON OF THE PERFORMANCES OF BIQUAD A AND BIQUAD B

CHAPTER V

COMPARISON OF THE PERFORMANCES OF BIQUAD A AND BIQUAD B

5.1 INTRODUCTION

The purpose of this Chapter is to present a detailed comparison of the performances of the biquadratic realizations described in Chapters 3 and 4*. First, the comparison is made, based on the theory introduced in Chapters 3 and 4. Further comparisons are then drawn from the results of digital computer simulations. The realizations are assumed to be implemented using one of the best available OA's (at the time of writing this thesis), namely, Fairchild μA715. Finally, experimental results of designs A-II and B, implemented using one of the lowest priced, commercial OA's, (μA741C), are given and compared.

5.2 COMPARISON - PART I

In this section, the important properties of A-I, A-II and B obtained previously in Chapters 3 and 4 are tabulated.

Table 5.1 gives, for LP, HP, BP, AP and N sections, the different sensitivities to the passive and active elements, the influence of the amplifier pole on Q_p and ω_p and the number of OA's required per second order section.

---

* In this Chapter, A-I, A-II and B are used to abbreviate Biquad A-Design I, Biquad A-Design II and Biquad B Design, respectively.

TABLE 5.1

COMPARISON OF THE PROPERTIES OF BIQUAD A AND BIQUAD B

REALIZATION	$\omega_p << B$						EFFECT OF FINITE-OA BANDWIDTH		NO. OF OA'S REQUIRED
	$\lvert S^{Q_p}_{R,C}\rvert$	$\lvert S^{\omega_p}_{R,C}\rvert$	$\lvert S^{Q_z}_{R,C}\rvert$	$\lvert S^{\omega_z}_{R,C}\rvert$	$S^{Q_p}_{A_0}$	$S^{\omega_p}_{A_0}$	$Q_p/\hat{Q}_{pa}$	$\omega_p/\hat{\omega}_{pa}$	
A-I	≤ 1	≤ 1	≤ 1	≤ 1	0	0	$1+4(\frac{Q_p}{A_0})^2-4Q_p^2(\frac{\omega_p}{B})^2$	$1+4\frac{Q_p}{A_0}\cdot\frac{\omega_p}{B}$	3
A-II	≤ 1	≤ 1	≤ 1	≤ 1	$\frac{Q_p}{A_0}$	0	$1+\frac{Q_p}{A_0}-\frac{1}{2}(\frac{\omega_p}{B})+\frac{7}{2}(\frac{Q_p}{A_0})(\frac{\omega_p}{B})-3Q_p(\frac{\omega_p}{B})^2$	$1+\frac{1}{2}\frac{\omega_p}{B}-\frac{1}{8}(\frac{\omega_p}{B})^2$	3
B	≤ 1	≤ 1	≤ 1	≤ 1	$\frac{4Q_p}{A_0}$	$-\frac{1}{A_0Q_p}$	$1+4(\frac{Q_p}{A})-2(\frac{\omega_p}{B})[1-2Q_p\frac{\omega_p}{B}+4\frac{Q_p}{A_0}]$	$1+2\frac{\omega_p}{B}$	2 *

* If circuit No. 10 in Table 4 is used, an isolation amplifier is necessary

The sensitivities with respect to the passive elements are of the same order. For $\omega_p << B$, A-I has the lowest $S^{\hat{Q}_{pa}}_{A_0}$ and $S^{\hat{\omega}_{pa}}_{A_0}$. This is also seen from the fact that $\hat{Q}_{pa}$ and $\hat{\omega}_{pa}$ are independent of the first order terms of (Q_p/A_0) and (ω_p/B). However, as ω_p is increased, $\hat{Q}_{pa}$ is enhanced much faster in A-I than in the other designs. Thus Q_p enhancement is the limiting factor of the useful frequency range for this design. We also observe that $\hat{Q}_{pa}$ has the lowest deviation in A-II as compared to the other designs. Thus A-II can be operated at relatively higher frequencies compared with A-I and B. This is verified using exact computer analysis in Section 5.3.

Table 5.2 lists, for A-II and B and for LP, HP, BP, AP and N sections, the total resistance (R_T), the number of resistors (R_N) and the number of capacitors (C_N), for the same total capacitance $C_T = 2C$ per section. C_{max}/C_{min}, R_{max}/R_{min} and R_{max} are also given.

As shown in Section 3.4, for A-I, the spread in capacitors is Q_p/m for a resistive spread of m Q_p $(m \geq 1)$. Thus, the total capacitance $= C(1 + Q_p/m)$. According to the available technology, the prices of good quality capacitors, whether in lumped or integrated form, are relatively high and increase as the value of capacitance increases. Hence, Design A-I does not appear to be useful for high Q_p realizations.

TABLE 5.2

COMPARISON OF THE PROPERTIES OF BIQUAD A AND BIQUAD B

REALIZATION	LP, HP, BP, AP				N				$\frac{C_{max}}{C_{min}}$	$\frac{R_{max}}{R_{min}}$	R_{max}
	R_T	R_N	C_T	C_N	R_T	R_N	C_T	C_N			
A-II	$R(2Q_p^{\frac{1}{2}} + 3 + \alpha + \frac{1}{\alpha})$ †	7	2C	2	$\simeq R(2Q_p^{\frac{1}{2}} + 10)$	9	2C	2	1	$2Q_p^{\frac{1}{2}}$	$RQ_p^{\frac{1}{2}}$
B	$R(Q_p + 4)$	5	2C	2	$\simeq R(Q_p + 7)$	6	2C	$\begin{matrix}2 \\ \omega_n \leq \omega_p \\ 3 \\ \omega_n > \omega_p\end{matrix}$	1*	Q_p	RQ_p

Note: i) R_T, R_N, C_T and C_N denote the total resistance, the number of resistors, the total capacitance and the number of capacitors, respectively.

ii) † $\alpha = 2Q_p^{\frac{1}{2}}/(1+Q_p^{\frac{1}{2}}) \simeq 2$ for $Q_p >> 1$

iii) * $\frac{C_{max}}{C_{min}} = 2$ for $\omega_n > \omega_p$

The results given in Table 5.2 are for a multiplier constant H = 2 in LP, HP and BP and H = 1 in AP realizations. For the N section, the values of H used are $\frac{1}{\alpha}$ ($\simeq \frac{1}{2}$) and $\frac{1}{2}$ in designs A-II and B, respectively. It is also assumed that ω_n is in the vicinity of ω_p which is mostly the case in practical applications. For other values of multiplier constants or $\frac{\omega_n}{\omega_p}$, R_T, C_T, etc., can be easily computed from Tables 3.3 and 4.2.

From Table 5.2, it is seen that as Q_p increases, A-II becomes more attractive, since its R_{max} is smaller and remains within practical limits for much higher values of Q_p. Also, the total resistance R_T (for high Q_p) has a much lower value in A-II than in B, for the same total capacitance. Conversely, the total capacitance in A-II will be much lower than in Design B for the same total resistance. Thus, the total substrate area required in Design A-II will be less than that required in Design B.

5.3 COMPARISON - PART II

In this section, the dependence of $\hat{Q}_{pa}$ and $\hat{\omega}_{pa}$ on the OA d.c. gain and corner frequency are investigated using exact computer analysis. At present, the useful frequency range of passive RC elements is much larger than that of OA's. Ideally, the values of A_0 and ω_c of the OA should be infinite. In practice, A_0 is finite and ω_c is at most, of the order of few kHz. Thus, the useful frequency range is determined by

the type of OA used, as well as the properties of the RC-active technique employed. Designs AI, AII and B are simulated using one of the best available OA's, namely, Fairchild μA715, whose typical d.c. gain (A_0) = 30,000 and gain-bandwidth product (B) = 65 MHz. The influence of A_0 and ω_c is illustrated by

$$1 - \Delta Q_n\% = [(\hat{Q}_{pa} - Q_p)/Q_p] \times 100$$

versus ω_p for values of Q_p in the range 50 to 500. Typical values of A_0 and ω_c for μA715 are assumed.

2 - $\Delta\omega_n\% = [(\hat{\omega}_{pa} - \omega_p)/\omega_p] \times 100$ versus ω_p for values of Q_p in the range 50 to 500. The same typical values of A_0 and ω_c are assumed.

3,4-$\Delta Q_n\%$ and $\Delta\omega_n\%$ versus $\Delta A_{0n}\%$ [$\Delta A_{0n} = (A_0 - A_{0\,typical})/A_{0\,typical}$] for A_0 varying by ± 50% about A_0 typical (Q_p and ω_p are the parameters).

5,6- $\Delta Q_n\%$ and $\Delta\omega_n\%$ versus $\Delta\omega_{cn}\%$ [$\Delta\omega_{cn} = (\omega_c - \omega_{c\,typical})/\omega_{c\,typical}$] for ω_c varying by ± 50% about ω_c typical (Q_p and ω_p are the parameters).

From the first set of curves ($\Delta Q_n\%$ versus ω_p for Q_p = 50,200 and 500), Fig. 5.1a, 5.1b and 5.1c, it is seen that

1) For $\omega_p \ll B$, $\Delta Q_n \simeq 0$ (or slightly negative), $-Q_p/A_0$ and $-4Q_p/A_0$ for A-I, A-II and B, respectively. This agrees with the approximate formulas of $\hat{Q}_{pa}/Q_p$ in Table 5.1.

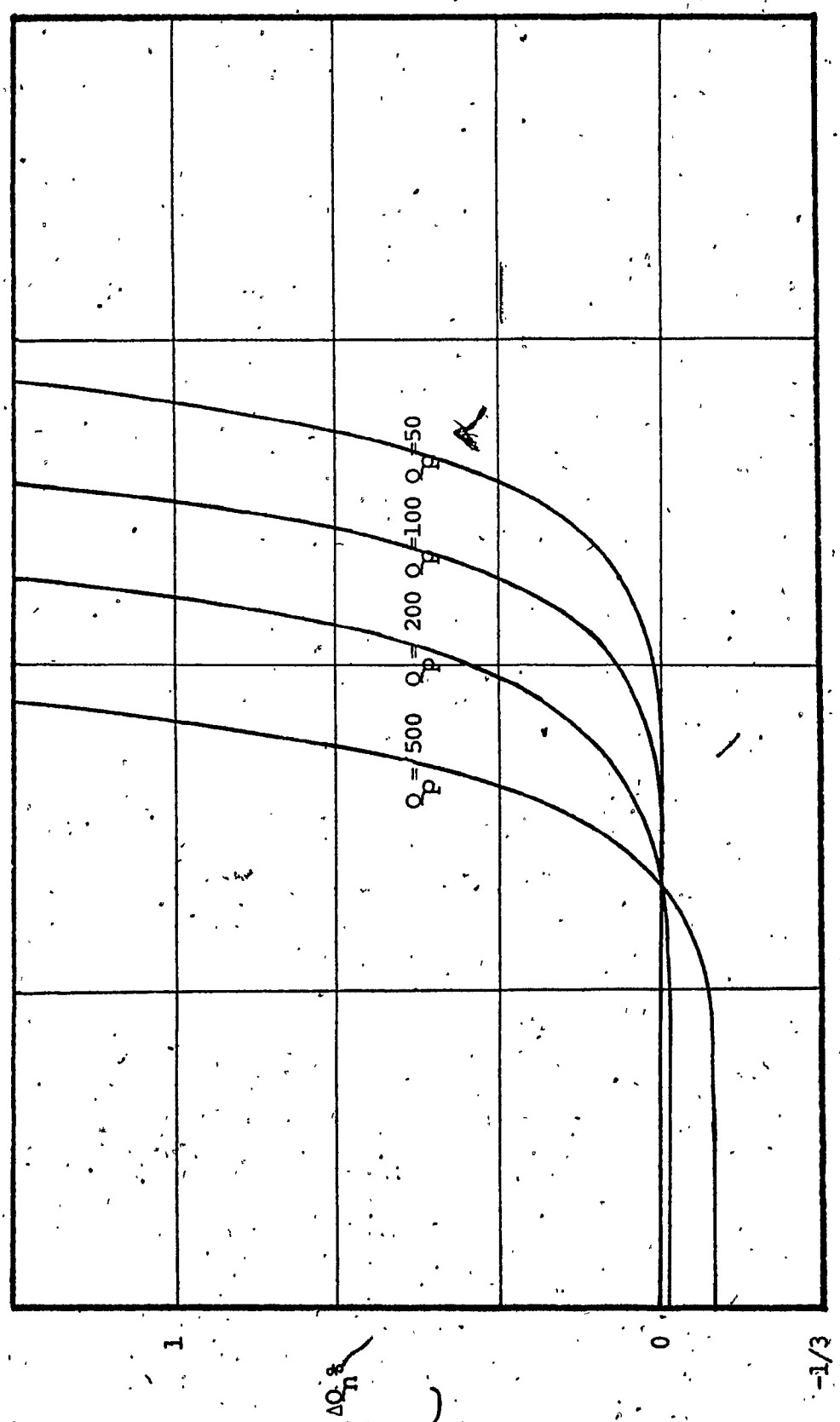

FIG. 5.1a ΔQ_n % VERSUS f_p FOR BIQUAD A - DESIGN I

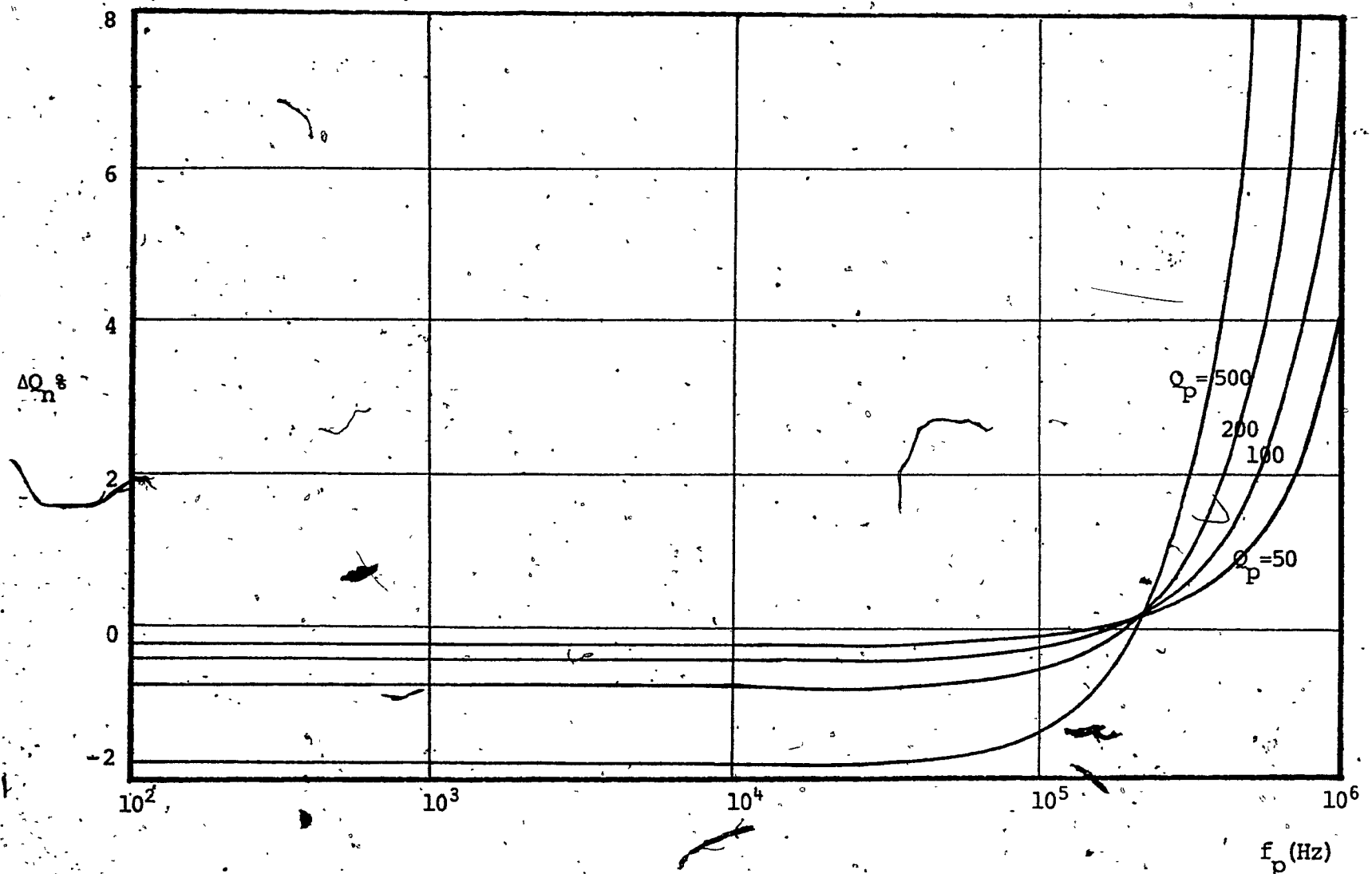

FIG. 5.1b ΔQ_n % VERSUS f_p FOR BIQUAD A - DESIGN II

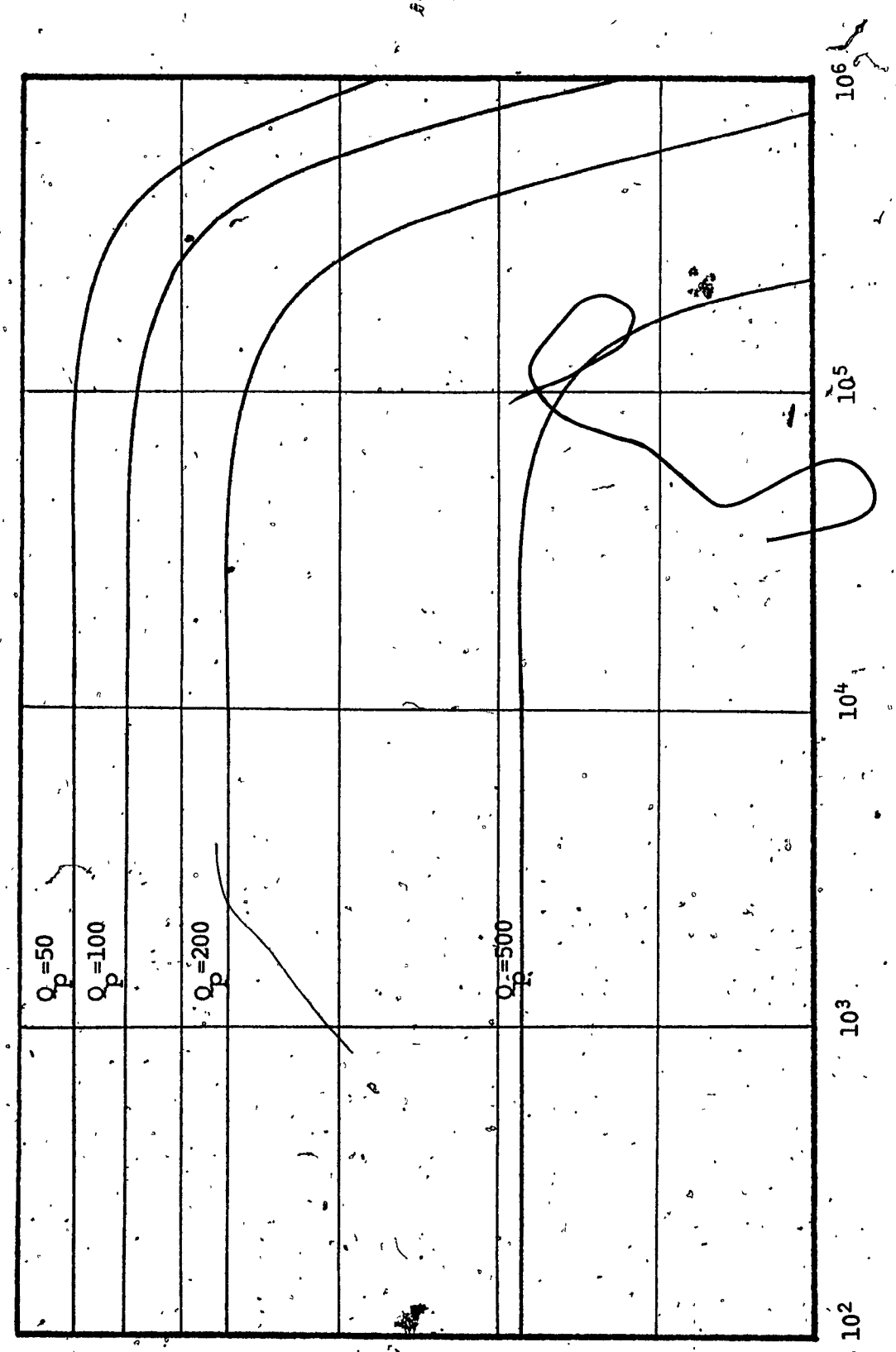

FIG. 5.1c ΔQ_n % VERSUS f_p FOR BIQUAD B

2) $|\Delta Q_n|$ remains almost constant over some range of ω_p. This value of ΔQ_n as well as the range over which it remains constant is lowest in A-I.

3) As ω_p increases, ΔQ_n becomes more negative in B, i.e., $\hat{Q}_{pa}$ decreases, while $\hat{Q}_{pa}$ increases in the other two designs. This Q enhancement starts at $\omega_p \approx 2KH_z$ in A-I and $\omega_p \approx 200\ KH_z$ in A-II.

4) All the curves in Fig. 5.1a intercept the ω_p axis at $\omega_p = \omega_c$ independent of the value of Q_p [as also predicted from (3.38a) by letting $Q_p/\hat{Q}_{pa} = 1$]. For $\omega_p > \omega_c$, there is a drastic increase in $\hat{Q}_{pa}$. Hence, for this design, the useful frequency range is severely limited. As the design has the lowest dependence of all on A_0 and ω_c below ω_c, it may still be useful for low frequency applications. However, it is recommended that OA's with as high ω_c as possible for the same B (gain-bandwidth product) be used for this design.

5) From Fig. 5.1b and 5.1c, it is seen that if a certain maximum percentage deviation is allowed in $\hat{Q}_{pa}$ due to the finite A_0 and B, then A-II is capable of realizing approximately four times the maximum Q_p obtained from Design B. This agrees with the approximate theoretical results (3.39a) and (4.29a)

In the second set of curves, Fig. 5.2, $\Delta\omega_n\%$ is plotted versus ω_p for Q_p = 50, 200 and 500. The following can be easily shown.

1) The lowest deviation $\Delta\omega_n$ is in A-I where the percentage deviation $\simeq -4(\frac{Q_p}{A_0})(\frac{\omega_p}{B})$. In most applications $4(\frac{Q_p}{A_0}) < 1$.

2) $\Delta\omega_n\%$ in A-II is $\simeq -\frac{\omega_p}{2B}$ and is slightly dependent on Q_p.

3) $\Delta\omega_n\%$ for Design B is $\simeq -\frac{2\omega_p}{B}$ which is independent of Q_p. These results all agree with theoretical predictions.

In practice, the deviations in Q_p and ω_p due to finite A_0 and ω_c or the tolerances in the passive elements are not important, as long as these deviations are within the tuning limits. Once a network is constructed, $\hat{Q}_{pa}$ and $\hat{\omega}_{pa}$ can be tuned to their nominal values as shown in Tables 3.3 and 4.2 After this post design adjustment, what is of significance is how $\hat{Q}_{pa}$ and $\hat{\omega}_{pa}$ will vary as A_0 and ω_c, as well as the passive elements change. The changes due to passive elements can be predicted from the temperature coefficients of the elements and the sensitivities to the passive elements. In practice, it is possible to cancel out the variations in resistors and capacitors by using resistors with temperature coefficients equal and opposite to those of the capacitors used. As A_0 and ω_c change due to temperature and power supply

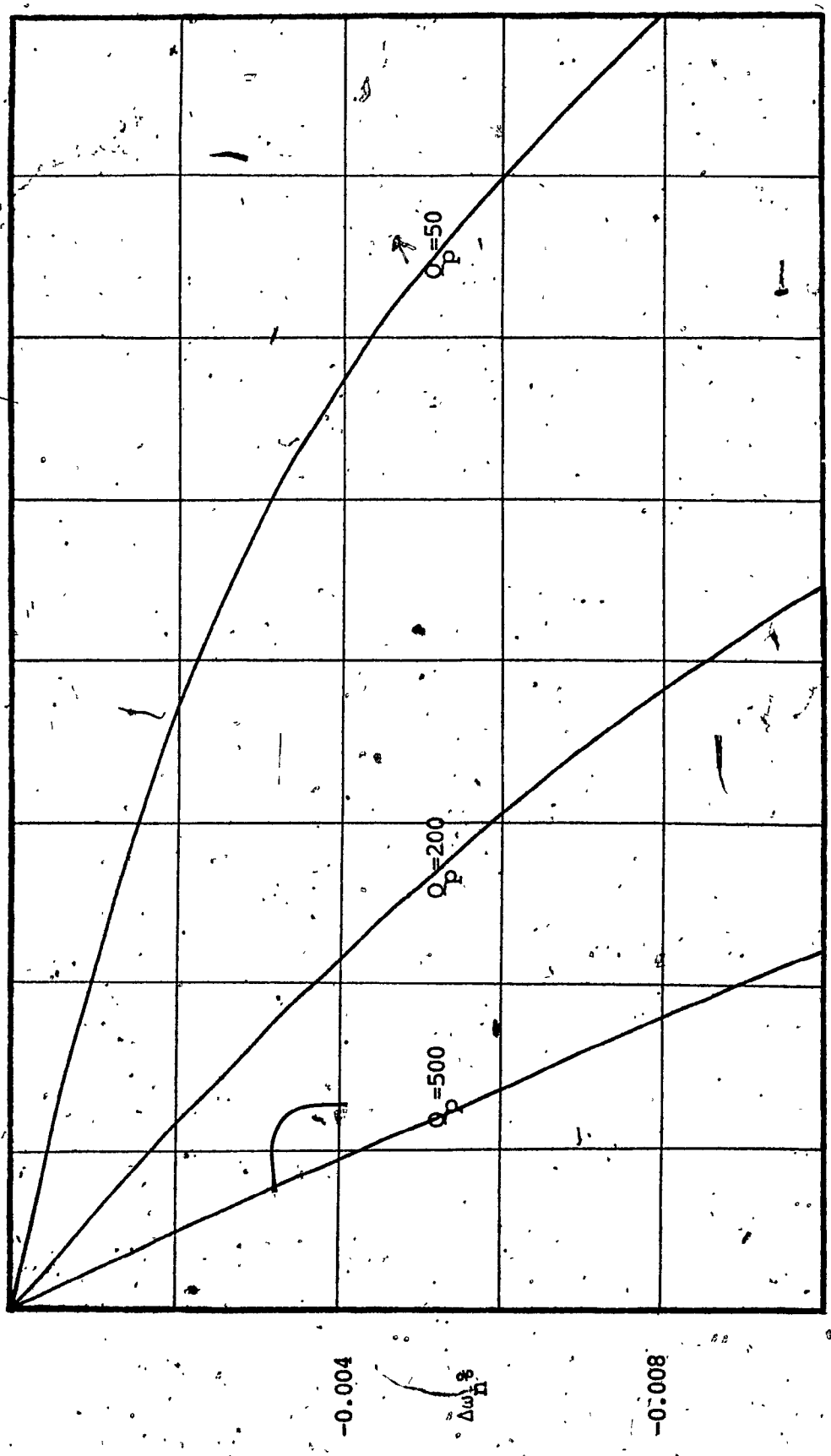

FIG. 5.2a $\Delta\omega_n$ % VERSUS f_p FOR BIQUAD A - DESIGN I

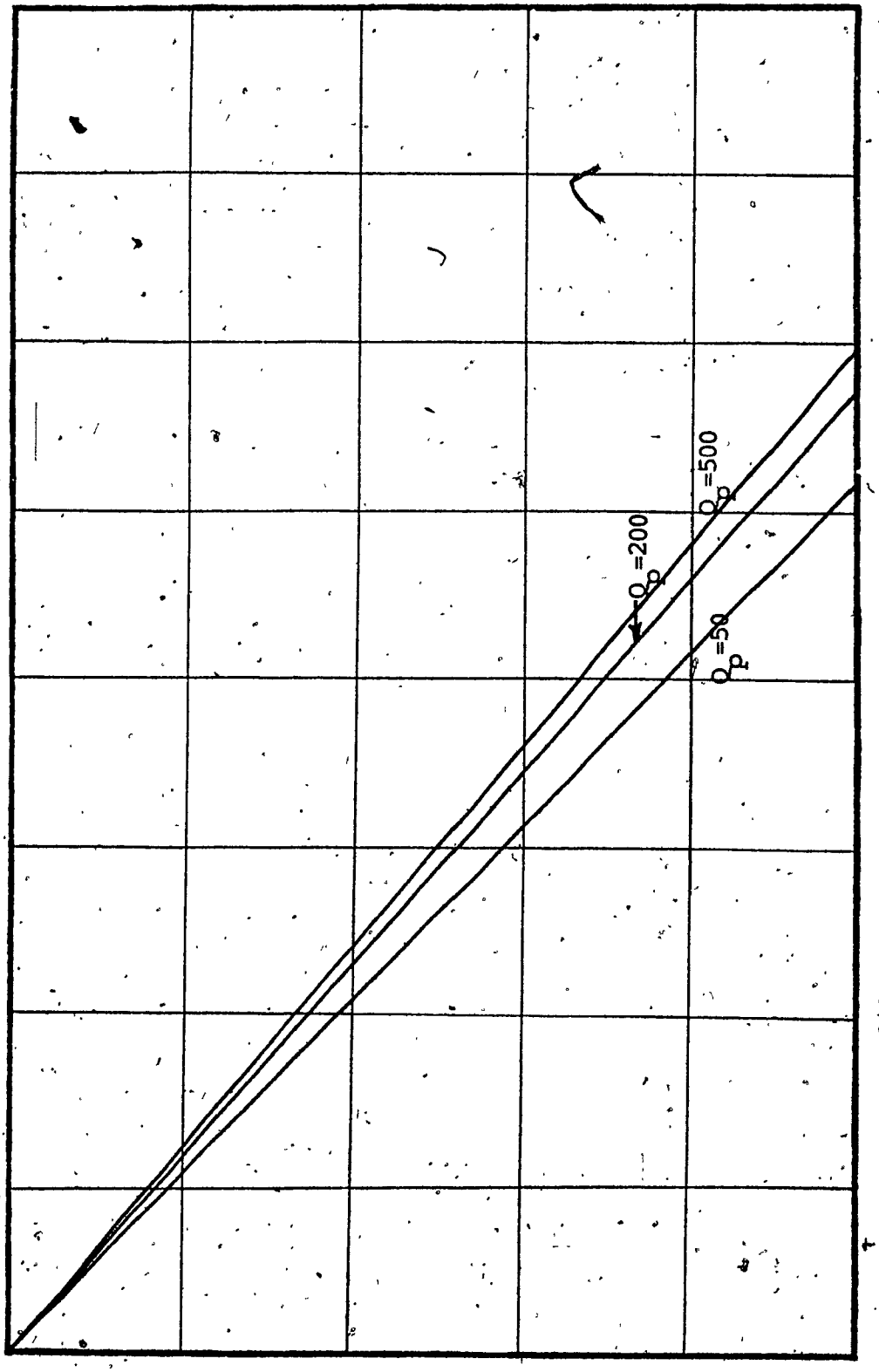

FIG. 5.2b $\Delta\omega_n$ % VERSUS f_p FOR BIQUAD A + DESIGN II

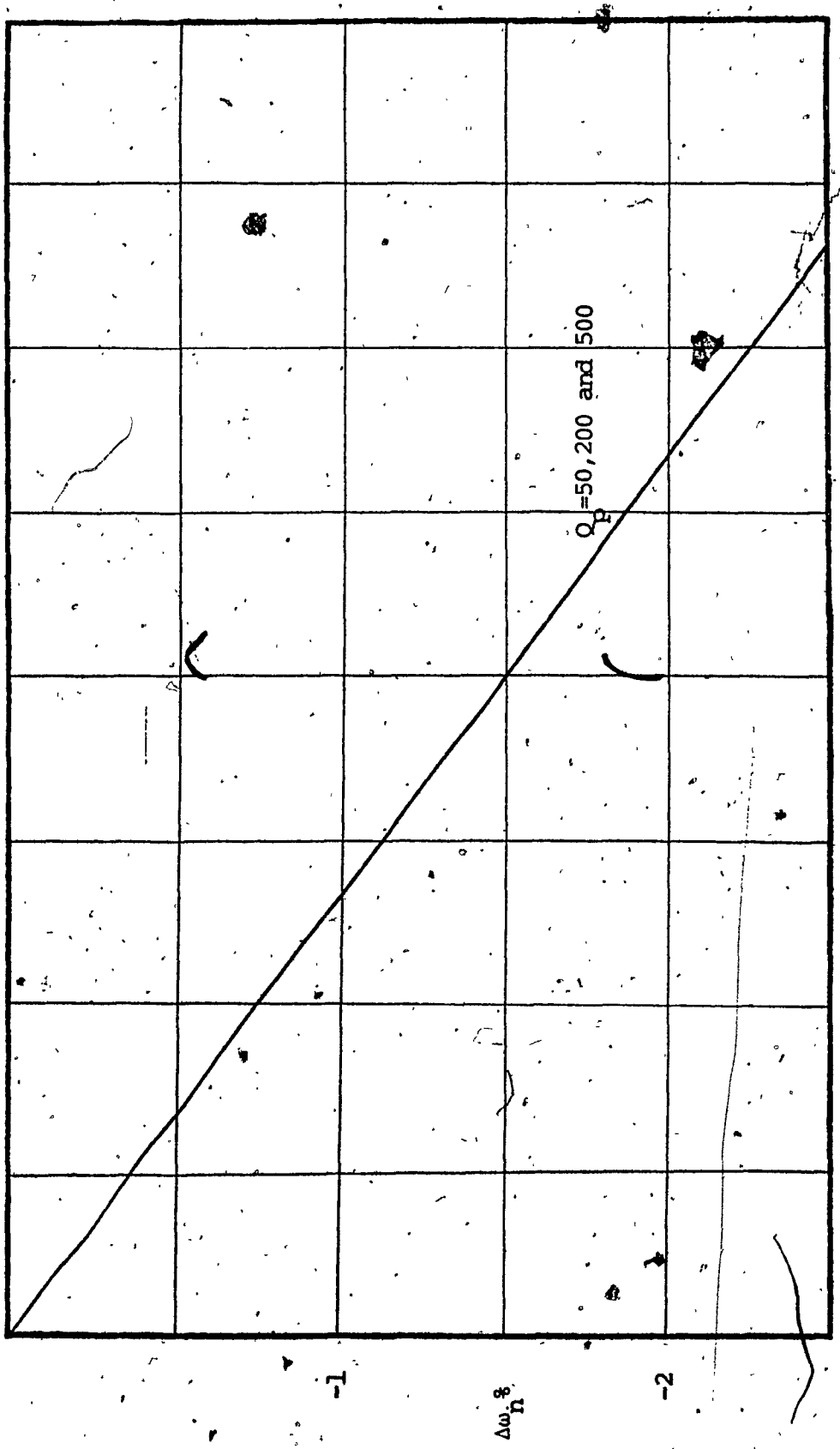

FIG. 5.2c $\Delta\omega_n\%$ VERSUS f_p FOR BIQUAD B

variations, the response may still be sensitive to these variations. From Figures 5.1 and 5.2, an idea can be obtained about the effect of gain-bandwidth variation (B) on $\hat{Q}_{pa}$ and $\hat{\omega}_{pa}$. The higher the initial deviations in $\hat{Q}_{pa}$ and $\hat{\omega}_{pa}$ from the nominal values $\hat{Q}_p$ and $\hat{\omega}_p$, the stronger the dependence of $\hat{Q}_{pa}$ and $\hat{\omega}_{pa}$ on A_0 and/or ω_c. Consequently, the changes in $\hat{Q}_{pa}$ and $\hat{\omega}_{pa}$ are larger as B changes for a given Q_p and ω_p. In sets 3-6 (Figures 5.3-5.6), $\hat{Q}_{pa}$ and $\hat{\omega}_{pa}$ are assumed to be adjusted to their nominal values for A_0 and ω_c at their typical values. Then the effect of A_0 variation up to ± 50% about A_0 typical (hence B) on $\hat{Q}_{pa}$ and $\hat{\omega}_{pa}$, as well as the effect of ± 50% variation in ω_c (hence B) on the same quantities are given, where ω_p and Q_p are taken as the parameters.

In the three sets of curves, Figures 5.3-5.6, it is seen that the deviations occurring in $\hat{Q}_{pa}$ and $\hat{\omega}_{pa}$ are smaller for the positive changes in ω_c and A compared with those occurring due to similar negative changes in ω_c and A_0.

From Figures 5.3a, 5.3b and 5.3c (ΔQ_n% versus ΔA_{0n}%), ΔQ_n is the smallest for small ω_p ($\omega_p \leq \omega_c$). As ω_p is increased, ΔQ_n in A-II becomes by far, the smallest amongst the three Designs. As an example, for 50% decrease in A_0, ω_p = 64 KH_z and Q_p = 400, A-I suffers from excessive Q enhancement, A-II has ΔQ_n% = -1 and B has ΔQ_n% = - 4.9.

From curve set 4 in Fig. 5.4 ($\Delta\omega_n$% versus ΔA_{0_n}%), it is seen that $\Delta\omega_n$ is proportional to $Q_p\omega_p$ in A-I, and has

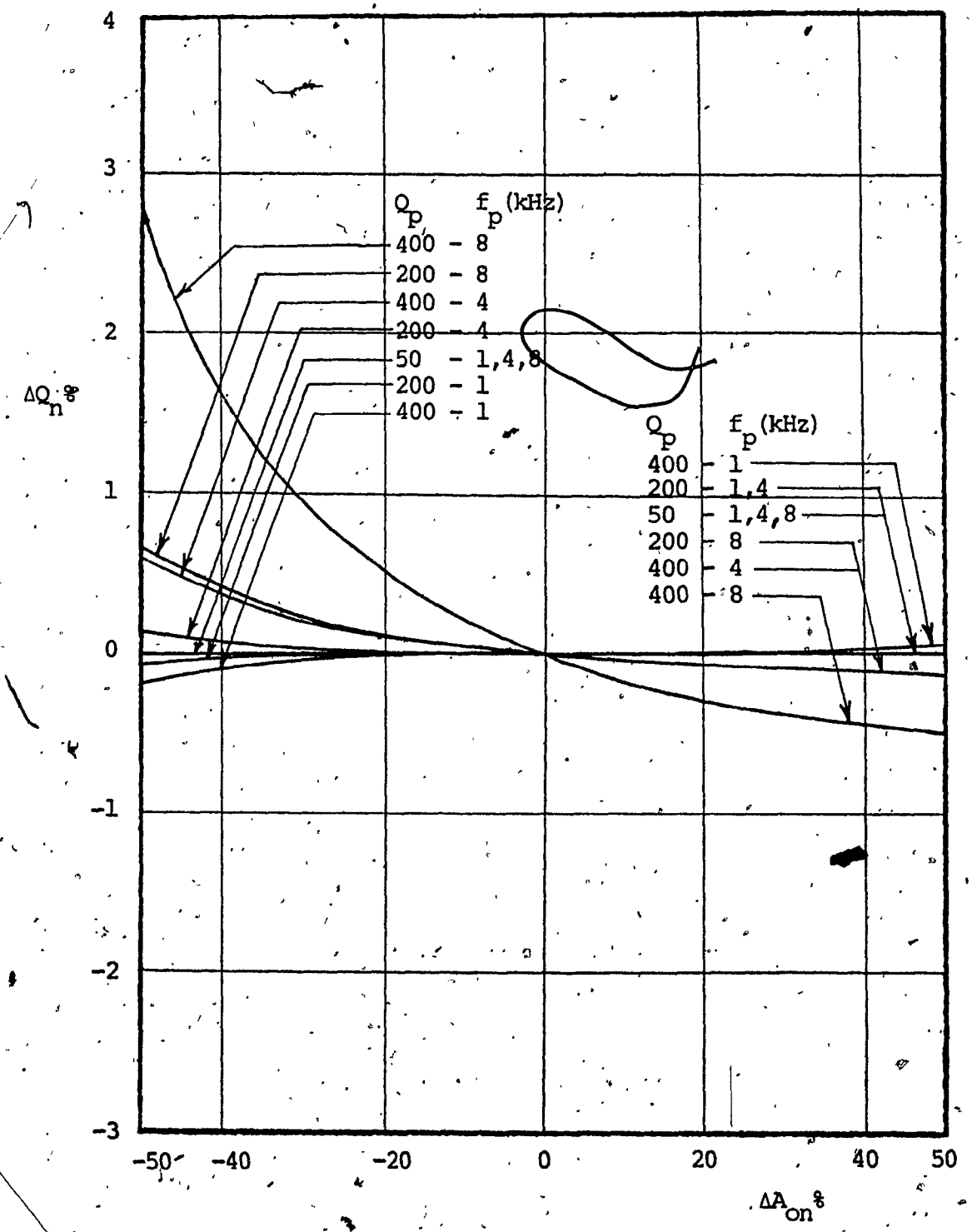

FIG. 5.3a ΔQ_n% VERSUS ΔA_{on}% FOR BIQUAD A - DESIGN I

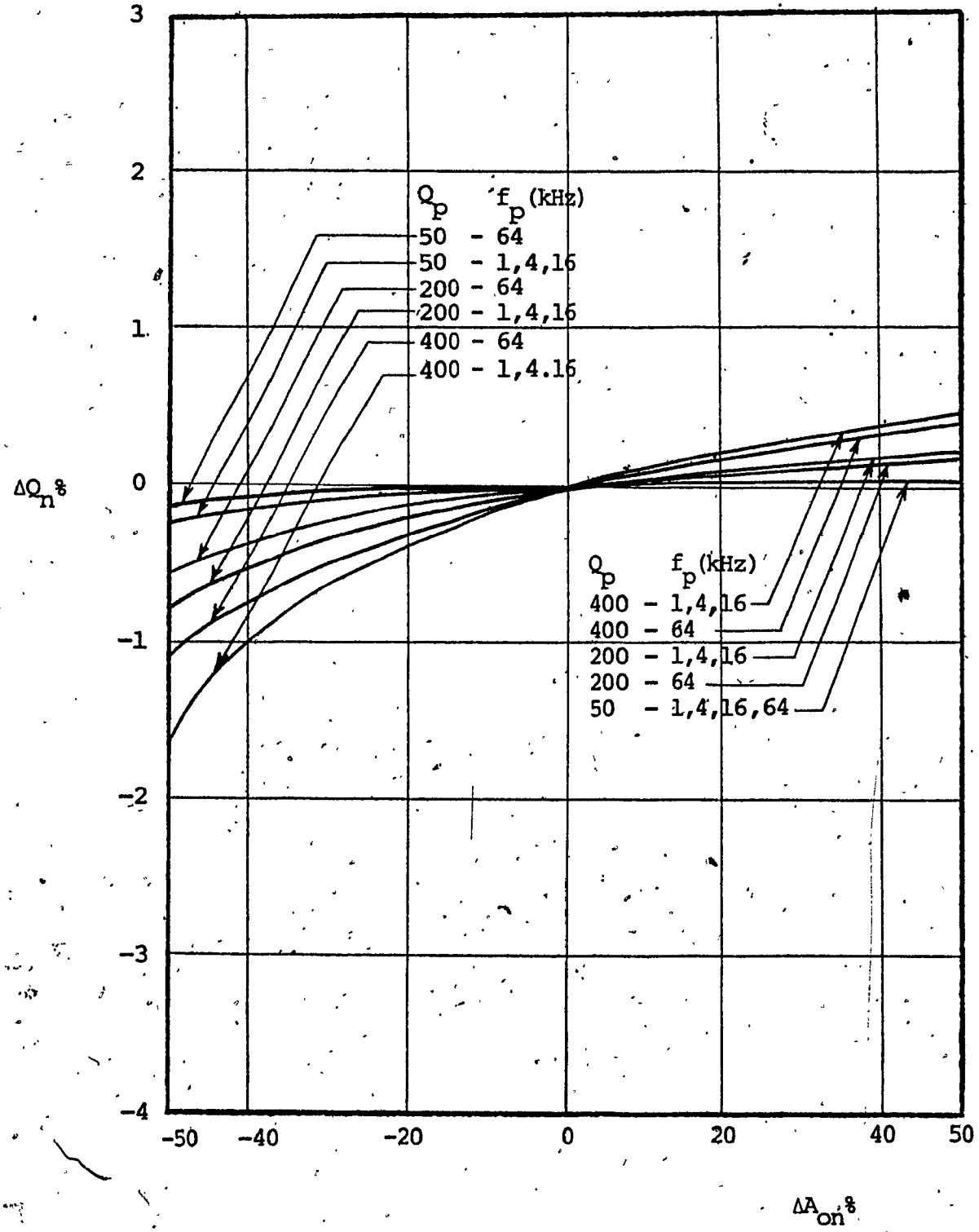

FIG. 5.3b ΔQ_n% VERSUS ΔA_{on}% FOR BIQUAD A - DESIGN II

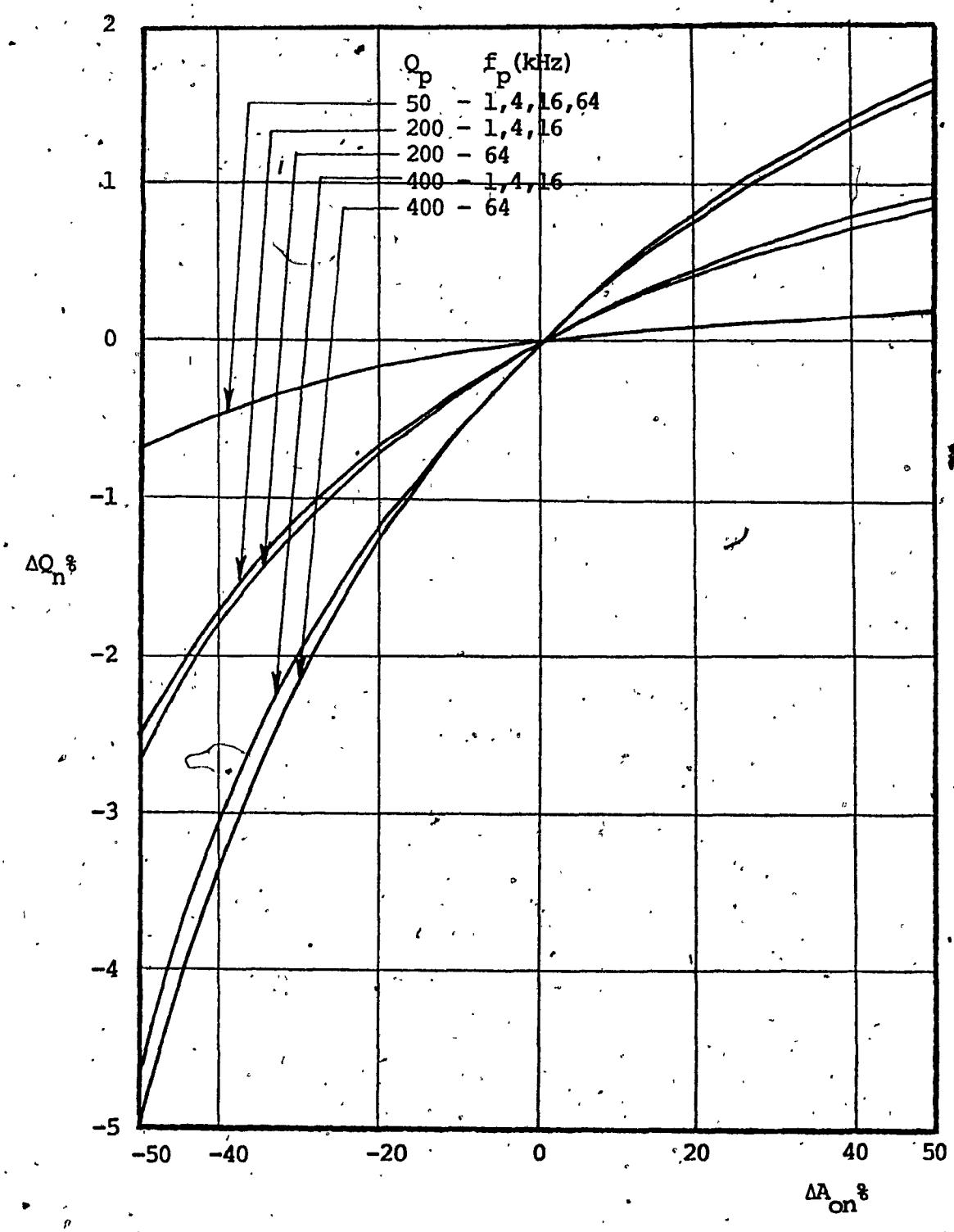

FIG. 5.3c ΔQ_n% VERSUS ΔA_{on}% FOR BIQUAD B

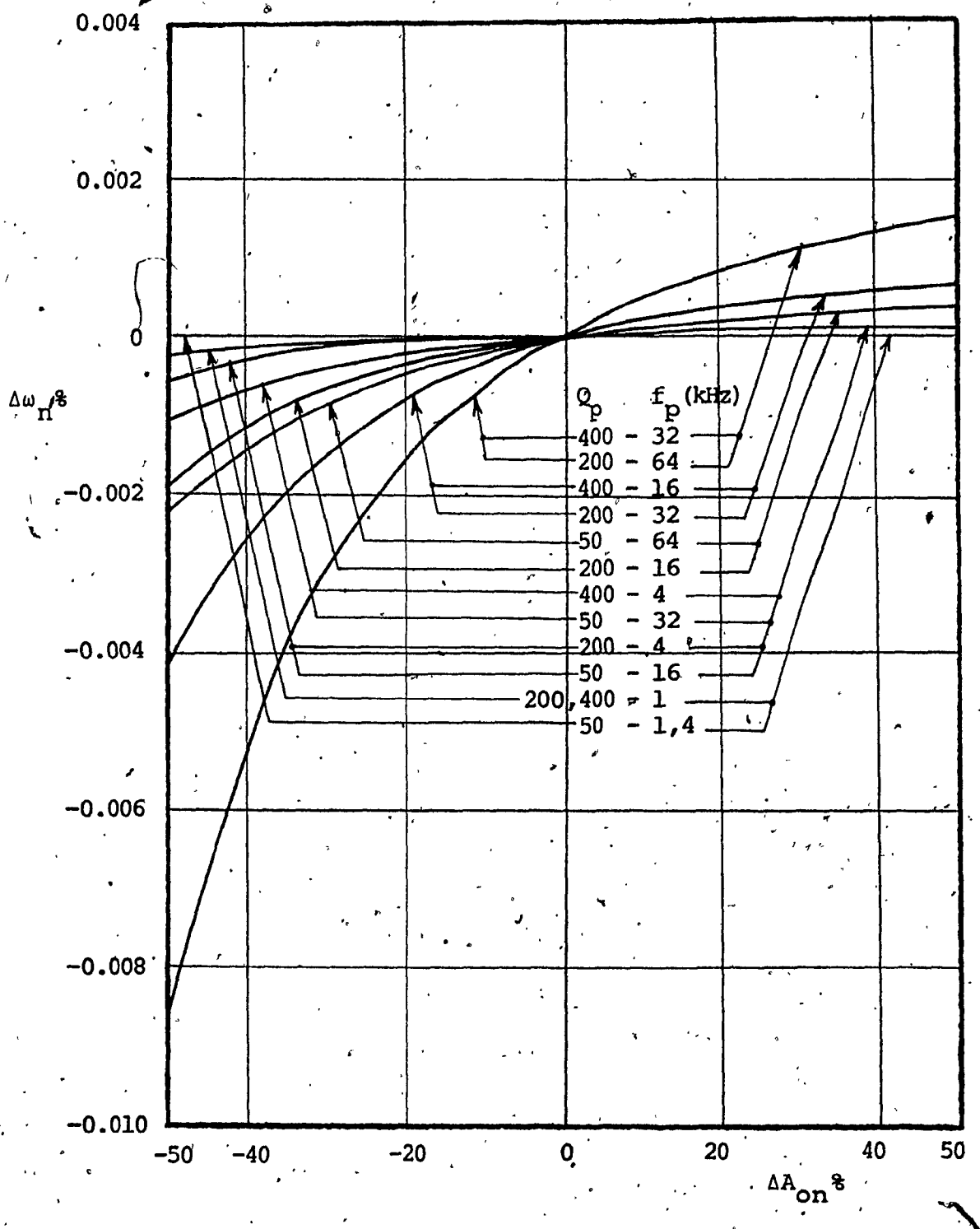

FIG. 5.4a $\Delta\omega_n$% VERSUS ΔA_{on}% FOR BIQUAD A - DESIGN I

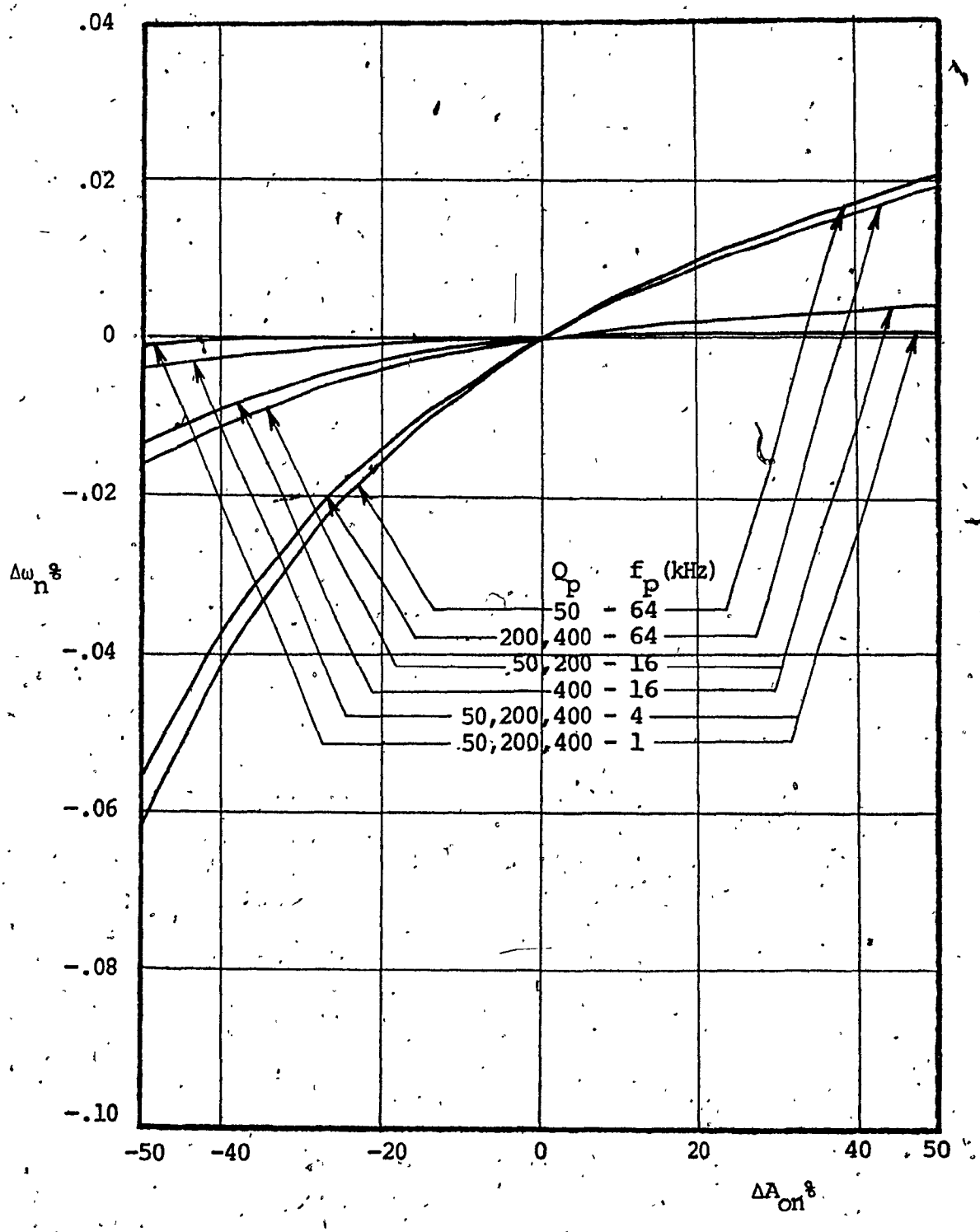

FIG. 5.4b $\Delta\omega_n$% VERSUS ΔA_{on}% FOR BIQUAD A - DESIGN II

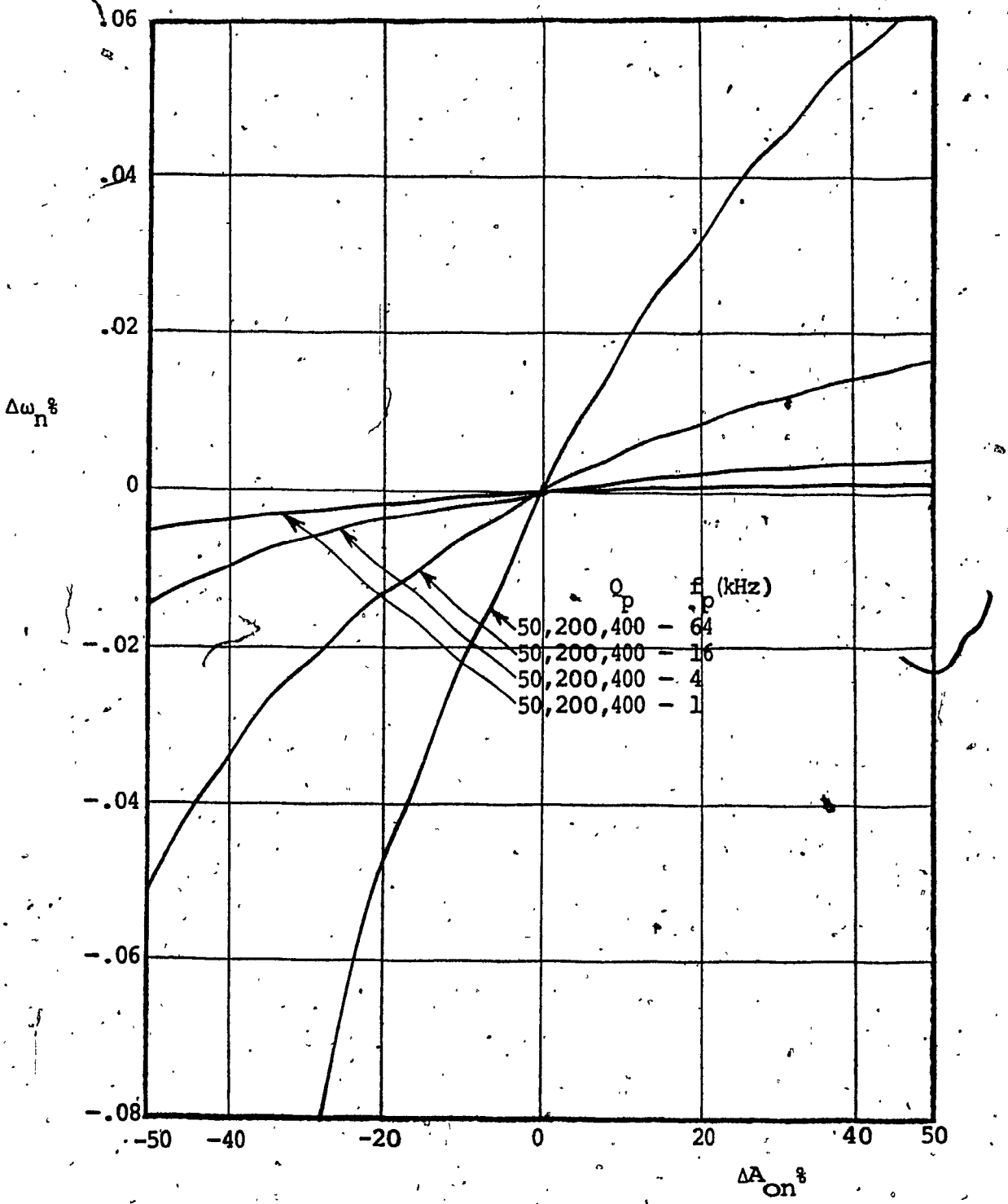

FIG. 5.4c $\Delta\omega_n$% VERSUS ΔA_{on}% FOR BIQUAD B

little dependence on Q_p while being proportional to ω_p in A-II and is independent of Q_p while being proportional to ω_p in B. This can be predicted also from Appendices A,B and C. The deviation $\Delta\omega_n$ in A-I is the smallest and that in B is four times that in A-II. Although A-I has the smallest deviation at all the ω_p's and Q_p's considered, it cannot be operated beyond ω_c at which the other two designs can still be used. This is because the limiting factor is imposed by Q enhancement which may lead to unstable operation, as shown in Fig. 5.1a.

From curve set 5 in Fig. 5.5 (Q_n% versus $\Delta\omega_{cn}$%), it is found that the deviations are the smallest in A-II.

Also, from Fig. 5.6 ($\Delta\omega_n$% versus $\Delta\omega_{cn}$%), the same conclusions can be made as those obtained from Fig. 5.4.

Hence from Figures 5.4, 5.5, and 5.6, we conclude that ΔQ_n% is the smallest in A-II for $\omega_p \geq 2KH_z$, whether due to changes in ω_c or A_0. Also, $\Delta\omega_n$ due to ΔA_{0_n} or $\Delta\omega_{cn}$ is proportional to $\omega_p Q_p$ in A-I, and has little dependence on Q_p, while being proportional to ω_p in A-II and independent of Q_p while being proportional to ω_p in Design B. The smallest deviation occurs in A-I, while that in A-II is approximately four times smaller than that encountered in Design B. The results of $\Delta\omega_n$% versus ΔA_{0_n}% and $\Delta\omega_{cn}$% may be misleading in A-I, since, as explained earlier, the limiting factor is imposed by ΔQ_n as ω_p is increased.

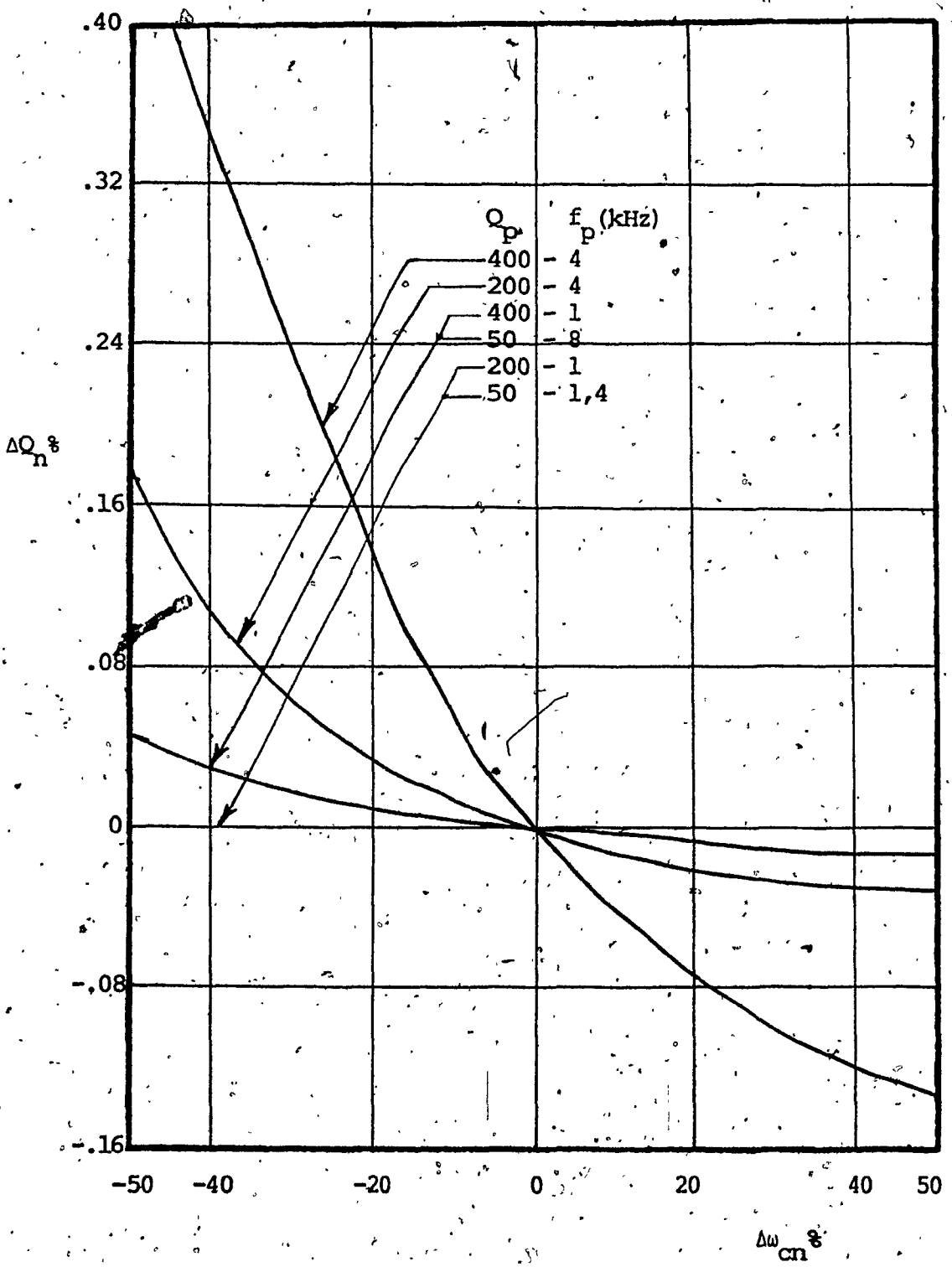

FIG. 5.5a ΔQ_n% VERSUS $\Delta\omega_{cn}$% FOR BIQUAD A - DESIGN II

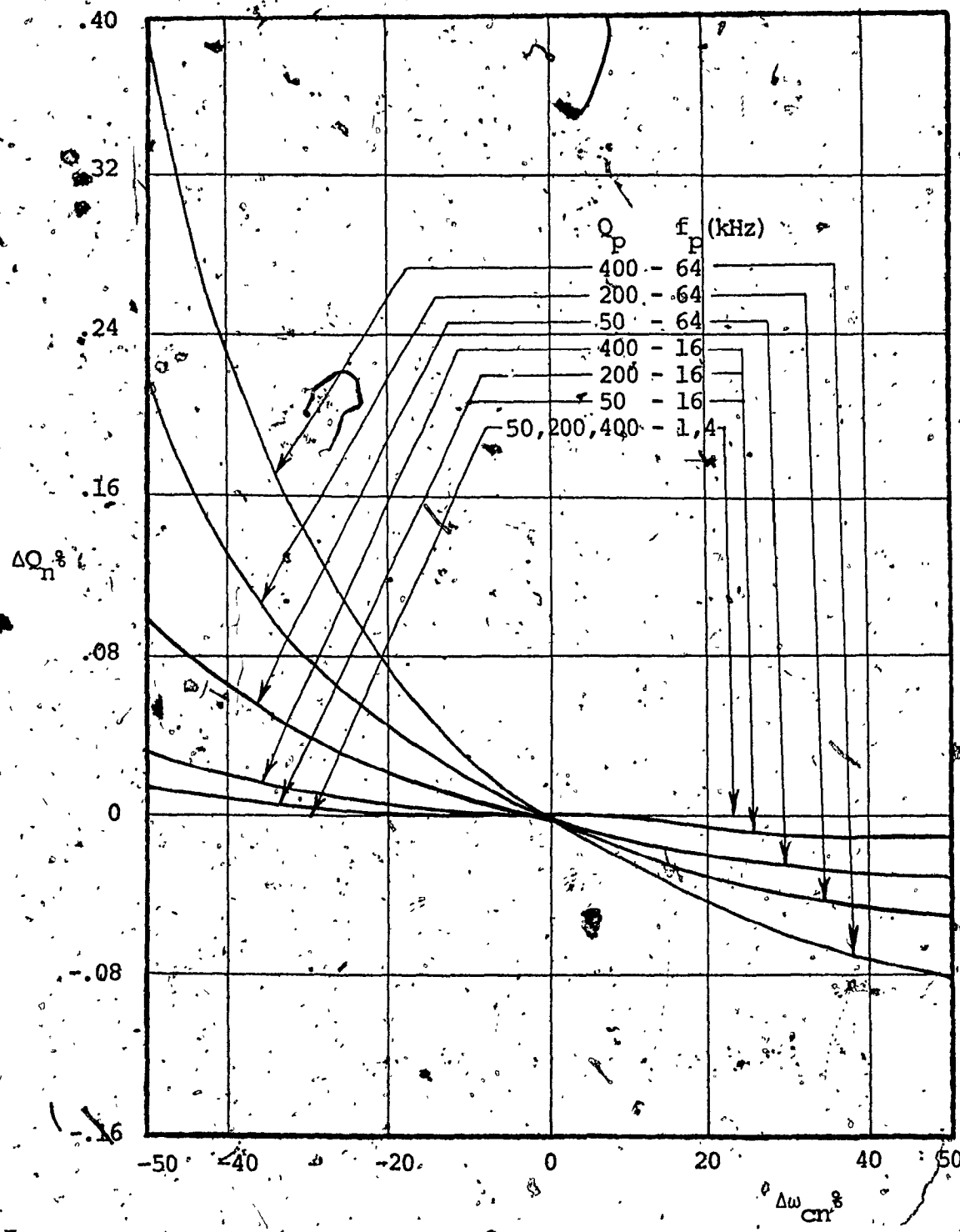

FIG. 5.5b ΔQ_n % VERSUS $\Delta\omega_{cn}$ % FOR BIQUAD A - DESIGN II

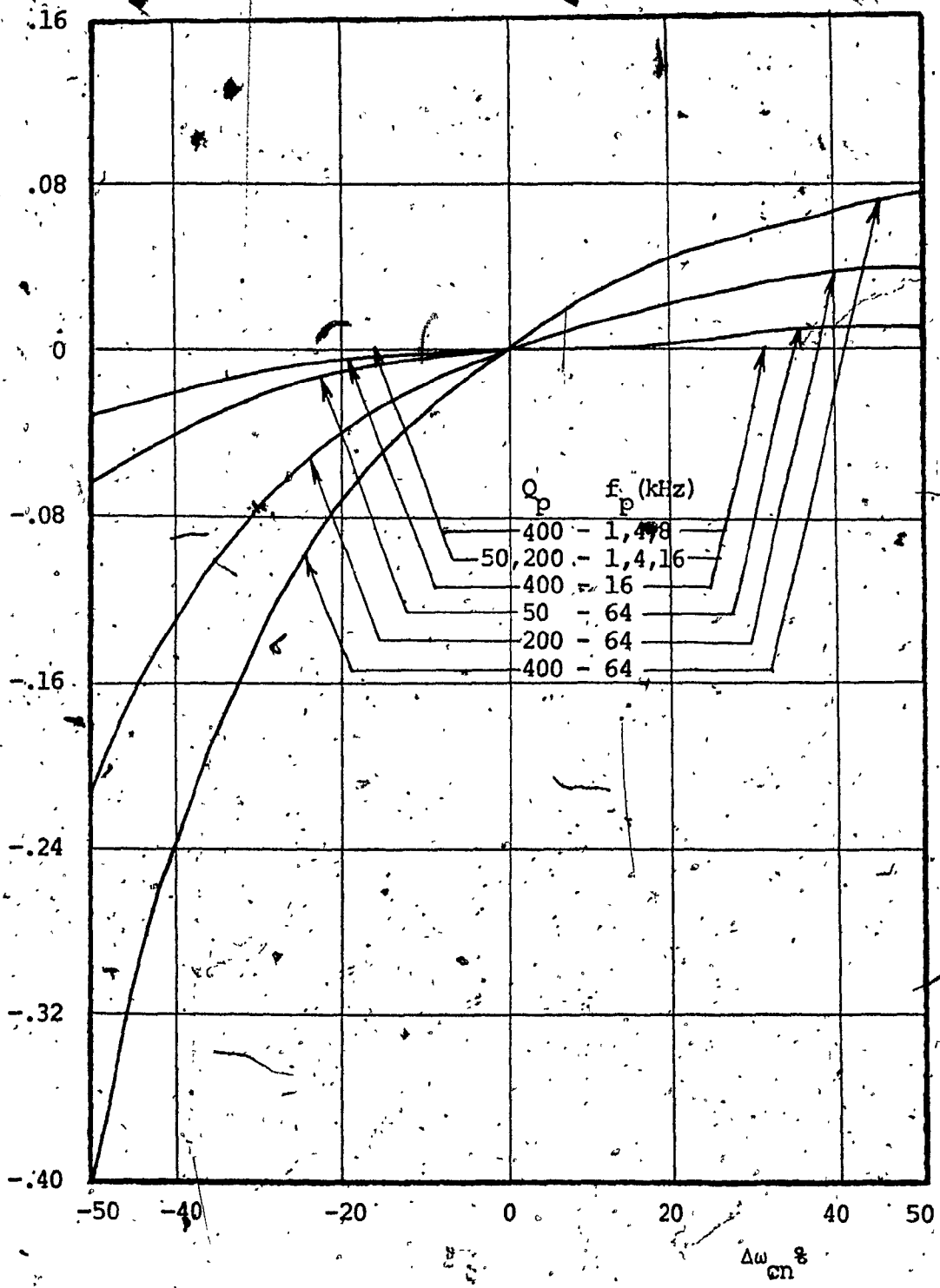

FIG. 5.5c ΔQ_n % VERSUS $\Delta\omega_{cn}$ % FOR BIQUAD B

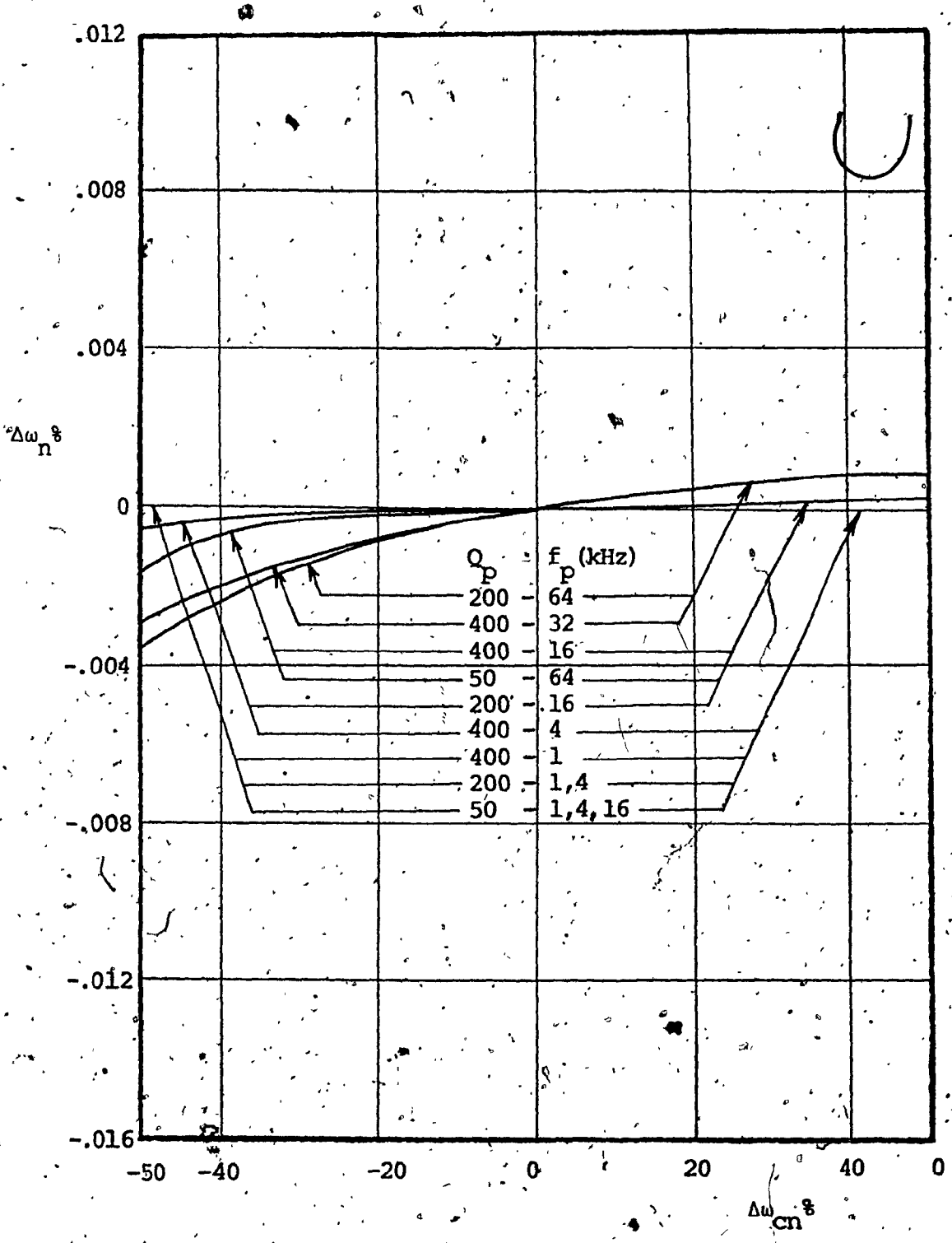

FIG. 5.6a $\Delta\omega_n$% VERSUS $\Delta\omega_{cn}$% OR BIQUAD A - DESIGN I

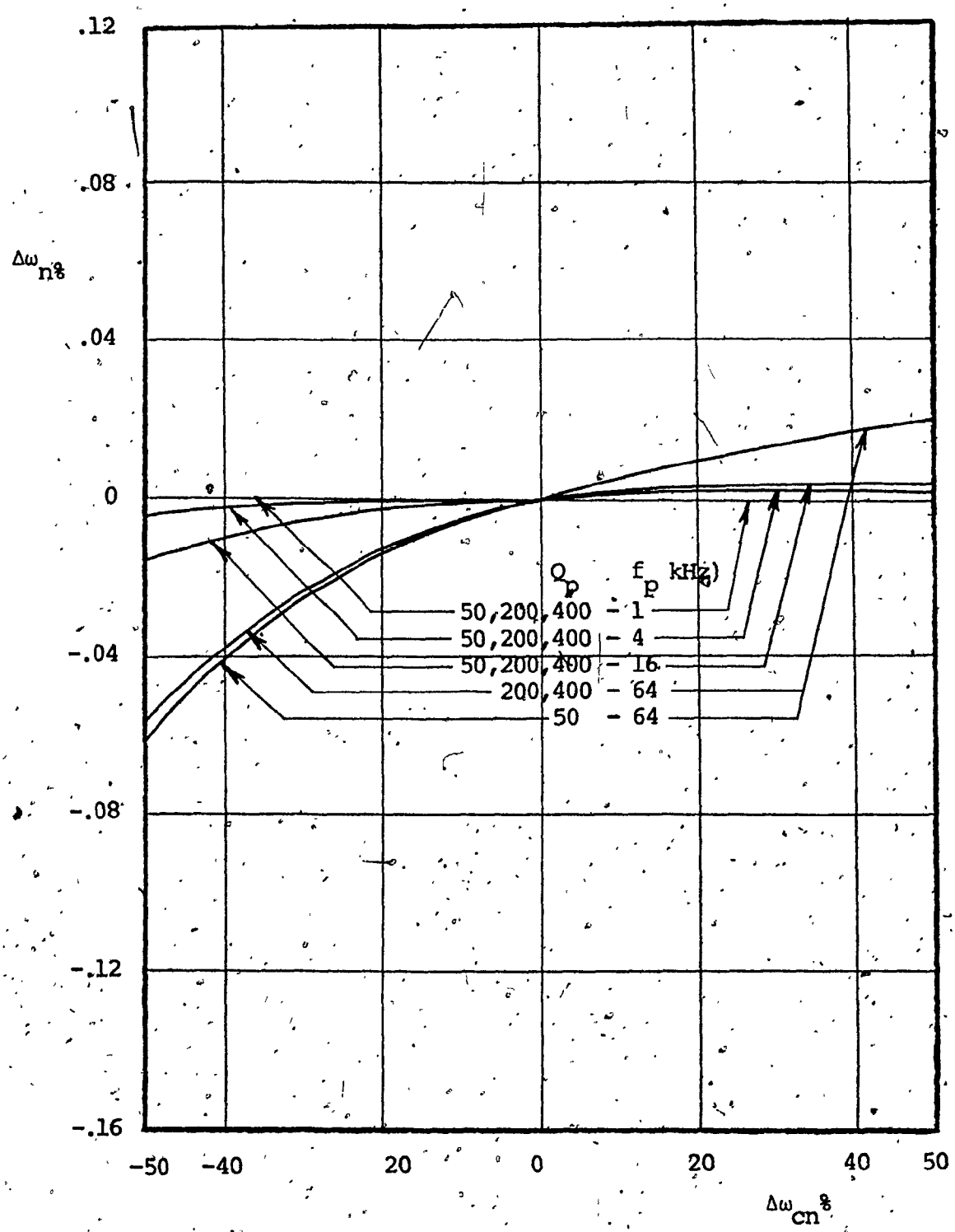

FIG. 5.6b $\Delta\omega_n$% VERSUS $\Delta\omega_{cn}$% FOR BIQUAD A - DESIGN II

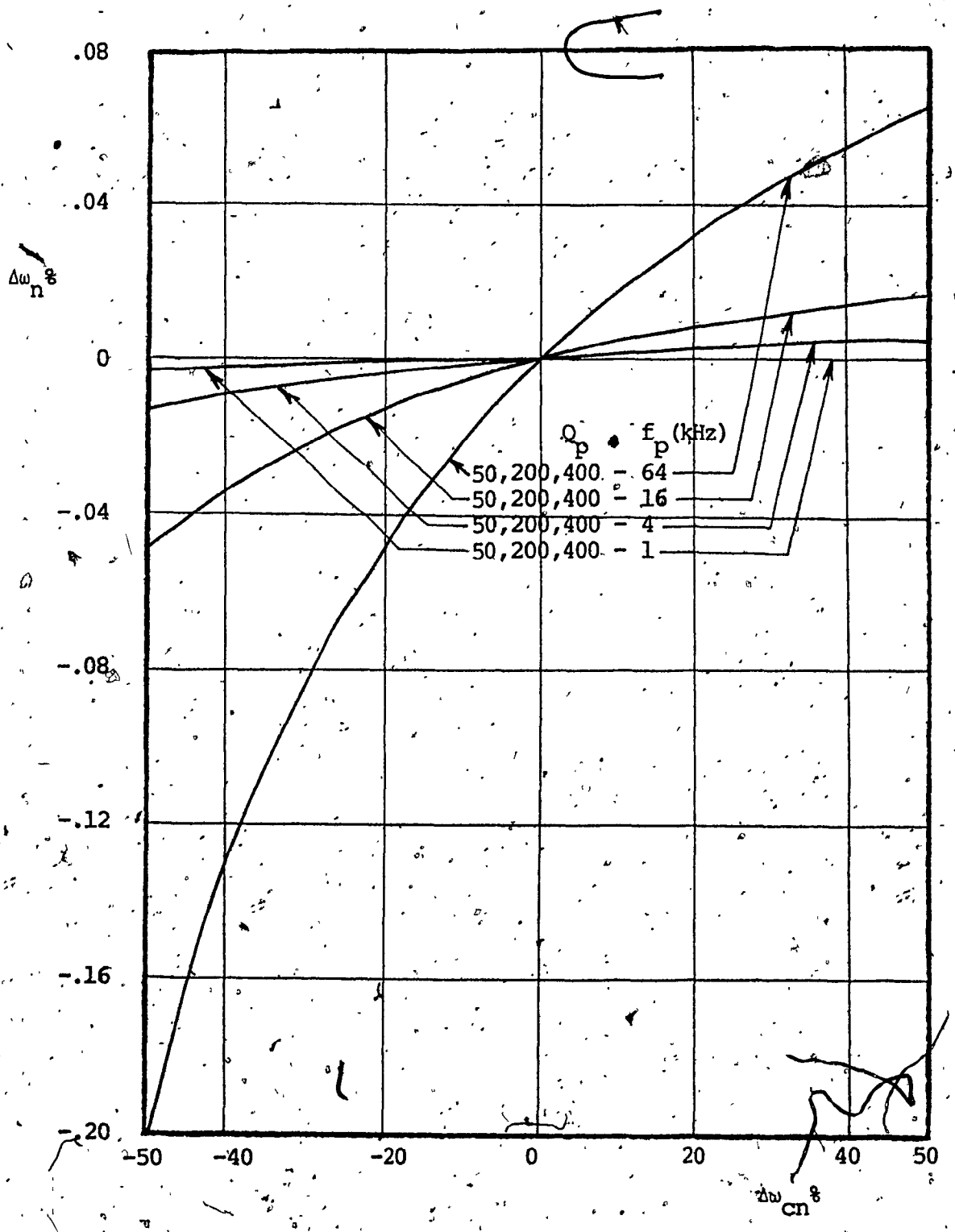

FIG. 5.6c $\Delta\omega_n$% VERSUS $\Delta\omega_{cn}$% FOR BIQUAD B

Thus, we may conclude that A-II has the largest useful bandwidth.

5.4 COMPARISON - PART III

In this section, the two filters designed in each of Sections 3.7 and 4.8 namely, the sixth order Chebychev low-pass filter and the sixth order elliptic band-pass filter, are compared. In Tables 5.3 and 5.4, the total resistance, R_{max} (largest resistor), R_{min} (smallest resistor), C_{max} (largest capacitor), C_{max}/C_{min}, and the numbers of resistors, capacitors and OA's per section in A-II and B realizations for both filters are given.

From the Tables, it is seen that as Q increases, the values of R_{max} are more attractive in A-II as previously explained. Also, when notch sections are used, the resistor tunable section in Design B needs an isolating OA. Thus, A-II becomes more advantageous, since it uses the same number of OA's in this case, while offering more attractive properties such as lower R_{max} for high Q realizations and lower sensitivities and dependence on the active elements.

After the filters were constructed, tuning was achieved easily in each filter for both A-II and B designs. The effect of the active parameters variation (due to the d.c. power supply variation) is shown in Figs. 5.1 and 5.2 for the L.P. and B.P. filters, respectively. From Fig. 5.1, for

TABLE 5.3

COMPARISON OF A-II AND B DESIGNS OF THE SIXTH ORDER LOW-PASS FILTER

SECTION	Q_p	TOTAL CABACITANCE	TOTAL RESISTANCE R_{max} R_{min}		C_{max} C_{max}/C_{min}		NUMBER OF RESISTORS		NUMBER OF CAPACITORS		NUMBER OF OA'S	
			A-II	B	A-II	B	A-II	B	A-II	B	A-II	B
1	0.7609	30.206	50.621 8.049 6.542	35.707 7.5 5.707	15.103 1	15.103 1	7	5	2	2	3	2
2	2.198	21.468	39.904 7.398 4.178	30.928 10.968 4.99	10.734 1	10.734 1	7	5	2	2	3	2
3	8.004	40.186	21.624 5.658 1.353	24.01 16.01 2.	20.093 1	20.093 1	7	5	2	2	3	2

Resistance in kilo ohms
Capacitance in nano farads

TABLE 5.4

COMPARISON OF A-II AND B DESIGNS OF THE SIXTH ORDER BAND-PASS FILTER

SECTION	Q_p	TOTAL CAPACITANCE	TOTAL RESISTANCE R_{max} / R_{min}		C_{max} / C_{max}/C_{min}		NUMBER OF RESISTORS		NUMBER OF CAPACITORS		NUMBER OF OA'S	
			A-II	B	A-II	B	A-II	B	A-II	B	A-II	B
1	32.468	106.104	33.370 11.396 1.175	72.935 64.935 2.	53.052 1	53.052 1	7	5	2	2	3	2
2	74.588	103.834	59.664 17.273 1.426	166.142 149.177 2.	51.917 1	51.917 ≈ 4.5	9	6	2	3	3	2 + buffer
3	74.59	108.422	54.731 17.273 1.948	182.588 149.180 2.	54.211 1	54.211 1	9	6	2	2	3	2 + buffer

Resistance in kilo ohms
Capacitance in nano farads

a d.c. power supply variation from ± 5V to ± 15V (input level = 0.05V), the deviation in the passband ripple is about 0.03 dB and 0.1 dB in A-II and B, respectively. In the B.P. filters, Fig. 5.8, for power supply variation from ± 7.5V to ± 15V(input level = 0.3V), the passband ripple remains less than 0.34 and 0.39 dB in A-II and B, respectively, while the deviation in the stopband is negligible.

In both filters using A-II and B, the responses were examined over the temperature range - 10°C to 70°C. The last peak displacement in the L.P. filters and the centre frequency displacement in the B.P. filters were found due to time constant changes from the passive element variations with temperature and were within the predicted values.

In conclusion, we observe that the Design II of Biquad A offers the most suitable techniques for high Q_p realizations amongst the three designs.

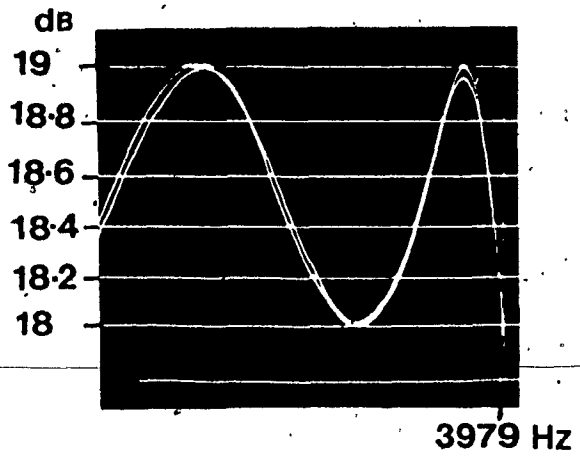

(a)

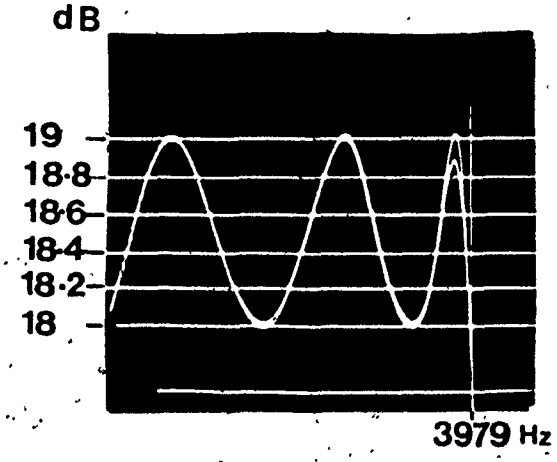

(b)

Fig. 5.7 The effect of variation of active parameters (due to power supply changes from ± 5V to ± 15V) on the frequency response of the sixth order Chebychev low-pass filter.

(a) Using A-II.

(b) Using B.

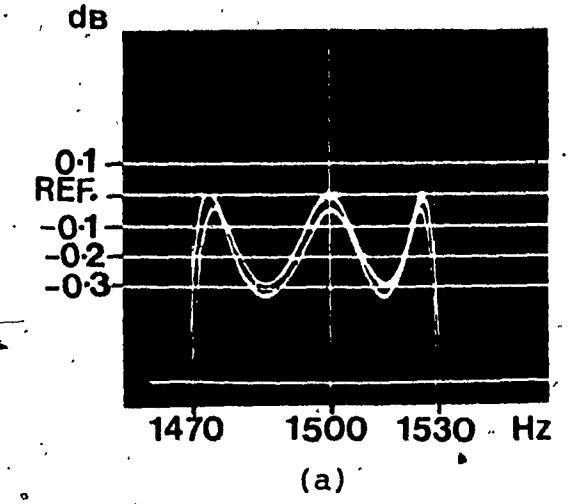

(a)

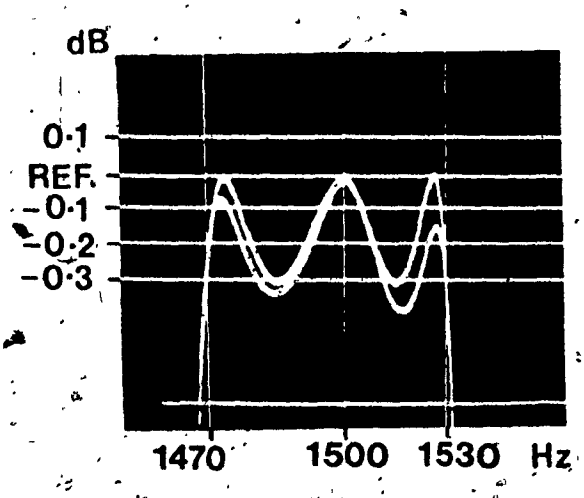

(b)

Fig. 5.8 The effect of variation of active parameters (due to power supply changes from ± 7.5V to ± 15V) on the frequency response of the sixth order elliptic band-pass filter.

(a) Using A-II.

(b) Using B.

CHAPTER VI

CONCLUSION

CHAPTER VI

CONCLUSION

Several high performance RC-active filter design techniques, suitable for direct as well as cascade synthesis procedures, have been developed and studied at length. The realizations use, as basic building-blocks, two types of current conversion type generalized immittance converters, termed CGICA and CGICB in the thesis.

For this purpose, two general configurations for direct synthesis procedures were first presented in Chapter II. One of these configurations, Structure A, uses CGICA's while the other configuration, Structure B, uses CGICB's as the active elements. A new configuration which is minimal with respect to the number of capacitors is obtained by suitably choosing the conversion functions h(s)'s of the CGICA's in Structure A. It is also shown that Structure B contains, as special cases, the realization due to Antoniou and the one due to Cobb and Su. It has been found that these synthesis techniques have the following attractive features:

i) No factorization of the transfer function is necessary.

ii) The synthesis is simple, since the elements are directly related to the coefficients of the transfer function.

iii) The numerator and denominator coefficients can be independently controlled by distinct elements and hence, the alignment of the designed network is expected to be relatively simple.

iv) The resulting realizations have very low sensitivity to element variations.

The minimal capacitor realization described in this thesis, while requiring 50% more OA's, than the one due to Antoniou, needs however, 50% less OA's than in Cobb and SU's minimal capacitor technique.

To take full advantage of integrated technology, filters should be manufactured in large quantities. This is facilitated by designing filters on the basis of the cascade synthesis approach. Hence, cascade synthesis methods are then developed in Chapters III and IV from the direct synthesis ones of Chapter II.

In particular, a stable (during activation) second order realization, Biquad A, is derived in Chapter III from Structure A, using the theory of singular elements. Two different desighs of this realization have been given, namely, Biquad A-Design 1 and Biquad A-Design II. Biquad A-Design I offers simultaneously zero $S_{A_0}^{Q_{pa}}$ and zero $S_{A_0}^{\omega_{pa}}$ while Biquad A-Design II offers low element spread, low $S_{A_0}^{Q_{pa}}$ and zero $S_{A_0}^{\omega_{pa}}$. It is, however, shown that Design II is

superior to Design I from the point of view of element spreads and operating frequency range. It is further shown that Design II has the following features which make it attractive for high Q-factor realizations:

i) Low sensitivity to passive element variations.

ii) Low Q_p sensitivity to d.c. gain variations of the OA's.

iii) Zero ω_p sensitivity to d.c. gain variations of the OA's.

iv) Low dependence of Q_p and ω_p on the finite bandwidth of the OA's.

v) Only three OA's per section are needed. Since the output can always be located at one of the OA output terminals, direct cascading of second order blocks is possible without isolating amplifiers.

vi) There is no spread in the capacitor values while the spread in the resistor values is at most, $2Q_p$.

vii) The filters use the minimum number of capacitors.

Biquad A-Design II has been used to design a number of second-order sections such as low-pass, high-pass, band-pass, notch and all-pass sections. By using these

sections, most of the practical filter specifications can be realized. These filter sections can be tuned easily by adjusting only three resistors. Several of the properties of the new realization are found attractive, as compared with high performance existing realizations, such as those due to KHN, TG and TH. Experimental results, using Design II proposed, show close agreement between theory and practice. Further, these results indicated that these realizations are insensitive to temperature and power supply variations.

There are many applications for which neither Q_p's required are very high, nor the specifications are stringent. In such cases, the high performance obtained from Biquad A may not be necessary and one may be willing to accept a reduced performance from a network, provided it offers other advantages.

Accordingly, in Chapter IV, another biquadratic realization, Biquad B, is obtained from Structure B. This realization, while sacrificing the performance at high Q_p and ω_p slightly, uses a lower number of OA's and results in a simpler network. This has also been used to design a number of universal second-order sections such as those obtained from Biquad A. Each section employs a CGICB which can be implemented by using two OA's. The sensitivites of Q_p, ω_p, Q_z, ω_z and also the multiplier constant of the realization have been found to be low with respect to the passive

and active element variations. A simple tuning sequence by adjusting only resistors has been described. With the exception of one of the notch sections in the twelve circuits considered, the output can be located at one of the OA output terminals. Consequently, cascading of these sections is possible without isolating amplifiers. The realizations are found to be free from low frequency unstable modes of operation. Furthermore, the amplifier pole does not introduce any high frequency unstable modes. Experimental results show close agreement between theory and practice. Also, these results indicate that these realizations are insensitive to temperature and power supply variations. The design procedure has been compared with those due to KHN, TG and TH and has been found to have comparable properties.

Finally, in Chapter V, the performances of Biquads A and B are compared. This comparison shows that Biquad A-Design II offers the largest useful frequency range of operation for a prescribed Q_p and/or ω_p accuracy. The maximum Q_p capability of Biquad B is about four times smaller than that of Biquad A-Design II. Also, the dependence of ω_p in Biquad B on the gain-bandwidth product of the OA's is four times higher than that in Biquad A-Design II. Biquad B, however, offers a simpler realization than Biquad A and uses a lower number of OA's per section excepting for one of the notch sections.* The performance of Biquad A-Design I is almost

---

*The notch sections, however, are often needed in realizing elliptic type transfer functions.

independent of the values of the active elements for $\omega_p \leq \omega_c$. However, the spread in capacitor and resistor values, as well as the rapid Q-enhancement limits the usefulness of this design. It is also shown in that Chapter that from the point of view of element spreads, total resistance for the same total capacitance or vice-versa, useful frequency range of operation, dependence on active elements, etc., Design II of Biquad A offers the most attractive technique for high Q_p realizations amongst all the three cascade design techniques presented in this thesis.

The author feels that it should be of interest to examine the effects of the finite impedance levels of OA's (such as differential input impedance, output impedance, etc.) on the designs presented in this thesis. The noise and dynamic range properties of the realizations have not been studied and should be looked into. Also, the possibility of extending the useful frequency range of operation of the designs presented in this thesis by incorporating lead networks in the structures to compensate for the phase lag introduced by the OA's should be investigated.

In conclusion, the author hopes that in view of the increasing use of active RC-filters in many areas such as instrumentation, control systems, data processing equipment, PCM systems, telephone equipment in transmission and switching, etc., the results obtained in this thesis would prove useful in practical applications.

REFERENCES

REFERENCES

[1] L.P. Huelsman, Ed., Active Filters: Lumped, Distributed, Integrated, Digital and Parametric, New York: McGraw-Hill, 1970.

[2] R.W. Newcomb, Active Integrated Circuit Synthesis, Englewood Cliffs, N.J.: Prentice-Hall, 1968.

[3] L.P. Huelsman, Ed., Active Filters: Lumped, Distributed, Integrated, Digital and Parametric., Ch. 2, New York: McGraw-Hill, 1970.

[4] S.K. Mitra, Analysis and Synthesis of Linear Active Networks, New York: Wiley, 1969.

[5] S.K. Mitra, Ed., Active Inductorless Filters, IEEE Press, 1971.

[6] S.K. Mitra, "Synthesizing Active Filters", IEEE Spectrum, January, 1969.

[7] G.S. Moschytz, "Inductorless Filters: A Survey", in Proc. 1970, Electron-Components Conf.

[8] J.G. Linvill, "RC Active Filters", Proc. IRE, Vol. 42, pp.555-564, Mar. 1954.

[9] T. Yanagisawa, "RC Active Networks Using Current Inversion Type Negative Impedance Converters", IRE Trans-Circuit Theory, Vol. CT-4, pp.140-144, Sept. 1957.

[10] E.S. Kuh, "Transfer Function Synthesis of Active RC Networks", 1960 IRE International Conv. Record, Vol. 8, pt. 2, pp.134-138.

[11] J.M. Spiress, "Synthesis of Active RC Networks", IRE Trans Circuit Theory, Vol. CT-8, pp.260-269, Sept. 1961.

[12] R.P. Sallen and E.L. Key, "A Practical Method of Designing RC Active Filters", IRE Trans. Circuit Theory, Vol. CT-2, pp.74-85, Mar. 1955.

[13] F.R. Bradley and R. McGoy, "Driftless dc amplifiers", Electronics, pp.144-148, Apr. 1954.

[14] G.S. Moschytz, "Miniaturized Filter Building Blocks Using Frequency Emphasizing Networks", Proc. Nat'l Electron. Conf., pp.634-639, 1967.

[15] G.S. Moschytz, "Active RC Filter Building Blocks Using Frequency Emphasizing Networks", IEEE J., Solid State Circuits, Vol. SC-2, pp.59-62, June, 1967.

[16] G.S. Moschytz, "Sallen and Key Filter Networks With Amplifier Gain Larger Than or Equal to Unity", IEEE J. Solid-State Circuits, Vol. SC-2, pp.114-116, Sept. 1967.

[17] W.J. Kerwin, L.P. Huelsman and R.W. Newcomb, "State Variable Synthesis for Insensitive Integrated Circuit Transfer Functions", IEEE J. Solid-State Circuits, Vol. SC-2, pp.87-92, Sept. 1967.

[18] R. Tarmi and M.S. Ghausi, "Very High-Q Insensitive Active RC Networks", IEEE Trans-Circuit Theory, Vol. CT-17, pp. 358-366, Aug. 1970.

[19] J. Tow, "Active RC Filters - A State Space Realization", Proc. IEEE, Vol. 56, pp.1137-1139, June, 1968.

[20] J. Tow, "Design Formulas for Active RC Filters Using Operational Amplifier Biquad", Electron.Lett., Vol. 5, pp.339-341, 1969.

[21] J. Tow, "A Step-by-Step Active Filter Design", IEEE Spectrum, Vol. 6, pp.64-68, Dec. 1969.

[22] L.C. Thomas, "The Biquad: Part I - Some Practical Design Considerations", IEEE Trans-Circuit Theory, Vol. CT-18, pp.350-357, May, 1971.

[23] L.C. Thomas, "The Biquad: Part II-A Multipurpose Active Filtering System", IEEE Trans-Circuit Theory, Vol. CT-18, pp.358-361, May, 1971.

[24] W.B. Mikhael and B.B. Bhattacharyya, "New-Minimal Capacitor Low Sensitivity RC Active Synthesis Procedure", Electron. Lett. Vol. 7, pp.694-696, Nov. 1971.

[25] W.B. Mikhael and B.B. Bhattacharyya, "A Simple Realization of Non-Minimum Phase Transfer Functions", Alta Frequenza, N.8, Vol. XLI, pp.629-631, August,1972.

[26] A. Antoniou, "Novel RC-Active Network Synthesis Using Generalized Immittance Converters", IEEE Trans-Circuit Theory, Vol. CT-17, pp.212-217, May, 1970.

[27] T.A. Hamilton and A.S. Sedra, "Some New Configurations for Active Filters", IEEE Trans. Circuit Theory, Vol. CT-19, pp.25-33, Jan. 1972.

[28] A. Antoniou, "New RC-Active Network Synthesis Procedures Using Negative-Impedance Converters", Proc. IEE (London), Vol. 114, pp.894-902, July, 1967.

[29] H.J. Orchard, "Inductorless Filters", Electron-Letters, Vol. 2, pp.224, Sept. 1966.

[30] J. Gorski-Popiel, "Horowitz Minimum Sensitivity Decomposition", Electron.Letters, Vol. 2, pp.334-335, Sept. 1966.

[31] A. Antoniou, "Realization of Gyrators Using Operational Amplifiers and their Use in RC-Active Network Synthesis", Proc. IEE, Vol. 116, pp.1838-1850, Nov. 1969.

[32] B.B. Bhattacharyya, Wasfy B. Mikhael and A. Antoniou, "Design of RC-Active Networks by Using Generalized Immittance Converters", IEEE International Symposium on Circuit Theory, pp.290-294, Apr. 1973.

[33] R.J. Widlar and J.N. Giles, "Designing With Off-the-Shelf Linear Microcircuits", Fairchild Application Bulletin, App. -124, January, 1966.

[34] Tobey, Graeme and Huelsman, Ed., Operational Amplifiers Design and Applications, New York: McGraw-Hill, 1971.

[35] J. Gorski-Popiel, "RC-ACtive Synthesis Using Positive Impedance Converters", Electron. Lett., Vol. 3, pp. 381-382, Aug. 1967.

[36] W.B. Mikhael and B.B. Bhattacharyya, "Stability Properties of Some RC-Active Realizations", Electron. Lett., Vol. 8, No. 11, pp.288-289, June, 1972.

[37] A. Antoniou, "Stability Properties of Some Gyrator Circuits", Electron.Lett., Vol. 4, pp.510-512, 1968.

[38] R.W. Newcomb, and B.D.O. Anderson, "State Variable Results for Minimal Capacitor Integrated Circuits", University of Stanford Electronics Laboratory Technical Report 6553-14.

[39] D.R. Cobb, and K.L. Su, "Open-Circuit Voltage Transfer Function Synthesis Using the Generalized Positive Impedance Converter", IEEE International Symposium on Circuit Theory, pp.345-349, Apr. 1972.

[40] H.J. Carlin and D.C. Youla, "Network Synthesis With Negative Resistors", Proc. Inst. Radio Engrs., 49, pp.907-920, 1961.

[41] H.J. Carlin, "Singular Network Elements", IEEE Trans. CT-11, pp.67-72, 1964.

[42] G. Martinelli, "On the Nullor", Proc. Inst. Elec. Electron. Engrs. Vol. 53, p.332, 1965.

[43] E. Butler, "The Operational Amplifier as a Network Element", Systems Theory Group Technical Report 86, Cornell University, U.S.A.

[44] A.C. Davies, "The Significance of Nullators, Norators, and Nullors in Active-Network Theory", Radio Electron. Engr. 34, pp.259-267, 1967.

[45] L.T. Bruton, "Biquadratic Sections Using Generalized Impedance Converters", The Radio and Electronic Engineer, Vol. 41, No. 11, Nov. 1971.

[46] Valihora, "Modern Technology Applied to Network Implementation", IEEE International Symposium on Circuit Theory, pp.169-173, Apr. 1972.

APPENDIX A

APPENDIX A.1

THE INFLUENCE OF THE AMPLIFIER POLE ON Q_p AND ω_p OF BIQUAD A - DESIGNS

Assuming ideal OA's, Q_p and ω_p of any RC-active network will be functions of the different resistors and capacitors only. Hence, we may write

$$Q_p = f_1 (R,C) \qquad (A.1)$$

and

$$\omega_p = g_1 (R,C) \qquad (A.2)$$

where R and C denote the resistive and capacitive parameters. From physical considerations, f_1 and g_1 are continuous functions of these elements.

Let the OA's in the network be identical. If the d.c. gain A_0 and the finite gain-bandwidth product B of the OA's are taken into consideration, Q_p and ω_p actually realized are $\hat{Q}_{pa}$ and $\hat{\omega}_{pa}$. Thus, we may write

$$\frac{\hat{Q}_{pa}}{Q_p} = f_2 (R,C,A_0,B) \qquad (A.3)$$

$$\frac{\hat{\omega}_{pa}}{\omega_p} = g_2 (R,C,A_0,B) \qquad (A.4)$$

Now, for ideal OA's $\hat{Q}_{pa} = Q_p$ and $\hat{\omega}_{pa} = \omega_p$ or

$$\lim_{\substack{A_0 \to \infty \\ B \to \infty}} \frac{\hat{Q}_{pa}}{Q_p} = 1^* \qquad (A.5)$$

and

$$\lim_{\substack{A_0 \to \infty \\ B \to \infty}} \frac{\hat{\omega}_{pa}}{\omega_p} = 1 \qquad (A.6)$$

Thus, from (A.3) to (A.6), we have

$$\frac{\hat{Q}_{pa}}{Q_p} = f_3\left(R, C, \frac{1}{A_0}, \frac{1}{B}\right) \qquad (A.7)$$

$$\frac{\hat{\omega}_{pa}}{\omega_p} = g_3\left(R, C, \frac{1}{A_0}, \frac{1}{B}\right) \qquad (A.8)$$

For any given design R's and C's can be expressed in terms of Q_p and ω_p. In studying the effect of A_0 and B, on the design, Q_p and ω_p can be regarded as normalizing constants and (A.7) and (A.8) may be rewritten as

$$\frac{\hat{Q}_{pa}}{Q_p} = f\left(\frac{Q_p}{A_0}, \frac{\omega_p}{B}\right) \qquad (A.9)$$

and

$$\frac{\hat{\omega}_{pa}}{\omega_p} = g\left(\frac{Q_p}{A_0}, \frac{\omega_p}{B}\right) \qquad (A.10)$$

---

* $B \to \infty$ implies $\omega_c = 2\pi f_c \to \infty$ where f_c is the amplifier pole.

where f and g are continuous functions of $(\frac{Q_p}{A_0})$ and $(\frac{\omega_p}{B})$, and $f(0,0) = g(0,0) = 1$. Expanding f and g in McLaurin series around the point $\frac{Q_p}{A_0} = \frac{\omega_p}{B} = 0$ and retaining up to second order terms, we have

$$\frac{\hat{Q}_{pa}}{Q_p} = 1 + a_1 \frac{Q_p}{A_0} + a_2 (\frac{Q_p}{A_0})^2 + b_1 \frac{\omega_p}{B} + b_2 (\frac{\omega_p}{B})^2 + c \frac{Q_p}{A} \cdot \frac{\omega_p}{B} \tag{A.11}$$

and

$$\frac{\hat{\omega}_{pa}}{\omega_p} = 1 + \alpha_1 \frac{Q_p}{A_0} + \alpha_2 (\frac{Q_p}{A_0})^2 + \beta_1 \frac{\omega_p}{B} + \beta_2 (\frac{\omega_p}{B})^2 + \gamma \frac{Q_p}{A_0} \cdot \frac{\omega_p}{B} \tag{A.12}$$

where a's, b's, α's, β's, c and γ are constants related to the derivatives of f and g with respect to $(\frac{Q_p}{A_0})$ and $(\frac{\omega_p}{B})$ evaluated at the $(0,0)$ point.

Assuming $Q_p < A_0$ and $\omega_p < B$, we may also have (up to second order terms)

$$\frac{Q_p}{\hat{Q}_{pa}} = 1 + d_1 \frac{Q_p}{A_0} + d_2 (\frac{Q_p}{A_0})^2 + e_1 \frac{\omega_p}{B} + e_2 (\frac{\omega_p}{B})^2 + h \frac{Q_p}{A_0} \cdot \frac{\omega_p}{B} \tag{A.13}$$

and

$$\frac{\omega_p}{\hat{\omega}_{pa}} = 1 + \theta_1\frac{Q_p}{A_0} + \theta_2\left(\frac{Q_p}{A_0}\right)^2 + \eta_1\frac{\omega_p}{B} + \eta_2\left(\frac{\omega_p}{B}\right)^2 + \nu\,\frac{Q_p}{A_0}\cdot\frac{\omega_p}{B} \qquad (A.14)$$

where d's, e's, θ's, η's, h and ν are constants.

The above formats (A.10) to (A.14) of $\frac{Q_p}{\hat{Q}_{pa}}$ or $\frac{\hat{Q}_{pa}}{Q_p}$ and $\frac{\omega_p}{\omega_{pa}}$ or $\frac{\hat{\omega}_{pa}}{\omega_p}$ are crucial to our subsequent discussion.

Using (3.27) to (3.29), that is, the constraints of Design I in Section 3.6, we obtain from (3.37)

$$\frac{Q_p}{\hat{Q}_{pa}}\left(1+\frac{4}{A_0}+\frac{8}{A_0^2}+\frac{8}{A_0^3}\right) = \frac{\omega_{pa}}{\omega_p}\left[1+\frac{4}{A_0}+\frac{4}{A_0^2}\left(1+\frac{1}{A_0}\right)\cdot(2+Q_p^2)\right]$$

$$+ 4Q_p\left(\frac{\omega_p}{B}\right)\left(\frac{\hat{\omega}_{pa}}{\omega_p}\right)\left[1+\frac{4}{A_0} - \left(\frac{\hat{\omega}_{pa}}{\omega_p}\right)^2\left(1+\frac{2}{A_0}+\frac{3}{A_0^2}\right)\right]$$

$$+ 4\left(\frac{\omega_p}{B}\right)^2\left(\frac{\hat{\omega}_{pa}}{\omega_p}\right)^3\left[\frac{\hat{\omega}_{pa}}{\omega_p}\frac{Q_p}{\hat{Q}_{pa}}\left(1+\frac{3}{A_0}\right) - (2+Q_p^2)\left(1+\frac{3}{A_0}\right)\right]$$

$$+ 4\left(\frac{\omega_p}{B}\right)^3\left(\frac{\hat{\omega}_{pa}}{\omega_p}\right)^4\left[\left(\frac{2}{Q_p}+Q_p\right)\frac{Q_p}{\hat{Q}_{pa}} + Q_p\cdot\frac{\hat{\omega}_{pa}}{\omega_p}\right] \qquad (A.15)$$

and

$$\left(\frac{\omega_p}{\hat{\omega}_{pa}}\right)^2\left(1+\frac{4}{A_0}+\frac{8}{A_0^2}+\frac{8}{A_0^3}\right) = \left(1+\frac{4}{A_0}+\frac{4}{A_0^2}+\frac{4}{A_0^3}\right)$$

$$+\frac{4}{Q_p}\frac{\omega_p}{B}\left[1-\frac{\hat{\omega}_{pa}}{\omega_p}\frac{\hat{Q}_p}{\hat{Q}_{pa}}\left(1+\frac{2}{A_0}+\frac{3}{A_0^2}\right)+\left(\frac{2+Q_p^2}{A_0}\right)\left(2+\frac{3}{A_0}\right)\right]$$

$$+4\left(\frac{\omega_p}{B}\right)^2\left[2+\frac{6}{A_0}-\left(\frac{\omega_{pa}}{\omega_p}\right)^2\left\{1-\frac{1}{Q_p}\left(\frac{Q_p}{\hat{Q}_{pa}}\right)^2\right\}\left(1+\frac{3}{A}\right)\right.$$

$$\left.-\left(\frac{2}{Q_p^2}+1\right)\frac{Q_p}{\hat{Q}_{pa}}\frac{\hat{\omega}_{pa}}{\omega_p}\left(1+\frac{3}{A_0}\right)\right]$$

$$-4\left(\frac{\omega_p}{B}\right)^3\frac{\hat{\omega}_{pa}}{\omega_p}\left[\frac{2}{Q_p}\left(\frac{Q_p}{\hat{Q}_{pa}}\right)+\left(\frac{2}{Q_p}+Q_p\right)\left\{1-\frac{1}{Q_p^2}\left(\frac{Q_p}{\hat{Q}_{pa}}\right)^2\right\}\frac{\hat{\omega}_{pa}}{\omega_p}\right.$$

$$\left.-\frac{1}{Q_p^2}\left(\frac{\hat{\omega}_{pa}}{\omega_p}\right)^2\left(\frac{Q_p}{\hat{Q}_{pa}}\right)\left\{2-\frac{1}{Q_p^2}\left(\frac{Q_p}{\hat{Q}_{pa}}\right)^2\right\}\right. \qquad \text{(A.16)}$$

Assuming $A_0 >> 1$, $Q_p >> 1$ and using the formats (A.11) to (A.14) to ignore terms which will introduce only third and higher order terms of $\left(\frac{Q_p}{A_0}\right)$ and $\left(\frac{\omega_p}{B}\right)$ in the final expressions for $\frac{Q_p}{\hat{Q}_{pa}}$ and $\frac{\omega_p}{\hat{\omega}_{pa}}$, we have from (A.13) and (A.14)

$$\left(\frac{\omega_p}{\hat{\omega}_{pa}}\right)^2 = 1 + \frac{4}{Q_p}\frac{\omega_p}{B} - \frac{4}{Q_p}\frac{\omega_p}{Q_p}\left(\frac{\hat{\omega}_{pa}}{\omega_p}\right)\left(\frac{Q_p}{\hat{Q}_{pa}}\right)$$

$$+ 8\,\frac{\omega_p}{B}\,\frac{Q_p}{A_0} \qquad \text{(A.17)}$$

and

$$\frac{Q_p}{\hat{Q}_{pa}} = \frac{\hat{\omega}_{pa}}{\omega_p} + 4\,\frac{Q_p^2}{A_0^2} + 4\,Q_p\,\frac{\omega_p}{B}\left(\frac{\hat{\omega}_{pa}}{\omega_p}\right)$$

$$- 4\,Q_p\,\frac{\omega_p}{B}\left(\frac{\hat{\omega}_{pa}}{\omega_p}\right)^3 - 4Q_p^2\left(\frac{\omega_p}{B}\right)^2 \qquad \text{(A.18)}$$

Substituting for $\frac{Q_p}{\hat{Q}_{pa}}$ from (A.16) in (A.15) yields

$$\left(\frac{\omega_p}{\hat{\omega}_{pa}}\right)^4 = 1 + \frac{4}{Q_p}\frac{\omega_p}{B} + 8\,\frac{Q_p}{A_0}\frac{\omega_p}{B} - \frac{4}{Q_p}\frac{\omega_p}{B}\left(\frac{\hat{\omega}_{pa}}{\omega_p}\right)^2 \qquad \text{(A.19)}$$

From (A.17) we obtain

$$2\left(\frac{\omega_p}{\hat{\omega}_{pa}}\right)^2 = 1 + \frac{4}{Q_p}\frac{\omega_p}{B} + 8\,\frac{Q_p}{A_0}\cdot\frac{\omega_p}{B}$$

$$\pm\sqrt{\left(1+\frac{4}{Q_p}\frac{\omega_p}{B}+8\,\frac{Q_p}{A_0}\frac{\omega_p}{B}\right)^2 - \frac{16}{Q_p}\frac{\omega_p}{B}} \qquad \text{(A.20)}$$

Taking only the positive sign of the square root since (A.6) has to be satisfied in the ideal case, we have

$$2\left(\frac{\omega_p}{\omega_{pa}}\right)^2 = 1 + 8\frac{Q_p}{A_0}\frac{\omega_p}{B} + \sqrt{\left(1+\frac{4}{Q_p}\frac{\omega_p}{B}+8\frac{Q_p}{A_0}\cdot\frac{\omega_p}{B}\right)^2 - \frac{16}{Q_p}\frac{\omega_p}{B}}$$

(A.21)

Retaining now only up to second order effects we have

$$\left(\frac{\omega_p}{\omega_{pa}}\right)^2 = 1 + 8\frac{Q_p}{A_0}\frac{\omega_p}{B} + \frac{4}{Q_p^2}\left(\frac{\omega_p}{B}\right)^2 \qquad (A.22)$$

Substituting (A.21) in (A.16), we have

$$\frac{Q_p}{\hat{Q}_{pa}} = 1 + 4\left(\frac{Q_p}{A_0}\right)^2 - 4Q_p^2\left(\frac{\omega_p}{B}\right)^2 + 4\frac{Q_p}{A_0}\frac{\omega_p}{B} \qquad (A.23)$$

For $Q_p >> 1$, $Q_p < A_0$, $\omega_p < B$ we have from (A.22)

$$\frac{\omega_p}{\hat{\omega}_{pa}} = 1 + 4\frac{Q_p}{A_0}\cdot\frac{\omega_p}{B} \qquad (A.24)$$

When the term $\frac{\omega_p}{B}$ becomes of any significance compared to 1, $Q_p\frac{\omega_p}{B}$ will be $>> \frac{1}{A_0}$, thus from (A.23) we obtain

$$\frac{Q_p}{\hat{Q}_{pa}} = 1 + 4\left(\frac{Q_p}{A_0}\right)^2 - 4Q_p\left(\frac{\omega_p}{B}\right)\left[Q_p\frac{\omega_p}{B} + \frac{1}{A_0}\right] =$$

$$\doteq 1 + 4\left(\frac{Q_p}{A_0}\right)^2 - 4Q_p^2\left(\frac{\omega_p}{B}\right)^2 \qquad (A.25)$$

Thus, we note from (A.24) and (A.25) that Q_p and ω_p are both independent of A_0 and B as far as first order effects are concerned.

APPENDIX A - 2

THE COMPUTER PROGRAM FOR CALCULATING THE EXACT VALUES OF $\hat{Q}_{pa}$ AND $\hat{\omega}_{pa}$, OF BIQUAD A - DESIGN I IMPLEMENTED USING μA7410A, FOR DIFFERENT VALUES OF Q_p AND ω_p

```
      PROGRAM HAHBY(INPUT,OUTPUT)
C THREE AMPLIFIER  ZERO D.C. ACTIVE SENSITIVITIES
      DIMENSIONXCOF(6),COF(6),ROOTR(6),ROOTI(6)
      M=5
      B=2.0*3.14159*1000000.0
      AO=100000.0
      DO 3 NQ=20,200,20
      QP=NQ
      X1=1.0
      X2=1.0
      X3=1.0
      EMX4=QP**2
      D1=1.0+1.0/X1+1.0/X2+1.0/(X1*X2)
      D2=1.0+X1+X1*X3+X1*X2*X3
      D3=(1.0+X1+X2+X1*X2)*(1.0+X3+EMX4)
      D4=1.0+X2+1.0/X3+1.0/(X1*X3)
      D5=(1.0+1.0/X3)*(1.0+X2+1.0/X1+X2/X1)
      AK=1.0
    2 DO 1 I=1,9
      CON=I
      FP=CON*AK
      WP=2.0*3.14159*FP
      XCOF(1)=(WP*WP)*(1.0+D4/AO+(D5/(AO*AO))*(1.0+1.0/AO))
      XCOF(2)=(WP/QP)*(1.0+D2/AO)+(WP*D3/(QP*AO*AO))*(1.0+1.0/AO)+2.0*D5
     3*WP*WP/(AO*B)+3.0*D5*WP*WP/(B*AO*AO)+D4*WP*WP/B
      XCOF(3)=1.+D1*(1.+1./AO+1./(AO*AO))/AO+WP*D2/(QP*B)+2.*WP*D3/(QP*A
     3O*B)+3.*WP*D3/(QP*B*AO*AO)+D5*WP*WP/(B*B)+3.*D5*WP*WP/(AO*B*B)
      XCOF(4)=D1*(1.0+2.0/AO+3.0/AO**2)/B+WP*D3/(QP*B*B)+3.0*WP*D3/(QP*A
     3O*B*B)+D5*WP*WP/(B*B*B)
      XCOF(5)=D1*(1.0+3.0/AO)/(B*B)+WP*D3/(QP*B*B*B)
      XCOF(6)=D1/(B*B*B)
      CALL POLRT(XCOF,COF,M,ROOTR,ROOTI,IER)
      WPACT=(ROOTI(1)**2+ROOTR(1)**2)**0.5
      QPACT=ABS(WPACT/(2.0*ROOTR(1)))
      FPACT=WPACT/(2.0*3.14159)
      DEVQP=(QPACT-QP)/QP
      DEVFP=(FPACT-FP)/FP
      PRINT 4,QP,QPACT,DEVQP
    4 FORMAT(4X,*IDEAL Q=*,F7.1,4X,*REALIZED Q=*,F10.4,4X,*NORMALIZED
     3DEVIATION(Q REALIZED-Q IDEAL/Q IDEAL)=*,F10.4)
      PRINT 5,FP,FPACT,DEVFP
    5 FORMAT(4X,*IDEAL RESONANT FREQ=*,F12.0,4X,*REALIZED RESON FREQ=*,F
     312.2,4X,*FP REALIZED-FP IDEAL/FP IDEAL=*,F14.6)
      PRINT 6,(ROOTR(J),ROOTI(J),J=1,5)
    6 FORMAT(4X,*ROOT REAL PART=*,E16.7,6X,*IMAG PART=*,E20.7,/)
    1 CONTINUE
      AK=10.0*AK
      IF(AK-10000000.0)2,3,3
    3 CONTINUE
      STOP
      END
```

APPENDIX B.

APPENDIX B.1

THE INFLUENCE OF THE AMPLIFIER POLE ON Q_p AND ω_p OF BIQUAD A - DESIGN II

Using (3.30) and (3.33), that is, the constraints of Design II in Section 3.7, we obtain from (3.37)

$$\left(\frac{\omega_p}{\omega_{pa}}\right)^2 \left[1 + \frac{2}{A_0}\left(1+Q_p^{-\frac{1}{2}}\right) + 2\left(\frac{1}{A_0^2}+\frac{1}{A_0^3}\right)\left(1+3Q_p^{-\frac{1}{2}}\right)\right] =$$

$$= 1 + 2\left(\frac{1+Q_p^{-\frac{1}{2}}}{A_0}\right)\left(1+\frac{1}{A_0}+\frac{1}{A_0^2}\right)$$

$$+ \left(\frac{\omega_p}{B}\right)\left\{\frac{1}{Q_p}\left(1+2Q_p^{\frac{1}{2}}+Q_p\right) - \frac{2}{Q_p}\left(\frac{\hat{\omega}_{pa}}{\omega_p}\right)\left(\frac{Q_p}{\hat{Q}_{pa}}\right)\left(1+Q_p^{-\frac{1}{2}}\right)\left(1+\frac{2}{A_0}+\frac{3}{A_0^2}\right)\right.$$

$$\left. + \frac{1}{Q_p A_0}\left(2+\frac{3}{A_0}\right)\left(3+4Q_p^{\frac{1}{2}}+5Q_p\right)\right\}$$

$$+ \left(\frac{\omega_p}{B}\right)^2\left[2\left(1+\frac{3}{A_0}\right)\left(1+3Q_p^{-\frac{1}{2}}\right) - \frac{1}{Q_p^2}\left(\frac{\hat{\omega}_{pa}}{\omega_p}\frac{Q_p}{\hat{Q}_{pa}}\right)\right.$$

$$\left. \cdot \left(1+\frac{3}{A_0}\right)\left(3+4Q_p^{\frac{1}{2}}+5Q_p\right) - 2\left(\frac{\hat{\omega}_{pa}}{\omega_p}\right)^2\left\{1-\frac{1}{Q_p^2}\left(\frac{Q_p}{\hat{Q}_{pa}}\right)^2\right\}\left(1+Q_p^{-\frac{1}{2}}\right)\left(1+\frac{3}{A_0}\right)\right]$$

$$+ \left(\frac{\omega_p}{B}\right)^3\left[\frac{2}{Q_p}\left(\frac{\hat{\omega}_{pa}}{\omega_p}\right)^3\left(\frac{Q_p}{\hat{Q}_{pa}}\right)\left\{2 - \frac{1}{Q_p^2}\left(\frac{Q_p}{\hat{Q}_{pa}}\right)^2\right\}\left(1+Q_p^{-\frac{1}{2}}\right) -\right.$$

$$\frac{1}{Q_p}\left(\frac{\hat{\omega}_{pa}}{\omega_p}\right)^2\left\{1-\frac{1}{Q_p^2}\left(\frac{Q_p}{\hat{Q}_{pa}}\right)^2\right\}\left(3+4Q_p^{\frac{1}{2}}+5Q_p\right)$$

$$-\frac{2}{Q_p}\left(\frac{\hat{\omega}_{pa}}{\omega_p}\,\frac{Q_p}{\hat{Q}_{pa}}\right)\left(1+3Q_p^{-\frac{1}{2}}\right) \qquad \text{(B.1)}$$

and

$$\frac{Q_p}{\hat{Q}_{pa}}\left[1+\frac{2}{A_0}\left(1+Q_p^{-\frac{1}{2}}\right)+2\left(\frac{1}{A_0^2}+\frac{1}{A_0^3}\right)\left(1+3Q_p^{-\frac{1}{2}}\right)\right] =$$

$$=\frac{\hat{\omega}_{pa}}{\omega_p}\left[1+\frac{1}{A_0}\left(1+2Q_p^{\frac{1}{2}}+Q_p\right)\right]$$

$$+2Q_p\,\frac{\omega_p}{B}\left(\frac{\hat{\omega}_{pa}}{\omega_p}\right)\left(1+Q_p^{-\frac{1}{2}}\right)\left[1-\left(\frac{\hat{\omega}_{pa}}{\omega_p}\right)\left(1+\frac{2}{A_0}+\frac{3}{A_0^2}\right)\right]$$

$$+\frac{\hat{\omega}_{pa}}{\omega_p}\,\frac{1}{A_0^2}\left(1+\frac{1}{A_0}\right)\left(3+4Q_p^{\frac{1}{2}}+5Q_p\right)+2\frac{Q_p}{A_0}\,\frac{\omega_p}{B}\left(\frac{\hat{\omega}_{pa}}{\omega_p}\right)\left(2+\frac{3}{A_0}\right)\left(1+3Q_p^{-\frac{1}{2}}\right)$$

$$+\left(\frac{\omega_p}{B}\right)^2\left(\frac{\hat{\omega}_{pa}}{\omega_p}\right)^2\left\{2\left(\frac{\hat{\omega}_{pa}}{\omega_p}\right)^2\frac{Q_p}{\hat{Q}_{pa}}\left(1+\frac{3}{A_0}\right)\left(1+Q_p^{-\frac{1}{2}}\right)\right.$$

$$\left.-\left(\frac{\hat{\omega}_{pa}}{\omega_p}\right)\left(1+\frac{3}{A_0}\right)\left(3+4Q_p^{\frac{1}{2}}+5Q_p\right)\right\}+\left(\frac{\omega_p}{B}\right)^3\left(\frac{\hat{\omega}_{pa}}{\omega_p}\right)^2\left\{\left(\frac{\hat{\omega}_{pa}}{\omega_p}\right)^2\frac{Q_p}{\hat{Q}_{pa}}\left(\frac{3}{Q_p}+4Q_p^{-\frac{1}{2}}+5\right)\right.$$

$$\left.+2Q_p\left(\frac{\hat{\omega}_{pa}}{\omega_p}\right)^3\left\{1-\frac{1}{Q_p^2}\left(\frac{Q_p}{\hat{Q}_{pa}}\right)^2\right\}\left(1+Q_p^{-\frac{1}{2}}\right)-2Q_p\left(\frac{\hat{\omega}_{pa}}{\omega_p}\right)\left(1+3Q_p^{-\frac{1}{2}}\right)\right\} \qquad \text{(B.2)}$$

Assuming $A_0 >> 1$, $Q_p >> 1$, and using formats (A.11) to (A.14) to ignore terms which will contribute only third and higher order terms of (Q_p/A_0) and (ω_p/B) in the final expressions for $Q_p/\hat{Q}_{pa}$ and $\omega_p/\hat{\omega}_{pa}$, we have from (B.1) and (B.2)

$$\left(\frac{\omega_p}{\hat{\omega}_{pa}}\right)^2 = 1 + \frac{\omega_p}{B} - \frac{5}{Q_p}\left(\frac{\omega_p}{B}\right) - \frac{2}{Q_p}\left(\frac{\omega_p}{B}\right)\left(\frac{\hat{\omega}_{pa}}{\omega_p}\right)\left(\frac{Q_p}{\hat{Q}_{pa}}\right) \qquad (B.3)$$

and

$$\frac{Q_p}{\hat{Q}_{pa}} = \frac{\hat{\omega}_{pa}}{\omega_p}\left(1+\frac{Q_p}{A_0}\right) + 5\frac{Q_p}{A_0^2} + 2Q_p\left(\frac{\omega_p}{B}\right)\left(\frac{\hat{\omega}_{pa}}{\omega_p}\right)\left\{1 - \left(\frac{\hat{\omega}_{pa}}{\omega_p}\right)^2\right\}$$

$$- 5Q_p\left(\frac{\omega_p}{B}\right)^2 + 4\left(\frac{Q_p}{A_0}\right)\left(\frac{\omega_p}{B}\right) \qquad (B.4)$$

Substituting for $\frac{Q_p}{\hat{Q}_{pa}}$ from (B.4) in (B.3) yields

$$\left(\frac{\omega_p}{\hat{\omega}_{pa}}\right)^4 - \left[1+\frac{\omega_p}{B} - \frac{5}{Q_p}\left(\frac{\omega_p}{B}\right)^2\right]\left(\frac{\omega_p}{\hat{\omega}_{pa}}\right)^2 + \frac{2}{Q_p}\left(\frac{\omega_p}{B}\right)\left(1+\frac{Q_p}{A_0}\right) = 0 \qquad (B.5)$$

Hence, using (A.6), we obtain from (B.5)

$$2\left(\frac{\omega_p}{\omega_{pa}}\right)^2 = 1 + \frac{\omega_p}{B} - \frac{5}{Q_p}\left(\frac{\omega_p}{B}\right)^2 + \sqrt{\left\{1 + \frac{\omega_p}{B} - 5\left(\frac{\omega_p}{B}\right)^2\right\}^2 - \frac{8}{Q_p}\frac{\omega_p}{B}\left(1+\frac{Q_p}{A_0}\right)} \qquad (B.6)$$

or

$$\left(\frac{\omega_p}{\omega_{pa}}\right)^2 \doteq 1 + \frac{\omega_p}{B}\left(1 - \frac{2}{Q_p} - \frac{5}{Q_p} - \frac{\omega_p}{B}\right) \qquad (B.7)$$

Hence, for $Q_p >> 1$, $\omega_p < B$, we have from (B.7),

$$\frac{\omega_p}{\omega_{pa}} \doteq 1 + \frac{1}{2}\frac{\omega_p}{B} - \frac{1}{8}\left(\frac{\omega_p}{B}\right)^2 \qquad (B.8)$$

Using (B.4), (B.7), (B.8) and the fact that $Q_p >> 1$, $A_0 >> 1$, $\omega_p < B$, $Q_p < A_0$, we have

$$\frac{Q_p}{Q_{pa}} \doteq 1 + \frac{Q_p}{A_0} - \frac{\omega_p}{2B} - 3Q_p\left(\frac{\omega_p}{B}\right)^2 + \frac{7}{2}\left(\frac{Q_p}{A_0}\right)\left(\frac{\omega_p}{B}\right) \qquad (B.9)$$

APPENDIX B - 2

THE COMPUTER PROGRAM FOR CALCULATING THE EXACT VALUES OF $\hat{Q}_{pa}$ AND $\hat{\omega}_{pa}$, OF BIQUAD A - DESIGN II IMPLEMENTED USING μA7410A FOR DIFFERENT VALUES OF Q_p AND ω_p

```
      PROGRAM EVA(INPUT,OUTPUT)
C THREE AMPLIFIER LOW SPREAD
      DIMENSIONXCOF(6),COF(6),ROOTR(6),ROOTI(6)
      M=5
      B=2.0*3.14159*1000000.0
      AO=100000.0
      DO 3 NQ=20,200,20
      QP=NQ
      X1=QP**0.5
      ALFM=2.0/(1.0+1.0/X1)
      X2=1.0
      X3=X1/ALFM
      EMX4=ALFM*X1
      D1=1.0+1.0/X1+1.0/X2+1.0/(X1*X2)
      D2=1.0+X1+X1*X3+X1*X2*X3
      D3=(1.0+X1+X2+X1*X2)*(1.0+X3+EMX4)
      D4=1.0+X2+1.0/X3+1.0/(X1*X3)
      D5=(1.0+1.0/X3)*(1.0+X2+1.0/X1+X2/X1)
      AK=1.0
    2 DO 1 I=1,9
      CON=I
      FP=CON*AK
      WP=2.0*3.14159*FP
      XCOF(1)=(WP*WP)*(1.0+D4/AO+(D5/(AO*AO))*(1.0+1.0/AO))
      XCOF(2)=(WP/QP)*(1.0+D2/AO)+(WP*D3/(QP*AO*AO))*(1.0+1.0/AO)+2.0*D5
     9*WP*WP/(AO*B)+3.0*D5*WP*WP/(B*AO*AO)+D4*WP*WP/B
      XCOF(3)=1.+D1*(1.+1./AO+1./(AO*AO))/AO+WP*D2/(QP*B)+2.*WP*D3/(QP*A
     80*B)+3.*WP*D3/(QP*B*AO*AO)+D5*WP*WP/(B*B)+3.*D5*WP*WP/(AO*B*B)
      XCOF(4)=D1*(1.0+2.0/AO+3.0/AO**2)/B+WP*D3/(QP*B*B)+3.0*WP*D3/(QP*A
     90*B*B)+D5*WP*WP/(B*B*B)
      XCOF(5)=D1*(1.0+3.0/AO)/(B*B)+WP*D3/(QP*B*B*B)
      XCOF(6)=D1/(B*B*B)
      CALL POLRT(XCOF,COF,M,ROOTR,ROOTI,IER)
      WPACT=(ROOTI(1)**2+ROOTR(1)**2)**0.5
      QPACT=ABS(WPACT/(2.0*ROOTR(1)))
      FPACT=WPACT/(2.0*3.14159)
      DEVQP=(QPACT-QP)/QP
      DEVFP=(FPACT-FP)/FP
      PRINT 4,QP,QPACT,DEVQP
    4 FORMAT(4X,*IDEAL Q=*,F7.1,4X,*REALIZED Q=*,F10.4,4X,*NORMALIZED
     3DEVIATION(Q REALIZED-Q IDEAL/Q IDEAL)=*,F10.4)
      PRINT 5,FP,FPACT,DEVFP
    5 FORMAT(4X,*IDEAL RESONANT FREQ=*,F12.0,4X,*REALIZED RESON FREQ=*,F
     812.2,4X,*FP REALIZED-FP IDEAL/FP IDEAL=*,F14.6)
      PRINT 6,(ROOTR(J),ROOTI(J),J=1,5)
    6 FORMAT(4X,*ROOT REAL PART=*,E16.7,6X,*IMAG PART=*,E20.7,/)
    1 CONTINUE
      AK=10.0*AK
      IF(AK-1000000.0)2,3,3
    3 CONTINUE
      STOP
      END
```

APPENDIX C

APPENDIX C.1

THE INFLUENCE OF THE AMPLIFIER POLE ON Q_p AND ω_p OF BIQUAD B

Assuming $A_0 >> 1, Q_p >> 1$ and using the formats (A.11 to A.14) to ignore those terms that contribute only third and higher order terms to the final expression for $\frac{Q_p}{\hat{Q}_{pa}}$ and $\frac{\omega_p}{\hat{\omega}_{pa}}$, we have from (4.23)

$$\left(\frac{\omega_p}{\hat{\omega}_{pa}}\right)^2 \doteq 1 + 4\frac{\omega_p}{B}\left\{1 - \frac{1}{2Q_p}\left(\frac{\omega_p}{\hat{\omega}_{pa}}\frac{Q_p}{\hat{Q}_{pa}}\right)\right\}$$

$$- \frac{1}{Q_p^2}\left(\frac{\omega_p}{\hat{\omega}_{pa}}\frac{Q_p}{\hat{Q}_{pa}}\right)\left(1 - \frac{\omega_p}{\hat{\omega}_{pa}}\frac{Q_p}{\hat{Q}_{pa}}\right)$$

$$+ \frac{2}{A_0}\left\{1 - \frac{2}{Q_p}\left(\frac{\omega_p}{\hat{\omega}_{pa}}\frac{Q_p}{\hat{Q}_{pa}}\right)\right\} + 2\left(\frac{\omega_p}{B}\right)^2\left\{1 - \left(\frac{\hat{\omega}_{pa}}{\omega_p}\right)^2\right\} \quad (C.1)$$

and

$$\frac{Q_p}{\hat{Q}_{pa}} = \frac{\hat{\omega}_{pa}}{\omega_p}\left[1 + 4\frac{Q_p}{A_0} + 2Q_p\frac{\omega_p}{B}\left\{1 - \left(\frac{\hat{\omega}_{pa}}{\omega_p}\right)^2\right\} - 4Q_p\left(\frac{\omega_p}{B}\right)^2\right] \quad (C.2)$$

From (C.2) we have

$$\frac{Q_p}{\hat{Q}_{pa}}\left(\frac{\omega_p}{\hat{\omega}_{pa}}\right) = 1 + 4\frac{Q_p}{A_0} + 2Q_p\frac{\omega_p}{B} - 4Q_p\left(\frac{\omega_p}{B}\right)^2 - 2Q_p\frac{\omega_p}{B}\left(\frac{\hat{\omega}_{pa}}{\omega_p}\right)^2 \quad (C.3)$$

and

$$\left(\frac{Q_p}{\hat{Q}_{pa}}\frac{\omega_p}{\hat{\omega}_{pa}}\right)^2 = 1 + 16\left(\frac{Q_p}{A_0}\right)^2 + 4Q_p^2\left(\frac{\omega_p}{B}\right)^2\left\{1 - \left(\frac{\hat{\omega}_{pa}}{\omega_p}\right)^2\right\}$$

$$+ 16Q_p^2\left(\frac{\omega_p}{B}\right)^4 + 8\frac{Q_p}{A_0}$$

$$+ 4Q_p\frac{\omega_p}{B}\left\{1 - \left(\frac{\hat{\omega}_{pa}}{\omega_p}\right)^2\right\} - 8Q_p\left(\frac{\omega_p}{B}\right)^2$$

$$+ 8Q_p\frac{Q_p}{A_0}\frac{\omega_p}{B}\left\{1 - \left(\frac{\hat{\omega}_{pa}}{\omega_p}\right)^2\right\} - 32Q_p\frac{Q_p}{A_0}\left(\frac{\omega_p}{B}\right)^2$$

$$- 16Q_p^2\left(\frac{\omega_p}{B}\right)^3\left\{1 - \left(\frac{\hat{\omega}_{pa}}{\omega_p}\right)^2\right\} \quad (C.4)$$

Substituting for $\left(\frac{Q_p}{\hat{Q}_{pa}}\frac{\omega_p}{\hat{\omega}_{pa}}\right)$ and its square from (C.4) and (C.5) in (C.1) and ignoring terms contributing only third and higher order terms, we have

$$\left(\frac{\omega_p}{\hat{\omega}_{pa}}\right)^4 - \left\{1 + 4\frac{\omega_p}{B} - 4\left(\frac{\omega_p}{B}\right)^2\right\}\left(\frac{\omega_p}{\hat{\omega}_{pa}}\right)^2$$

$$- 2\frac{\omega_p}{B}\left(\frac{4}{A_0} + 2\frac{\omega_p}{B} - \frac{2}{Q_p}\right) = 0 \quad (C.5)$$

Using (A.6) and (C.5) we have

$$2\left(\frac{\omega_p}{\hat{\omega}_{pa}}\right)^2 = 1 + 4\frac{\omega_p}{B} - 4\left(\frac{\omega_p}{B}\right)^2 \pm \sqrt{1 + 4\frac{\omega_p}{B} - 4\left(\frac{\omega_p}{B}\right)^2 + 8\frac{\omega_p}{B}\left(\frac{4}{A_0} + 2\frac{\omega_p}{B} - \frac{2}{Q_p}\right)} \qquad (C.6)$$

Hence

$$\left(\frac{\omega_p}{\hat{\omega}_{pa}}\right)^2 \doteq 1 + 4\frac{\omega_p}{B} \qquad (C.7)$$

or

$$\frac{\omega_p}{\hat{\omega}_{pa}} \doteq 1 + 2\frac{\omega_p}{B} \qquad (C.8)$$

From (C.2), (C.7) and (C.8), we obtain

$$\frac{Q_p}{\hat{Q}_{pa}} \doteq 1 + 4\frac{Q_p}{A_0} - 2\frac{\omega_p}{B} + 4Q_p\left(\frac{\omega_p}{B}\right)^2 - 8\frac{Q_p}{A_0}\frac{\omega_p}{B} \qquad (C.9)$$

APPENDIX C - 2

THE COMPUTER PROGRAM FOR CALCULATING THE EXACT VALUES OF $\hat{Q}_{pa}$ AND $\hat{\omega}_{pa}$, OF BIQUAD B IMPLEMENTED USING μA7410A, FOR DIFFERENT VALUES OF Q_p AND ω_p

```
      PROGRAM VICTOR(INPUT,OUTPUT)
TWO AMPLIFIER CIRCUIT
      DIMENSIONXCOF(5),COF(5),ROOTR(5),ROOTI(5)
      M=4
      B=2.0*3.14159*1000000.0
      AO=100000.0
      DO 3 NQ=20,200,20
      QP=NQ
      AK=1.0
    2 DO 1 I=1,9
      CON=I
      FP=CON*AK
      WP=2.0*3.14159*FP
      XCOF(1)=(1.+(1./AO+1./(AO*AO))*(1.+1./QP))*WP*WP
      XCOF(2)=(1./(WP*QP)+2.*(1.+1./AO)*(2.+1./QP)/(AO*WP)+2.*(1.+2./AO)
     *(1.+1./QP)/B)*WP*WP
      XCOF(3)=(1./(WP*WP)+2.*(1.+1./AO)/(AO*WP*WP)+2.*(1.+2./AO)*(2.+1./
     *QP)/(B*WP)+2.*(1.+1./QP)/(B*B))*WP*WP
      XCOF(4)=(2.*(1.+2./AO)/(B*WP*WP)+2.*(2.+1./QP)/(WP*B))*WP*WP
      XCOF(5)=2./(B*B)
      CALL POLRT(XCOF,COF,M,ROOTR,ROOTI,IER)
      WPACT=(ROOTI(1)**2+ROOTR(1)**2)**0.5
      QPACT=ABS(WPACT/(2.0*ROOTR(1)))
      FPACT=WPACT/(2.0*3.14159)
      DEVQP=(QPACT-QP)/QP
      DEVFP=(FPACT-FP)/FP
      PRINT 4,QP,QPACT,DEVQP
    4 FORMAT(4X,*IDEAL Q=*,F7.1,4X,*REALIZED Q=*,F10.4,4X,*NORMALIZED
     *DEVIATION(Q REALIZED-Q IDEAL/Q IDEAL)=*,F10.4)
      PRINT 5,FP,FPACT,DEVFP
    5 FORMAT(4X,*IDEAL RESONANT FREQ=*,F12.0,4X,*REALIZED RESON FREQ=*,F
     *12.2,4X,*FP REALIZED-FP IDEAL/FP IDEAL=*,F14.6)
      PRINT 6,(ROOTR(J),ROOTI(J),J=1,4)
    6 FORMAT(4X,*ROOT REAL PART=*,E16.7,6X,*IMAG PART=*,E20.7,/)
    1 CONTINUE
      AK=10.0*AK
      IF(AK-1000000.0)2,3,3
    3 CONTINUE
      STOP
      END
```